European Society
ESGAR
Gastrointestinal and Abdominal Radiology

Insights into Imaging

Education and strategies in European radiology

ESGAR 2015 Book of Abstracts / Volume 6 / Supplement 2 / June 2015

ESGAR 2015 / June 9 – 12 / Paris, France
26th Annual Meeting and Postgraduate Course

ESR
European Society of Radiology

European Society
ESGAR
Gastrointestinal and Abdominal Radiology

JUNE 9-12

ESGAR 2015

PARIS
FRANCE

European Society of Gastrointestinal and Abdominal Radiology

BOOK OF ABSTRACTS

INCLUDES ABSTRACTS OF SCIENTIFIC PRESENTATIONS

IMPORTANT ADDRESSES

ORGANISING SECRETARIAT

Central ESGAR Office
Neutorgasse 9
AT – 1010 Vienna, Austria
Phone: +43 1 535 89 27
Fax: +43 1 535 70 37
E-Mail: office@esgar.org

WEBSITE

www.esgar.org

CONFERENCE VENUE

CNIT
2 Place de la Défense
FR – 92053 Paris, France

CME CREDITS

The 'ESGAR – THE EUROPEAN SOCIETY OF GASTRO-INTESTINAL AND ABDOMINAL RADIOLOGY' (or) 'ESGAR 2015 – 26th ESGAR Annual Meeting' is accredited by the European Accreditation Council for Continuing Medical Education (EACCME) to provide the following CME activity for medical specialists. The EACCME is an institution of the European Union of Medical Specialists (UEMS), www.uems.net.

The 'ESGAR 2015 – 26th ESGAR Annual Meeting' is designated for a maximum of (or 'for up to') 23 hours of European external CME credits. Each medical specialist should claim only those hours of credit that he/she actually spent in the educational activity.

Date of publishing: June 2015

JOINT SESSION

European Society of Urogenital Radiology

SPONSORS

ESGAR wishes to gratefully acknowledge the support of its Corporate Members:

Bayer HealthCare

BRACCO

GE Healthcare

Guerbet Contrast for Life

PHILIPS

The Final Programme of ESGAR 2015 is available on the ESGAR website www.esgar.org

DOI 10.1007/s13244-015-0412-2

TABLE OF CONTENTS

ESGAR EXECUTIVE COMMITTEE

PRESIDENT
L. Martí-Bonmatí (Valencia/ES)

PRESIDENT-ELECT
C. Matos (Brussels/BE)

VICE PRESIDENT
S. Halligan (London/UK)

SECRETARY
A. Palkó (Szeged/HU)

TREASURER
S. Jackson (Plymouth/UK)

PAST PRESIDENT
F. Caseiro Alves (Coimbra/PT)

EDUCATION COMMITTEE
R.G.H. Beets-Tan (Maastricht/NL)

MEMBERSHIP COMMITTEE
T. Helmberger (Munich/DE)

WORKSHOP COMMITTEE
A. Laghi (Latina/IT)

MEETING PRESIDENT
Y. Menu (Paris/FR)

PRE-MEETING PRESIDENT
V. Valek (Brno/CZ)

PRE-PRE-MEETING PRESIDENT
P. Prassopoulos (Alexandroupolis/GR)

PAST MEETING PRESIDENT
G.H. Mostbeck (Vienna/AT)

MEMBERS AT LARGE
P. Prassopoulos (Alexandroupolis/GR)
J. Stoker (Amsterdam/NL)
M. Zins (Paris/FR)

LANGUAGE ABSTRACT EDITOR

S. Jackson (Plymouth/UK)

ESGAR 2015 MEETING PRESIDENT

Prof. Yves Menu
Saint Antoine Hospital
Pierre-et-Marie Curie University (Paris VI)
Assistance Publique-Hopitaux de Paris
157, Rue du Faubourg St-Antoine
FR – 75571 Paris, France

ESGAR 2015 PROGRAMME COMMITTEE

CHAIRMAN
F. Caseiro Alves (Coimbra/PT)

MEMBERS
R.G.H. Beets-Tan (Maastricht/NL)
S. Halligan (London/UK)
T. Helmberger (Munich/DE)
S. Jackson (Plymouth/UK)
A. Laghi (Latina/IT)
C. Matos (Brussels/BE)
L. Martí-Bonmatí (Valencia/ES)
Y. Menu (Paris/FR)
G.H. Mostbeck (Vienna/AT)
A. Palkó (Szeged/HU)
P. Prassopoulos (Alexandroupolis/GR)
J. Stoker (Amsterdam/NL)
V. Valek (Brno/CZ)
M. Zins (Paris/FR)

ESGAR 2015 LOCAL ORGANISING COMMITTEE

C. Aubé (Angers/FR)
S. Aufort (Castelnau Le Lez/FR)
M.F. Bellin (Le Kremlin Bicêtre/FR)
J. Cazejust (Paris/FR)
B. Dupas (Nantes/FR)
Y. Gandon (Rennes/FR)
B. Guiu (Dijon/FR)
C. Hoeffel (Reims/FR)
A. Luciani (Creteil/FR)
O. Lucidarme (Paris/FR)
F. Pilleul (Lyon/FR)
T. Pousse (La Rochefoucauld/FR)
P. Soyer (Paris/FR)
J.-P. Tasu (Poitiers/FR)
V. Vilgrain (Clichy/FR)
M. Zins (Paris/FR)

ABSTRACT REVIEWING PANEL

D. Akata (Ankara/TR)
O. Akhan (Ankara/TR)
C. Aubé (Angers/FR)
C. Ayuso (Barcelona/ES)
M.A. Bali (Brussels/BE)
C. Bartolozzi (Pisa/IT)
R.G.H. Beets-Tan (Maastricht/NL)
M.F. Bellin (Le Kremlin Bicêtre/FR)
P. Boraschi (Pisa/IT)
R. Bouzas (Vigo/ES)
G. Brancatelli (Palermo/IT)
D.J. Breen (Southampton/UK)
F. Caseiro Alves (Coimbra/PT)
C. Catalano (Rome/IT)
J. Cazejust (Paris/FR)
N. Courcoutsakis (Alexandroupolis/GR)
E. Delabrousse (Besancon/FR)
R.F. Dondelinger (Liège/BE)
M. D'Onofrio (Verona/IT)
B. Dupas (Nantes/FR)
N. Elmas (Izmir/TR)
H. Fenlon (Dublin/IE)
B. Fox (Plymouth/UK)
A.H. Freeman (Cambridge/UK)
A. Furlan (Pittsburgh, PA/US)
Y. Gandon (Rennes/FR)
S. Gourtsoyianni (London/UK)
L. Guimaraes (Porto/PT)
J.A. Guthrie (Leeds/UK)
S. Halligan (London/UK)
T. Helmberger (Munich/DE)
C. Hoeffel (Reims/FR)
P. Huppert (Darmstadt/DE)
F. Iafrate (Rome/IT)
S. Jackson (Plymouth/UK)
M. Karcaaltincaba (Ankara/TR)
S.H. Kim (Busan/KR)
H.-U. Laasch (Manchester/UK)
A. Laghi (Latina/IT)
J.S. Lameris (Amsterdam/NL)
E. Leen (London/UK)
P. Lefere (Roeselare/BE)
M. Lewin (Villejuif/FR)
D.J. Lomas (Cambridge/UK)
A. Luciani (Creteil/FR)
O. Lucidarme (Paris/FR)
M. Maas (Maastricht/NL)
F. Maccioni (Rome/IT)
R. Manfredi (Verona/IT)
T. Mang (Vienna/AT)
D. Marin (Durham, NC/US)
B. Marincek (Cleveland, OH/US)
L. Martí-Bonmatí (Valencia/ES)
D.F. Martin (Manchester/UK)
G.F. Maskell (Truro/UK)
C. Matos (Brussels/BE)
R.M. Mendelson (Perth, WA/AU)
Y. Menu (Paris/FR)
G. Morana (Treviso/IT)
M. Morrin (Dublin/IE)
G.H. Mostbeck (Vienna/AT)
E. Neri (Pisa/IT)
B. Op De Beeck (Edegem/BE)
A. Palkó (Szeged/HU)
P.L. Pereira (Heilbronn/DE)
F. Pilleul (Lyon/FR)
P. Pokieser (Vienna/AT)
T. Pousse (La Rochefoucauld/FR)
P. Prassopoulos (Alexandroupolis/GR)
M. Puckett (Torquay/UK)
J. Puig Domingo (Sabadell/ES)
C. Ridereau-Zins (Angers/FR)
M. Ronot (Clichy/FR)
L.H. Ros Mendoza (Zaragoza/ES)
E.J. Rummeny (Munich/DE)
W. Schima (Vienna/AT)
S. Schmidt-Kobbe (Lausanne/CH)
O. Seror (Bondy/FR)
P. Sidhu (London/UK)
S. Skehan (Dublin/IE)
S. Somers (Dundas, ON/CA)
M. Staunton (Cork/IE)
J. Stoker (Amsterdam/NL)
C. Stoupis (Maennedorf/CH)
Z. Tarjan (Stevenage/UK)
J.-P. Tasu (Poitiers/FR)
S.A. Taylor (London/UK)
S. Terraz (Geneva/CH)
C. Triantopoulou (Athens/GR)
V. Valek (Brno/CZ)
D. Vanbeckevoort (Leuven/BE)
V. Vilgrain (Clichy/FR)
M.-P. Vullierme (Clichy/FR)
D. Weishaupt (Zurich/CH)
S.D. Yarmenitis (Athens/GR)
C.J. Zech (Basel/CH)
M. Zins (Paris/FR)

POSTER JURY

D. Akata (Ankara/TR)
A.J. Aschoff (Kempten/DE)
M.A. Bali (Brussels/BE)
R.G.H. Beets-Tan (Maastricht/NL)
P. Boraschi (Pisa/IT)
R. Bouzas (Vigo/ES)
G. Brancatelli (Palermo/IT)
F. Caseiro Alves (Coimbra/PT)
J. Cazejust (Paris/FR)
N. Courcoutsakis (Alexandroupolis/GR)
L. Crocetti (Pisa/IT)
R.F. Dondelinger (Liège/BE)
M. D'Onofrio (Verona/IT)
N. Elmas (Izmir/TR)
H. Fenlon (Dublin/IE)
B. Fox (Plymouth/UK)
A.H. Freeman (Cambridge/UK)
A. Furlan (Pittsburgh, PA/US)
L. Guimaraes (Porto/PT)
J.A. Guthrie (Leeds/UK)
S. Halligan (London/UK)
T. Helmberger (Munich/DE)
F. Iafrate (Rome/IT)
S. Jackson (Plymouth/UK)
M. Karcaaltincaba (Ankara/TR)
C. Kay (Bradford/UK)
S.H. Kim (Busan/KR)
A. Laghi (Latina/IT)
J.S. Lameris (Amsterdam/NL)
T. Lauenstein (Essen/DE)
P. Lefere (Roeselare/BE)
M. Lewin (Villejuif/FR)
D.J. Lomas (Cambridge/UK)
O. Lucidarme (Paris/FR)
M. Maas (Maastricht/NL)
F. Maccioni (Rome/IT)
A. Madureira (Porto/PT)
D.E. Malone (Dublin/IE)
R. Manfredi (Verona/IT)
T. Mang (Vienna/AT)
D. Marin (Durham, NC/US)
B. Marincek (Cleveland, OH/US)
L. Martí-Bonmatí (Valencia/ES)
D.F. Martin (Manchester/UK)
C. Matos (Brussels/BE)
R.M. Mendelson (Perth, WA/AU)
Y. Menu (Paris/FR)
G. Morana (Treviso/IT)
M. Morrin (Dublin/IE)
G.H. Mostbeck (Vienna/AT)
E. Neri (Pisa/IT)
B. Op de Beeck (Edegem/BE)
A. Palkó (Szeged/HU)
N. Papanikolaou (Heraklion/GR)
P. Pokieser (Vienna/AT)
P. Prassopoulos (Alexandroupolis/GR)
M. Puckett (Torquay/UK)
C. Ridereau-Zins (Angers/FR)
G.A. Rollandi (Genoa/IT)
M. Ronot (Clichy/FR)
L.H. Ros Mendoza (Zaragoza/ES)
E.J. Rummeny (Munich/DE)
W. Schima (Vienna/AT)
S. Schmidt-Kobbe (Lausanne/CH)
S. Skehan (Dublin/IE)
S. Somers (Dundas, ON/CA)
M. Staunton (Cork/IE)
J. Stoker (Amsterdam/NL)
C. Stoupis (Maennedorf/CH)
Z. Tarjan (Stevenage/UK)
J.-P. Tasu (Poitiers/FR)
S.A. Taylor (London/UK)
C. Triantopoulou (Athens/GR)
V. Valek (Brno/CZ)
D. Vanbeckevoort (Leuven/BE)
J. Venancio (Lisbon/PT)
V. Vilgrain (Clichy/FR)
M.-P. Vullierme (Clichy/FR)
D. Weishaupt (Zurich/CH)
S.D. Yarmenitis (Athens/GR)
C.J. Zech (Basel/CH)
M. Zins (Paris/FR)


European Society
ESGAR
Gastrointestinal and Abdominal Radiology

11:00 - 12:30 **Leonard de Vinci**

Scientific Session SS 1

Diffuse liver disease I

SS 1.01

Inter-examination repeatability of hepatic shear-wave speed estimated by acoustic radiation force impulse imaging in adults with non-alcoholic fatty liver disease

E. Heba, M. Andre, T. Wolfson, M.S. Middleton, R. Loomba, C. Sirlin; San Diego, CA/US

Purpose: To assess inter-examination repeatability of hepatic shear-wave speed (SWS) estimated by acoustic radiation force impulse (ARFI) imaging in adults with known or suspected non-alcoholic fatty liver disease (NAFLD).

Material and Methods: In this prospective, IRB-approved, HIPAA-compliant study, subjects referred from the hepatology clinic underwent two ultrasound examinations (inter-examination time 5–10 min) using a 4C1 convex array transducer (Siemens Acuson™ S3000 scanner). Supine subjects were scanned intercostally. In each examination, 10–14 consecutive ARFI acquisitions were made in separate breath-holds in regions of interest placed in the right lobe of the liver > 2 cm below liver capsule. SWS values from each acquisition were recorded. Cohort means ± standard deviations (SDs) and medians were calculated. The intraclass correlation coefficient (ICC) between examinations was computed with 95% confidence intervals (CIs).

Results: 35 adult subjects were enrolled (17 M, 18 F; mean body mass index [BMI] 29.9 ± 4.8 kg/m^2; range 17.8–38.7 kg/m^2). For subjects in examination 1, the median SWS was 1.20 m/s, range 0.81–3.59 m/s with cohort mean coefficient of variation 0.21. In examination 2, cohort median was 1.18 m/s, range 1.25–3.57 m/s with mean coefficient of variation 0.19. ICC between examinations was 0.887 (0.788–0.941).

Conclusion: Quantitative ARFI shows high inter-examination repeatability with no statistically significant differences between sessions, supporting its use for evaluation of SWS as a quantitative imaging biomarker of liver fibrosis.

SS 1.02

Evaluating fibrosis in patients with non-alcoholic fatty steatohepatitis: non-invasive assessment with MR elastography

L. Costa-Silva, A. Lima, S. Ferolla, T.C.A. Ferrari; Belo Horizonte/BR

Purpose: To evaluate the diagnostic accuracy of magnetic resonance elastography (MRE) as a method to help in diagnosing fibrosis in patients with non-alcoholic steatohepatitis (NASH).

Material and Methods: This prospective study was institutional review board approved, and informed consent was obtained. It was conducted in 69 patients with NASH and in 13 healthy volunteers, with no history of liver disease/alcohol intake who underwent MRE. Liver stiffness was calculated. 20 patients were excluded. Patients with NASH had their biopsy within 24 months of MRE (median: 2.0 months; mean: 4.3 months). Independent-sample t-test and one-way ANOVA were used to compare stiffness with fibrosis noted on biopsy between NASH population and volunteers, and among subgroups classified by METAVIR score, respectively. The degree of fibrosis on biopsy and liver stiffness were correlated using Spearman's correlation coefficient.

Results: Analysis included 49 subjects (36 patients with NASH and 13 healthy volunteers). Mean stiffness for control group (2.30kPa±0.25kPa) was significantly lower than for NASH group (3.68kPa±1.67kPa)(p=0.05). MRE mean stiffness measurements increased according to the histologic stage (METAVIR) (p<0.001), with significant correlation between increasing fibrosis stage and stiffness values (r=0.77, p<0.001). On comparing all categorical biopsy result groups, there were significant differences between them (p<0.001).

Conclusion: MRE stiffness correlated with severity of fibrosis, which supports previous findings that MRE is a non-invasive and effective method for detection and assessment of liver fibrosis and may represent a valuable tool to finely discern hepatic fibrosis non-invasively.

SS 1.03

Effect of respiration on MR elastography-based wave quality, liver stiffness and inter-examination repeatability

K. Wang[1], T. Wolfson[1], M.S. Middleton[1], J. Chen[2], K. Glaser[2], M. Yin[2], P. Rossman[2], R. Ehman[2], C. Sirlin[1]; [1]San Diego, CA/US, [2]Rochester, NY/US

Purpose: To assess the effect of respiration on MR elastography (MRE)-based wave quality, liver stiffness, and inter-examination repeatability.

Material and Methods: After providing written informed consent, enrolled subjects underwent 2D- and 3D-MRE 3T examinations on inspiration, and expiration. Between examinations, volunteers were removed from and then repositioned on the scanner table. Regions of interest (ROIs) were placed on liver stiffness maps where wave signal-to-noise was high. ROI size was recorded as a metric of wave quality. Liver stiffness ROI values were documented. Intraclass correlation coefficients (ICC) were estimated as a metric of inter-examination repeatability for the two respiratory phases separately, and compared by bootstrap-based testing. The effects of respiration on ROI size and stiffness value were examined with linear mixed-effect models.

Results: Nine adult volunteers were enrolled in this study. For 2D-MRE, mean ROI size was smaller (2182 vs. 2552 pixels, p = 0.011) and mean stiffness larger (2.04 vs. 1.93 kPa, p = 0.008) on inspiration than expiration. For 3D-MRE, mean ROI sizes were similar (3056 vs. 3088 pixels, p = 0.20); mean stiffnesses were larger (1.54 vs. 1.44 kPa, p < 0.001) on inspiration than expiration. ICCs were not different at inspiration vs. expiration for either technique.

Conclusion: 2D-, but not 3D-MRE wave quality was worse on inspiration than expiration. Liver stiffness was greater on inspiration than expiration for 2D- and 3D-MRE. Inter-examination repeatability was unaffected by acquisition respiration phase.

SS 1.04

Optimal number of 2D shear wave elastography measurements for diagnosing liver fibrosis severity

V. Vilgrain[1], C. Cassinotto[2], V.Y.-F. Leung[3], G. Ferraioli[4], M. Ronot[1], M. Friedrich-Rust[5], S. Pol[6], A. Guibal[7], R. Zheng[8], S. Francque[9], P. Zoumpoulis[10], I. Sporea[11], M. Thiele[12], J. Trebicka[13], E. Herrmann[5]; [1]Clichy/FR, [2]Pessac/FR, [3]Shatin/HK, [4]Pavia/IT, [5]Frankfurt/DE, [6]Paris/FR, [7]Perpignan/FR, [8]Guangzhou/CN, [9]Edegem/BE, [10]Athens/GR, [11]Timisoara/RO, [12]Odense/DK, [13]Bonn/DE

Purpose: To determine the optimal number of 2D shear wave elastography (2D-SWE) measurements to assess liver fibrosis severity.

Material and Methods: 452 patients from 13 sites with 3 2D-SWE measurements and liver biopsy were retrospectively collected. AUROC was calculated for F1 vs. ≥F2, ≤F2 vs. ≥F3, and ≤F3 vs. F4 using the first, the first two, and the three SWE measurements. In addition, factors associated with increased variability were searched.

Results: Etiologies were chronic hepatitis C (HCV, n=108), hepatitis B (HBV, n=116), non-alcoholic fatty liver disease (NAFLD, n=69) or other liver diseases (n=159). 38.7% of the patients had minimal or no fibrosis, 15.9% had significant fibrosis, 11.9% had severe fibrosis and 33.4% had cirrhosis. 2D-SWE performance assessed by AUROC was not significantly higher using the median value of three measurements than to the first measurement (0.801 and 0.795 for F1 vs. ≥F2, 0.872 and 0.858 for ≤F2 vs. ≥F3, and 0.958 and 0.952 for ≤F3 vs. F4, respectively). On univariate analysis, the following factors were associated with increased variability: BMI, weight, prevalence of metabolic syndrome and etiology (p=0.00019, p=0.002, p=0.0056 and p=0.029, respectively). On multivariate analysis, only higher BMI was significantly associated with increased variability (p=0.0023).

Conclusion: 2D-SWE diagnostic performance for assessing fibrosis severity was similar using either the median of three measurements or the first measurement. Higher BMI was the most important factor for higher variability between different 2D-SWE measurements.

SS 1.05

Cirrhosis diagnosis using liver stiffness measurement: discrepancies between fibrotest, transient elastography and shear wave elastography

L. Bour, M. Monteanu, L. Chami, P. Ollo Flores, J. Prado Marques, I. Huynh-Charlier, T. Poynard, O. Lucidarme; Paris/FR

Purpose: To assess the added value of SWE and B mode ultrasound particularly in case of discrepancies between TE and FT for the F4 diagnosis.
Material and Methods: 215 patients with chronic hepatitis with reliable TE, FT, SWE measurement and B mode ultrasound evaluation were included. Cut-offs for F4 were: FT=0.74 and TE/SWE=14.5kPa. Six B mode ultrasound signs were considered for F4: splenomegaly, other vascular signs for portal hypertension, atrophy of segment IV, other liver dysmorphic conditions, ascites and HCC. Steatosis was also assessed using controlled attenuation parameter (CAP) with FS.
Results: In 184 (86%) cases, TE and FT were concordant for non-F4 (N=171 (80%)) or F4 (N=13 (6%)). Among the 31 discordant cases, F4 was staged with FT only in 20 (9%) patients (F4-FT group) and with TE only in 11 (5%) patients (F4-TE group). F4-FT group had a tendency to exhibit more steatosis than F4-TE with respective CAP values: 266dB and 210dB (p=0.18). Comparing F4-FT and F4-TE groups, respectively: the median numbers of B mode signs for cirrhosis were 2 and 1 (p=0.09); SWE staged F4 in 19% and 73% cases (p=0.04) and median SWE values were 9.3 and 17.4 kPa (p<0.01).
Conclusion: SWE found similar results than TE in case of discrepancies with FT while B mode signs for cirrhosis were in favor of FT results. Steatosis could lead to an underestimation of TE and SWE values.

SS 1.06

A comparison of 3T and 7T 2D adiabatic multi-echo spectroscopic imaging sequence with spherical k-space sampling 31P-MRSI of the liver in healthy volunteers

J.H. Runge[1], W.J.M. Van Der Kemp[2], D.W.J. Klomp[2], P.R. Luijten[2], A.J. Nederveen[1], J. Stoker[1]; [1]Amsterdam/NL, [2]Utrecht/NL

Purpose: Liver diseases are a major global health concern often requiring invasive assessment by needle biopsy, especially if the degree of inflammation needs to be ascertained. ^{31}P-MR spectroscopic imaging (MRSI) allows non-invasive probing of important liver metabolites that are linked with inflammatory processes. Recently, the adiabatic multi-echo spectroscopic imaging sequence with spherical k-space sampling (AMESING) was introduced at 7T, using localised T_2 information for signal-to-noise ratio (SNR) gain. If AMESING could be implemented for liver MRSI, its localised spectra could reduce the need for invasive biopsy for liver inflammatory status assessment.
Material and Methods: Ten male volunteers underwent 2D AMESING MRSI at 3T and 7T after a minimum four-hour fast. SNRs of FID-only and T_2-weighted sum spectra were calculated using maximum peak amplitudes and the SD of the noise. Statistical comparisons were performed with the Wilcoxon signed-rank test.
Results: For the first time, liver metabolites' T_2 values at 7T were measured: PE (55.6±3.5 ms), PC (51.2±2.3 ms), Pi (46.4±1.1 ms), GPE (44.0±0.8 ms), GPC (50.4±0.8 ms) and α-ATP (18.2±0.4 ms). In conjunction with higher field strength and improved coil setup, these allowed a total 3.2× SNR gain using T_2-weighted averaging at 7T compared to 3T FID only.
Conclusion: 7T AMESING MRSI can provide high-SNR spectral maps of liver metabolites including localised T_2 information which may benefit the diagnostic workup of liver disease and avoid biopsy.

SS 1.07

Simultaneous quantification of liver steatosis and iron overload with multiecho MR imaging in diffuse liver disorders, with histological validation

M. França[1], A. Alberich-Bayarri[2], L. Martí-Bonmatí[2], P. Oliveira[1], J.A. Oliveira[1], J.R. Vizcaino-Vasquez[1], F. Costa[1], G. Porto[1], H. Pessegueiro-Miranda[1]; [1]Porto/PT, [2]Valencia/ES

Purpose: To validate a quantitative MR imaging protocol for simultaneous assessment of liver fat and iron, as imaging biomarkers in different diffuse liver disorders.
Material and Methods: Consecutive patients who had clinically indicated liver biopsy were recruited. A 3.0T MR examination using a single breath-hold multiecho chemical shift (ME-CSh) GRE sequence (TR/TE=10/0.99, 1.69, 2.39, 3.09, 3.79, 4.49, 5.19, 5.89, 6.59, 7.29, 7.99, 8.69 ms) was performed. Proton density fat fraction (PDFF) and R2* quantification were calculated with own-developed software using magnitude and phase reconstruction, T1 bias and T2* correction. A ROI was placed within the biopsied liver segment. Biopsy was used as the gold standard for steatosis (0–3), iron deposits (0–4) grading, and inflammation and fibrosis (ISHAK score).
Results: 109 patients were enrolled. Median MR-calculated PDFF was 4.65% (IQR: 4.66%). PDFF showed significant differences between steatosis grades and correlated strongly with histology (R=0.817; p<0.001). Mean and median iron-related R2* were 106 Hz, 42 Hz (IQR 31 Hz). R2* measurements demonstrated significant differences between iron histological grading and a strong correlation with histology (R=0.718, p<0.001). Using analysis of variance and logistic regression, PDFF measurements were not confounded by the presence of iron, inflammation or fibrosis. ROC analysis estimated a PDFF cut-off value of 5.75% to diagnose liver steatosis (AUC=0.996).
Conclusion: MR-calculated PDFF and R2* may be used for measuring steatosis and iron deposits in different diffuse liver disorders with a single breath-hold ME-CSh-GRE sequence.

SS 1.08

Agreement between map- and region of interest-based hepatic proton density fat fraction estimation

P. Manning, C. Park, K. Wang, A. Gamst, T. Wolfson, R. Loomba, C. Sirlin; San Diego, CA/US

Purpose: To compare under varying scan conditions the agreement between parametric maps and standard region-of-interest (ROI)-based methods for hepatic proton density fat fraction (PDFF) estimation in non-alcoholic fatty liver disease (NAFLD).
Material and Methods: 31 adult patients with known or suspected NAFLD undergoing clinical gadoxetic acid-enhanced liver MRI were recruited for multi-echo magnitude-based MRI. Scans at flip angles of 10° and 50° were obtained before and after administration of gadoxetic acid over echo numbers ranging from two to six, giving 20 independent scan conditions per patient. For each scan variation, PDFF was calculated in two ways: 1) ROIs were placed onto each source image and mean signal intensities in ROIs entered into a previously validated matlab-based fitting algorithm and 2) Automated fitting was applied pixel by pixel to generate a "parametric map" of PDFF for the full hepatic region. Values from each method were recorded at corresponding locations. Agreement between ROI-based and map-based PDFF was examined using univariate regression analyses.
Results: Over all conditions tested, agreement was excellent between map- and ROI-based PDFF estimation. For the 20 scan variations, total mean (and range) for linear regression slope, intercept, and R^2 were, respectively: 1.000 (0.994-1.013), 0.114 (-0.022-0.274)%, and 1.000 (0.998-1.000).
Conclusion: Agreement between map- and ROI-based PDFF estimation is nearly perfect over a wide range of conditions. The approaches can be performed interchangeably in clinical and research applications.

SS 1.09

Intra-voxel incoherent motion diffusion-weighted (IVIM-DW) MR imaging in the evaluation of diffuse liver inflammation and fibrosis: correlation with liver biopsy

M. França[1], A. Alberich-Bayarri[2], L. Martí-Bonmatí[2], P. Oliveira[1], S. Guimaraes[1], J.R. Vizcaino-Vasquez[1], G. Porto[1], H. Pessegueiro-Miranda[1]; [1]Porto/PT, [2]Valencia/ES

Purpose: To investigate the reliability of IVIM-DW for assessing liver inflammation and fibrosis in diffuse liver disorders.
Material and Methods: 75 consecutive patients with diverse liver disorders and clinically indicated liver biopsy were recruited to perform a single-shot echo-planar 2D IVIM-DW sequence, respiratory-triggered, with 6 b values (0, 50, 200, 400, 600, 800 s/mm^2). Calculated parameters were measured from a mono (ADC)- and biexponential (D, D*, f) model equation expressing signal attenuation as a function of b values. Quantification of these parameters was performed with own-developed software, selecting an ROI in the biopsied liver segment. Biopsy was used as gold standard for grading liver inflammation and fibrosis (ISHAK score). Steatosis (0-3) and iron deposits (0-4) were also registered.
Results: For histological inflammation grading, patient's distribution was (grade/n): none/6; mild/56; moderate/13. Fibrosis grading distribution was: F0-F1/46; F2-F3/17; F4-F6/12. Also, 24 patients had liver steatosis while 36 had iron deposition. ADC values showed significant differences between grades of ISHAK necroinflammatory activity and fibrosis scores (p<0.05), with weak correlation with histological results. D* and f also showed significant differences (p<0.05) between ISHAK necroinflammatory grades. Only D values demonstrated significant differences between grades of steatosis or iron deposits.
Conclusion: IVIM-DW-derived parameters may stage liver inflammation and fibrosis in diffuse liver disorders, even in the presence of steatosis or iron deposits.

SS 1.10

Inter-reader reproducibility of hepatic proton density fat fraction estimation

J.C. Hooker, C. Park, S. Liao, T.-A. Le, M.S. Middleton, J. Chen, T. Wolfson, R. Loomba, C. Sirlin; San Diego, CA/US

Purpose: To investigate inter-reader reproducibility of hepatic proton density fat fraction (PDFF) estimated by magnitude-based magnetic resonance imaging (M-MRI) in adult non-alcoholic steatohepatitis (NASH).

Material and Methods: Adults with biopsy-proven NASH enrolled in this study underwent one (n = 5) or two different-day (n = 45) 3T liver M-MRI scans (GE, Milwaukee, WI). Blinded interpretation was conducted by four readers with varying experience. Readers placed three regions of interest (ROIs) centrally within each of the nine liver segments (27 ROIs total) on source images, avoiding artifact and major vasculature. ROIs were copied onto parametric PDFF maps from which PDFF values were recorded. Whole-liver and individual-segment PDFF values were summarized descriptively. Intraclass correlation coefficients (ICCs) were computed across readers for whole-liver and individual-segment PDFF estimations. 95% confidence intervals (CIs) were calculated using bootstrap-based methods to adjust for within-subject dependencies.

Results: Fifty adults were enrolled in this study (26 M, 24 F). Mean whole-liver PDFF was 16.8% and ranged from 4.8 to 33.4% depending on the reader. Individual-segment PDFF ranged from 2.9 to 37.4% depending on the reader and segment. Whole-liver ICC was 0.965 (0.952, 0.975). Individual-segment ICCs ranged from 0.933 (0.889–0.958) for segment 1–0.983 (0.973–0.987) for segment 8. Mean individual-segment ICC was 0.964 with a SD of 0.018.

Conclusion: Whole-liver and individual-segment PDFF estimation by M-MRI showed high inter-reader reproducibility, despite variable experience of readers.

11:00 - 12:30 **Goethe**

Scientific Session SS 2
The small bowel and beyond

SS 2.01

Intra- and inter-observer reproducibility of MR enterography indexes for the assessment of disease activity in Crohn's disease using central readers

J. Rimola[1], S.A. Taylor[2], C. Santillan[3], K. Horsthuis[4], G. Zou[5], J. Panés[1], I. Ordas[1], W. Sandborn[3], J. Stoker[4], L. Stitt[5], K. Reena[5], G. D'Haens[4], M.K. Vandervoort[5], B.G. Feagan[5], B.G. Levesque[5]; [1]Barcelona/ES, [2]London/UK, [3]San Diego, CA/US, [4]Amsterdam/NL, [5]London, ON/CA

Purpose: Reproducibility is a critical property of magnetic resonance enterography (MRE) Crohn's disease activity indices if they are to be used in clinical trials. We evaluated the reproducibility of two MRE disease activity instruments, the MaRIA and London indices, when centrally read in a multi-center trial setting.

Material and Methods: Four central readers from Europe and North America reviewed 50 MRE of patients with a spectrum of Crohn's disease activity and location. Readers assessed the MaRIA and London indices, pre-specified individual MRE findings, and a global rating of severity based on a visual analogue scale (VAS). Intraclass correlation coefficients (ICCs) for intra- and inter-rater agreement were calculated for each assessment.

Results: Intra-rater ICCs (95% confidence intervals) for the MaRIA, London, London Extended indices and the VAS were 0.89 (0.84–0.91), 0.84 (0.76–0.88), 0.81 (0.71–0.85) and 0.86 (0.81–0.90). Corresponding inter-rater ICCs were 0.71 (0.61–0.77), 0.50 (0.32–0.62), 0.56 (0.40–0.64), and 0.71 (0.62–0.77). The correlation between each reader's VAS and the MaRIA, London, and London Extended indices were 0.79 (0.71–0.85), 0.68 (0.58– 0.77) and 0.67 (0.58–0.76), respectively.

Conclusion: There was "almost perfect" intra-rater reproducibility of centrally read MaRIA and London indices. Inter-rater agreement was "substantial" for the MaRIA and "moderate" for the London indices. The MaRIA index appears to have the best operating characteristics.

SS 2.02

Changes in segmental small bowel motility measured by MRI can detect early response to anti-TNF therapy

A. Plumb, A. Menys, G. Bhatnagar, D. Prezzi, J. Makanyanga, E. Russo, T. Orchard, S.A. Taylor; London/UK

Purpose: To determine if small bowel (SB) motility measured by MRI improves in response to anti-TNF therapy for Crohn's disease (CD).

Material and Methods: Ethical permission was waived. 27 patients underwent cine MRI pre- and post-treatment with anti-TNFs (>6 months of treatment; "late imaging" group). 11 additional patients were imaged at baseline and after 12–14 weeks of treatment ("early imaging" group). Response to anti-TNFs was defined using a composite measure of all clinical data for the "late imaging" group, and using the Harvey–Bradshaw Index for the "early imaging" group. Changes in SB motility were quantified using a validated optic flow algorithm and compared between responders and non-responders using the Mann–Whitney U test and receiver operating characteristic (ROC) curves.

Results: Anti-TNF responders had significantly greater improvements in motility (mean change=136% of baseline) than non-responders (mean change=106%, $p<0.001$). An improvement in MRI-measured motility was 92% sensitive (identifying 22/24 responders) and 79% specific (identifying 11/14 non-responders) for response to anti-TNFs. This was true for both the "early imaging" (Sn: 86%; Sp: 100%) and "late imaging" groups (Sn: 94%; Sp: 70%). The area under the ROC curve for changes in motility was 83% (95% CI: 67–98%).

Conclusion: Increased MRI-measured SB motility is highly sensitive and moderately specific for response to anti-TNF therapy for Crohn's disease, even as early as 12–14 weeks. These data suggest that MRI may permit early identification of response/non-response to anti-TNFs, allowing personalized treatment regimes.

SS 2.03

MR enterography in patients with known Crohn's disease: prediction of patency capsule retention

M.-M. Amitai, E. Klang, N. Rozendorn, U. Kopylov, S. Ben-Horin, A. Eliakim; Ramat Gan/IL

Purpose: The main complication of capsule endoscopy (CE) in Crohn's disease (CD) is capsule retention. Evaluation of small bowel patency is recommended before CE using cross-sectional imaging or PC. Our aim was to evaluate the ability of MRE to predict PC retention, and to identify its most predictive imaging features.
Material and Methods: 57 patients underwent MRE followed by PC. A radiologist gave a positive or negative prediction for PC retention based on the MRE. Diseased segments (DS) on the MRE were evaluated for: number of DS, stenosis and prestenotic dilatations, maximal stenosis length, maximal wall thickness. Association of these imaging features with PC retention was evaluated.
Results: The radiologist gave a positive prediction of PC retention in 30/57 patients. PC retention occurred in 13/57 patients and was predicted by MRE in 12/13 cases. The sensitivity, specificity, PPV and NPV for prediction of PC retention were 92.3%, 59%, 40% and 96.3%, respectively. DS were found in 45/57 patients. The mean maximal stenosis length (9.7 cm vs. 7 cm, p=0.04) and the mean number of prestenotic dilatations (1.9 vs. 1, p=0.02) were significantly associated with PC retention.
Conclusion: MRE has high NPV and sensitivity but low PPV and specificity for PC retention. When capsule retention is suggested by MRE, PC should be performed before CE. Maximal stenosis length and number of prestenotic dilatations were significantly associated with PC retention.

SS 2.04

The role of diffusion-weighted MRI in assessment of inflammatory bowel disease

C. Schmid-Tannwald[1], C. Schmid-Tannwald[1], J.F. Morelli[2], B. Ertl-Wagner[1], M.F. Reiser[1], C. Rist[1]; [1]Munich/DE, [2]Baltimore, MD/US

Purpose: To evaluate the role of diffusion-weighted MRI (DW-MRI) in detecting and differentiating acute from chronic bowel inflammation in patients with Crohn's disease.
Material and Methods: MR enteroclysis (MRE) examinations with DW-MRI were reviewed from 24 patients with histologically proven Crohn's disease. Segments of bowel were evaluated for acute and chronic inflammation in three different reviews of the MRE images—T2w alone, T2w+DWI and T2+CET1w. Mean ADC values of normal bowel segments, as well as bowel segments with acute and chronic inflammation were calculated and compared.
Results: 144 bowel segments in total were reviewed. Inflammation was present in 46 segments. Acute inflammation was present in 32 segments, chronic inflammation in 14. 98 bowel segments showed no inflammatory activity. Sensitivity for differentiation between normal and inflamed bowel segments was 0.6, 0.67 and 0.86 on T2w, T2w+DWI and T2+CET1w datasets, respectively. Sensitivity for differentiation between acute and chronically inflamed bowel segments was 0.85, 0.91 and 0.96, respectively. The mean ADC value of normal bowel (2.18 +/- 0.37 x 10-3 mm^2/s) was statistically significantly greater than the mean of inflamed bowel segments ($p<0.001$). The mean ADC value of acutely inflamed bowel segments was statistically significantly lower than that of chronically inflamed bowel segments (1.09+/-0.18 vs. 1.55 +/-0.21 x 10-3 mm^2/s) ($p<0.001$).
Conclusion: DW-MRI improves detection and differentiation of acute versus chronic inflammatory changes of the bowel in patients with Crohn's disease compared to T2w-images alone.

SS 2.05

MRI as a potential "one-stop-shop" staging tool for colon cancer: can it replace CT for local staging?

M.J. Lahaye[1], D.M.J. Lambregts[1], E. Nerad[2], G.L. Beets[1], R.G.H. Beets-Tan[1]; [1]Maastricht/NL, [2]Eindhoven/NL

Purpose: CT is routinely used for staging of colon cancer. In the revised Dutch guidelines, MRI is recommended for liver staging because of its superiority to CT. If MRI proves valuable to also stage the local tumor, it could be used as a 'one-stop-shop' tool with the added benefit of avoiding radiation and nephrotoxic contrasts. Aim of this prospective study was to evaluate the performance of MRI for local staging of colon cancer.
Material and Methods: In an ongoing pilot study, we included 26 patients with colon cancer, undergoing MRI (1.5T) including T2TSE, BTFE and DWI sequences of the whole abdomen. Two experienced readers independently evaluated the examinations and scored; tumor location, T-stage (T1-2 vs. T3-4), nearby fascia/serosal involvement and N-stage (N0/N+). Histopathology was the reference standard.
Results: Histology found 18/26 T3-4 tumors, 6/26 fascia involvement and 9/26 N+ tumors. Both readers correctly identified all tumors with MRI. For assessment of T-stage, fascia involvement and N-stage, Reader 1 had a sensitivity/specificity of 93%/64%, 100%/79% and 67%/82%. For Reader 2, results were 88%/66%, 83%/75% and 64%/86%. Interobserver agreement was moderate to almost perfect (κ0.43, 0.44 and 0.84).
Conclusion: Our pilot data suggest that MRI has a high sensitivity for detecting colon tumors and most important prognostic factors. MRI may thus replace CT in staging colon cancer. If the FOXTROT trial will prove that neoadjuvant chemotherapy for locally advanced colon tumor will affect outcome, MRI has potential to accurately identify high-risk patients.

SS 2.06

withdrawn by the authors

SS 2.07

MR of the small bowel at 1.5T and 3T: a single patient comparison

L. Filipe, A. Gaber, L. Monnier-Cholley, L. Arrivé, Y. Menu; Paris/FR

Purpose: This study is a systematic comparison of 3T and 1.5T examinations of the small bowel performed in the same patient.
Material and Methods: 107 consecutive patients who underwent both 3T and 1.5T MR of the small bowel were selected. Independent experts established the standard, determined comparability and eliminated 22 cases with significant interval events hampering comparison. The population comprised mostly patients with Crohn's disease (74/85). Two blinded readers reviewed in consensus examinations in separate sessions and graded (1–5) the features of small bowel disease (mural and trans-mural lesions, obstruction, mesenteric lesions) and the level of artefacts. McNemar' test was used to discriminate differences within paired values.
Results: There were no significant differences for the evaluation of wall thickening, stenosis, obstruction, mesenteric abnormalities, despite large sample size. Only trends were observed. Unlike previous studies, ulcers and fistulae were identified similarly. Mucosal enhancement was significantly better appreciated at 1.5T.
Conclusion: Unlike previous study showing a benefit for the detection of ulcers, there was no clear advantage of 3T over 1.5T for small bowel evaluation in our larger population. Conversely, 1.5T proved to be more reliable for the evaluation of mucosal enhancement. This was in part related to both a higher level of artefacts and a decrease of contrast to noise ratio on T1 imaging. Study limitations include delay between examinations, absence of pathological gold standard, and non-random order of tests.

SS 2.08

PET/MRI enterography: feasibility and first results for the evaluation of intestinal inflammation and malignancies

L. Lenga[1], K. Beiderwellen[1], B. Gomez[1], P. Heusch[2], L. Umutlu[1], J. Langhorst[1], T. Lauenstein[1]; [1]Essen/DE, [2]Dusseldorf/DE

Purpose: To implement integrated PET/MR enterography for a multimodal assessment of intestinal pathologies.
Material and Methods: 21 patients with bowel malignancies, Crohn's disease or fever of unknown origin (male: n=14, female: n=5, age: 57±13 years) underwent PET/MR enterography (Biograph mMR, Siemens Healthcare, Erlangen, Germany) with either [^{18}F]FDG (n=12) or [^{68}Ga]-DOTATOC (n=9). For small bowel distension, a contrast solution (1500cc of mannitol and locust bean gum) was ingested. The following sequences were acquired: a) coronal TrueFISP; b) coronal T2w HASTE with fat saturation; c) coronal T1w 3D VIBE pre- and post-gadolinium; d) axial and coronal T1w 2D FLASH post-gadolinium. Datasets were reviewed with regard to co-registration of anatomical structures based on a 3-point scale (3: good co-registration, 2: slight misregistration, 1: significant misregistration) and image quality using a 4-point scale (1: non-diagnostic –4: excellent quality). Furthermore, visualization of intestinal and extraintestinal pathologies was described.
Results: PET/MR enterography was well tolerated by all patients. High overall image quality was achieved (mean score MRI: 3.2, PET: 2.3) with good co-registration of PET and MRI (mean: 2.61-2.95). PET/MR enterography allowed for an excellent visualization of intestinal pathologies including inflammatory and tumor manifestations. Furthermore, lymph node metastases were depicted in two patients.
Conclusion: PET/MR enterography is technically feasible and offers good co-registration of bowel structures. This new method enables a multimodal assessment of bowel lesions in malignant and inflammatory disease.

SS 2.09
The role of gadolinium in MR evaluation of perianal fistulas
G. Brahm, B. Sreeharsha, S. Thipphavong, K.S. Jhaveri; Toronto, ON/CA

Purpose: To retrospectively assess the utility of gadolinium when evaluating perianal fistulas in Crohn's disease on MRI.
Material and Methods: MR examinations of 98 consecutive patients with Crohn's disease were evaluated by two abdominal radiologists. First read included pre-gad T2W (axial and coronal) and STIR followed by second read with post-gadolinium dynamic enhanced axial images, noting the fistula opening, type, complexity and any abscess. Individual reads were compared to a consensus read and a statistician was used for analysis utilizing the McNemar test.
Results: 144 fistulas were present in 98 cases. Pre-gad images accurately detected 246 of 288 tracts (85%). Post-gad images improved detection in 14/288 tracts (p value < 0.001). There was mild improvement in assessing the internal opening with gadolinium (5/246 or 2%), however not statistically significant (p value = 0.063). There was no improved accuracy in determining the type or detection of abscesses with gadolinium. In determining the complexity, gadolinium provided improved accuracy in 9 % (17 of 196) (p < 0.001). This was most significant in fistulas with multiple tracts (accuracy improved by 16 %). There was no significant improvement in accuracy with simple (p value = 1.00) and single-branched fistulas (p value = 0.25).
Conclusion: Gadolinium-enhanced images provided no significant additional benefit in determining the internal opening, type of fistula or the detection of abscesses. Gadolinium-enhanced images do however provide improved accuracy in characterizing the complexity of perianal fistulas.

11:00 - 12:30 **Darwin 3**

Scientific Session SS 3
Mesentery, appendix and colon

SS 3.01
Is there a connection between mesenteric panniculitis and lymphoma?
V. Khasminsky, E. Atar, G. Bachar; Petah Tikva/IL

Purpose: Mesenteric panniculitis has long been associated with malignancy and lymphomas especially. Our aim was to elucidate the connection between mesenteric panniculitis and malignancy by establishing its prevalence among patients with known diagnosis of lymphoma and comparing it to the prevalence in general population and in a matched control group.
Material and Methods: We retrospectively evaluated CT and PET-CT examinations of 166 patients with established diagnosis of non-Hodgkin lymphoma. Mesenteric panniculitis was identified on the basis of five CT imaging signs described in literature. To distinguish mesenteric panniculitis from the involvement of mesentery by lymphoma, we relied on PET-CT evidence of FDG uptake in the mesenterium. For each lymphoma patient, we also chose two control subjects matched for age, gender and examination time period, for a total of 330 subjects.
Results: Mesenteric panniculitis was identified in 3 patients out of 166 in the lymphoma group (prevalence 1.8%) and in 7 patients out of 330 in the control group (prevalence 2.1%). None of the patients from the control group developed malignancy during the follow-up of 24 to 60 months.
Conclusion: The prevalence of mesenteric panniculitis among patients with NHL was similar to its prevalence in the control group and in general population. This runs contrary to the proposition that mesenteric panniculitis is associated with lymphomas. This obviates the need to recommend searching for malignancy in case of incidental discovery of mesenteric panniculitis.

SS 3.02
In vivo study of microcirculation in a murine model of pseudomyxoma peritonei using the intravoxel incoherent motion method for the assessment of antiangiogenic drugs
A. Dohan[1], C. Eveno[1], C. Pimpie[1], P. Bonnin[1], F. Duchat[2], M. Pocard[1], P. Soyer[1]; [1]Paris/FR, [2]Dijon/FR

Purpose: Pseudomyxoma peritonei (PMP) is characterized by mucinous ascites confined to the peritoneal cavity. The aim of this study was to monitor an antiangiogenic treatment in a murine model with the intravoxel incoherent motion (IVIM)-derived parameters obtained by MRI at 1.5T.
Material and Methods: Twenty nude mice orthotopically xenografted with human PMP had T2-spin echo MRI 8 weeks after the graft. All mice underwent diffusion-weighted images with 13 b values to fit the IVIM-derived parameters, namely, the pure-diffusion coefficient and the perfusion-related diffusion fraction and coefficient. Fitting was obtained using an automated MATLAB script. Ten mice were treated with Sorafenib (60mg/kg/j), and ten untreated mice were used as controls. MRI acquisitions were repeated 1 week and 4 weeks after the beginning of the treatment. Then, mice were killed and tumor angiogenesis was quantified with blood analysis and histological markers.
Results: The pure-diffusion coefficient and the perfusion fraction were not different between the 2 groups at the different times ($p<0.05$). Perfusion-related diffusion coefficient decreased at the first week in the treated group ($p=0.5$) and became significantly lower at the fourth week ($p<0.05$). It remained stable in the control group. Histological markers confirmed a greater vessel density in the tumor compared to treated group ($p<0.05$). Serum levels of VEGF, PlGF, and TGF-β were lower in the treated group ($p<0.01$).
Conclusion: IVIM parameters are useful to monitor the effect of an antiangiogenic drug in a murine model of PMP.

SS 3.03
Diagnosis of pseudomyxoma peritonei with MR imaging
A. Dohan, R. Dautry, Y. Guerrache, C. Eveno, M. Boudiaf, M. Pocard, P. Soyer; Paris/FR

Purpose: To identify imaging criteria that help to discriminate between pseudomyxoma peritonei (PMP) and peritoneal carcinomatosis (PC) from other origins on magnetic resonance (MR) imaging using a retrospective analysis.
Material and Methods: The preoperative MR imaging examinations of 45 consecutive patients with PMP were compared to those observed in 98 patients with PC from various origins (colorectal, n=45; ovarian, n=45; mesothelioma peritonei, n=8). Two abdominal radiologists blinded to the final diagnosis evaluated MR imaging examinations for the presence of 10 morphological and

functional criteria using a standardized form. Sensitivity, specificity and accuracy were calculated for each criterion. ROC curve analysis was used to determine the combination of criteria that yielded best accuracy.
Results: Presence of appendiceal mucocele had a sensitivity of 15% and a specificity of 100%. Presence of more than 10 mucinous lesions with a thick wall (MLTW) (greater than 4 mm) had a sensitivity of 85% and a specificity of 60%. A jelly/water ratio>0.5 had a sensitivity of 80% and a specificity of 80%. Presence of the butterfly sign had a specificity of 100% and a sensitivity of 65%. ROC analysis showed that the presence of 3 signs among the following four (appendiceal mucocele, jelly/water ratio>0.5, >10 MLTW, butterfly sign) yielded best degrees of accuracy (AUC=0.82).
Conclusion: A combination of three criteria was very accurate for the diagnosis of PMP and helps discriminate between PMP and PC. The combination of these criteria may reduce misdiagnoses.

SS 3.04
CT findings of intra-abdominal complications secondary to ventriculoperitoneal shunt
J.-J. Chung, E.-S. Cho, J.-S. Yu, J.H. Kim; Seoul/KR

Purpose: To evaluate the abdominopelvic (AP) CT findings of the intra-abdominal complications secondary to ventriculoperitoneal (VP) shunts for hydrocephalus.
Material and Methods: The CT images of 76 patients (M:F=34:42) who underwent VP shunt placement and AP CT because of shunt-related abdominal symptoms were reviewed retrospectively. Various CT images were analyzed with regard to the location of the shunting catheter tip; site, size, wall, and septa of localized fluid collection; peritoneal thickening; omentomesentery infiltration; abscess; bowel perforation; abdominal wall infiltration; and thickening of the catheter track wall.
Results: A total of 84 VP shunting catheters were introduced in 76 patients: 68 patients had a unilateral catheter inserted and 8 patients had bilateral catheters inserted. The mean period between the last VP shunting operation and CT was 11.1 months (range 1 week–115 months). Nineteen patients (25.0%) were pathologically diagnosed with VP shunt-related complications: 13 cases (17.1%) of shunt infection, 8 cases (10.5%) of CSF pseudocyst, 5 cases (6.6%) of abdominal abscess, 4 cases (5.3%) of infected fluid collection, and one case (1.3%) of bowel perforation. Microorganisms were cultured from the tip of the shunting catheter or peritoneal fluid in 14 patients (18.4%).
Conclusion: On AP CT, various intra-abdominal complications secondary to VP shunt were shown, of which shunt infection was the most common, followed by CSF pseudocyst, abdominal abscess, and infected fluid collection.

SS 3.05
Predicting underlying masses in appendiceal mucoceles
S. Chaudhry, A. Mcnaught, R. Vajpeyi, R. Chetty, S. Ghai; Toronto, ON/CA

Purpose: Appendiceal mucocele is a well-recognized but uncommon radiological entity. However, the term mucocele is non-specific and can indicate a build-up of normal secretions due to obstruction (benign/inflammatory mucocele), or occur in the presence of neoplasms (mucinous cystadenoma/cystadenocarcinoma). The purpose of this study was to determine whether dilation of the appendix not extending to its base/origin is a predictor for underlying neoplasm rather than inflammatory etiology. This may aid in limiting the number of repeat procedures needed and the risk of inadvertent spilling of neoplastic cells.
Material and Methods: Following institutional IRB, radiology reports between 2012 and 2013 containing the term “mucocele” were identified. The corresponding CT images were reviewed and correlated with pathology reports in patients who had undergone surgery. In particular, presence or absence of appendiceal dilation to its base was assessed.
Results: A total of 21 cases met the criteria. All 15 cases, where the base of the appendix was not dilated, but the distention was limited to the distal appendix, were mucinous neoplasms on histopathology. However, 3/18 mucinous neoplasms had dilation to the appendiceal base. All 3/3 benign mucoceles/inflammatory etiology also had dilation to the appendiceal base.
Conclusion: Our study demonstrated that appendiceal dilation not extending to the base is a strong predictor of an underlying mucinous neoplasm (cystadenoma/cystadenocarcinoma), while dilation extending to the base/origin of the appendix can be seen due to inflammation or underlying neoplasm.

SS 3.06
Inconclusive cases of 2-mSv CT in adolescents and young adults with suspected appendicitis: advantages of additional review of thin sections using multiplanar sliding-slab averaging technique
Y.J. Lee[1], B. Kim[1], Y. Ko[1], K.E. Cho[1], S.S. Hong[2], D.H. Kim[1], H. Song[2], K.H. Lee[1]; [1]Seongnam-Si, Gyeonggi-do/KR, [2]Seoul/KR

Purpose: To assess the advantages of additional multiplanar sliding-slab averaging (SSA) review of 2-mm-thick (thin) sections over stack review of 5-mm-thick (thick) sections in inconclusive 2-mSv CT cases in adolescents and young adults with suspected appendicitis.
Material and Methods: IRB approved this retrospective study and waived informed consent requirement. We included 149 patients (mean age, 28.0 years; 61 males; 88 females) in whom original CT reports were inconclusive for diagnosis of appendicitis. Five radiologists independently reviewed the thick sections in stack mode and then the thin sections using SSA. In each review, they rated the likelihood of appendicitis and the appendix visualization in 5- and 3-point Likert scales, respectively. Diagnostic performance and confidence were compared between two reviews using receiver operating characteristic (ROC) analysis, McNemar tests, and Wilcoxon signed rank tests.
Results: The pooled area under the ROC curve (AUC) was 0.90 and 0.93 for stack and SSA reviews, respectively, (90% CI for difference, [0.002, 0.06], P = 0.087). The differences were not always statistically significant, but SSA review tended to increase individual readers' AUC (range, 0.86–0.93 vs. 0.87–0.97, stack vs. SSA review); improve confidence in diagnosing (mean score, 3.6–4.7 vs. 3.9–4.7) or ruling out (1.6–2.1 vs. 1.5–1.9) appendicitis; reduce indeterminate interpretations (0%–15% vs. 0%–11%); and enhance normal appendix visualization (1.1–1.7 vs. 1.1–1.9).
Conclusion: Additional SSA review of thin sections tends to improve diagnostic performance and confidence when conventional stack review of thick sections is inconclusive.

SS 3.07
Periportal edema caused by acute appendicitis
I.A. Tamir, O. Benjaminov, E. Atar, G. Bachar; Petah Tikva/IL

Purpose: Periportal edema is a possible sequel of a wide range of diseases. Although non-specific, the identification of periportal edema by MDCT examination brings the radiologist for a thorough quest after the possible cause. All the relevant pivotal textbooks and atlases give a long differential diagnosis list of all the possible causes of periportal edema. Acute appendicitis is not included as a possible cause of periportal edema.
Material and Methods: The aim of this study is to determine the interrelated connection between periportal edema and acute appendicitis. We consecutively and chronologically studied 181 patients, from 19 to 92 years old, between January 2010 and August 2013, who were diagnosed with acute appendicitis. All the studies were evaluated by 2 senior radiologists who approved the imagistic diagnosis of appendicitis with the presence or absence of periportal edema.
Results: Periportal edema was identified in 29 patients of 181 studied (16 %). Although the difference was statistically non-significant, the mean age of periportal edematous group stood on 42±18 compared with the control group 48±16 (P=0.298). We additionally found increased frequency with complicated cases as gangrenous appendicitis (n=13), periappendicular abscess (n=5) and peritonitis (n=2).
Conclusion: Periportal edema is a possible sequel of acute appendicitis, especially with its complicated forms or with the younger adult population. Acute appendicitis should be included in the differential diagnosis as a possible cause of periportal edema.

SS 3.08
withdrawn by the authors

SS 3.09

Assessment of imaging criteria to predict stage III colon cancer using multidetector computed tomography

E. Rollvén, L. Blomqvist, M. Abraham Nordling, T. Holm; Stockholm/SE

Purpose: To study different imaging criteria for prediction of stage III disease in colon cancer using multidetector computed tomography (MDCT).

Material and Methods: From 483 consecutive patients who underwent elective primary resection during 2008-2011, a cohort of 119 patients who had performed preoperative MDCT was identified. MDCT's were reviewed with assessment of the number of lymph nodes, their anatomical distribution, size, size ratio, internal heterogeneity, presence of irregular outer border and contrast enhancement. Sensitivity, specificity, PPV and NPV for each studied image criteria for prediction of stage III disease were calculated.

Results: Of 119 patients, 80 were stage I-II and 39 were stage III. Of the studied criteria, internal heterogeneity in at least one lymph node resulted in the best performance with a sensitivity and specificity of 79 and 84%. Presence of irregular outer border resulted in a sensitivity and specificity of 59 and 81%. If both internal heterogeneity and/or irregular outer border was used as a criterion, this resulted in a sensitivity and specificity of 85% and 75%. None of the size criteria used was predictive for stage III disease.

Conclusion: When performing preoperative MDCT in patients with colon cancer, the imaging criteria that allow best prediction of stage III disease are either presence of at least one lymph node with internal heterogeneity or internal heterogeneity and/or irregular outer border. These criteria have to be validated in a prospective study.

SS 3.10

Paraduodenal hernia: clinical and imaging findings in 5 patients with emphasis on multi-detector CT findings

I.Y. Kim, Y.T. Kim, H.C. Shin; Cheonan/KR

Purpose: To review the clinical and radiologic features of paraduodenal hernia and to derive useful radiographic and multi-detector CT (MDCT) findings to assist in diagnosis.

Material and Methods: Retrospective review of medical records revealed 5 patients with surgically proven paraduodenal hernia (from September 2006 to September 2011) who had 5 MDCT scans and one small-bowel follow-through (SBFT) images and all abdominal plain film. Two radiologists reviewed those images with consensus and classified as right paraduodenal hernia and left paraduodenal hernia.

Results: There were 3 cases of left paraduodenal hernia and 2 cases of right paraduodenal hernia. Male and female sex ratio was 4:1. Mean age is 52.2 (age range 30–71). CT signs common to both types of paraduodenal hernia included evidence of small-bowel obstruction; clustering of small bowel; stretched, displaced, crowed, and engorged mesenteric vessels; and displacement of other bowel segments. Left-sided paraduodenal hernias demonstrated a saclike mass of small-bowel loops interposed between the stomach and pancreatic tail. All paraduodenal hernias were diagnosed confidently at retrospective review of CT and SBFT findings. Abdomen plain film suggestively diagnosed at retrospective review of paraduodenal hernia with 60% of accuracy.

Conclusion: Paraduodenal hernias are an important and underdiagnosed condition. Left-sided paraduodenal hernias are more common and accurate diagnosis is important for proper treatment. MDCT may allow confident diagnosis in all patients; however, abdomen plain film and SBFT have its role in the diagnosis.

11:00 - 12:30 **Darwin 4**

Scientific Session SS 4

Focal liver lesions on non-cirrhotic liver

SS 4.01

How accurate is [18F]-FDG PET/MRI for the depiction of liver lesions?

L. Lenga[1], K. Beiderwellen[1], V. Ruhlmann[1], P. Heusch[2], L. Geraldo[1], L. Umutlu[1], T. Lauenstein[1]; [1]Essen/DE, [2]Dusseldorf/DE

Purpose: To compare the diagnostic accuracy of [^{18}F]FDG-PET/CT with PET/MRI for the detection of hepatic tumors.

Material and Methods: 32 patients with different malignancies underwent [18F]FDG-PET/CT (Biograph mCT 128, Siemens Healthcare, Erlangen, Germany) and subsequent PET/MRI of the liver (Biograph mMR, Siemens Healthcare, Erlangen, Germany). Two readers assessed images concerning lesion characterization (benign, indeterminate, malignant), conspicuity (4-point scale) and diagnostic confidence (3-point scale). An imaging follow-up of more than 75 days (185±92 days) and/or histopathological specimen served as standard of reference. Sensitivity, specificity, positive predictive value (PPV) and negative predictive value (NPV) were calculated for both modalities. Accuracy was determined by calculating the area under the receiver operating characteristic (ROC) curve. Values of conspicuity and diagnostic confidence were compared using Wilcoxon-signed rank test.

Results: The standard of reference revealed 113 liver lesions in 26 patients (malignant: n=45; benign: n=68). For PET/MRI a higher accuracy (PET/CT: 82.4%; PET/MRI: 96.1%; p<0.001) as well as sensitivity (67.8% vs. 92.2%, p<0.01) and NPV (82.0% vs. 95.1%, p<0.05) was observed. PET/MRI offered higher lesion conspicuity (PET/CT: 2.0±1.1 [median: 2; range 0–3]; PET/MRI: 2.8±0.5 [median: 3; range 0–3]; p<0.001) and diagnostic confidence (PET/CT: 2.0±0.8 [median: 2; range: 1–3]; PET/MRI 2.6±0.6 [median: 3; range: 1–3]; p<0.001).

Conclusion: PET/MRI offers higher diagnostic accuracy compared to PET/CT for the detection of hepatic lesions and can be considered a powerful alternative method for liver imaging.

SS 4.02

Prediction of therapeutic response after FOLFOX and FOLFIRI treatment in patients with liver metastasis from colorectal cancer using computerized CT texture analysis

S.J. Ahn, J.H. Kim, S.J. Park, J.K. Han, B.I. Choi; Seoul/KR

Purpose: To determine whether the pretreatment CT texture analysis of hepatic metastasis from colorectal cancer is predictive of response after cytotoxic chemotherapy.

Material and Methods: The study included 145 patients with liver metastasis from colorectal cancer who underwent CT scan before and after forth cycles of cytotoxic chemotherapy using FOLFOX and FOLFIRI. Computerized CT texture of hepatic metastasis was quantified using pretreatment CT in both 2D and 3D analysis. We analyzed an independent predictor for response using multivariate logistic regression analysis. We also compared texture analysis between each CT machines. Response evaluation based on RECIST criteria. For statistical analysis, t-test and Kruskal–Wallis test was applied.

Results: 55 responding and 90 non-responding patients were evaluated. Responding groups had a significantly different mean attenuation, skewness, homogeneity, percentile CT attenuation, GLCM moments in 2D analysis and mean attenuation, standard deviation, entropy, homogeneity, percentile CT attenuation, GLCM moments in 3D analysis (P<0.05). Skewness (odds ratio, 6.739) in 2D, mean attenuation (odds ratio, 2.587), standard deviation (odds ratio, 3.163) in 3D were independent predictors for therapeutic response (P<0.05). However, only skewness (p=0.213) in 2D showed no significant different between each CT machines.

Conclusion: CT texture analysis using pretreatment CT is useful for prediction of therapeutic response evaluation after cytotoxic chemotherapy in patients with liver metastasis from colorectal cancer. Skewness in 2D was an independent predictor regardless of CT machines.

SS 4.03

MR imaging features for improved diagnosis of HCC in the non-cirrhotic liver: multi-center evaluation

M.A. Fischer[1], D.A. Raptis[1], O.F. Donati[1], G. Sotiropoulos[2], J. Mccall[3], A. Bartlett[3], P. Bachellier[4], A. Frilling[5], S. Breitenstein[1], P.-A. Clavien[1], H. Alkadhi[1], M.A. Patak[1]; [1]Zurich/CH, [2]Essen/DE, [3]Auckland/NZ, [4]Strasbourg/FR, [5]London/UK

Purpose: To determine MR imaging features for the differentiation between hepatocellular carcinoma (HCC) and benign hepatocellular tumors in the non-cirrhotic liver.

Material and Methods: 107 consecutive patients without liver cirrhosis (46 male; 45±14 years) who underwent liver resection due to suspicion of HCC were included in this multi-center study. The following imaging features were assessed: lesion diameter and demarcation, satellite lesions, central scar, capsule, fat content, hemorrhage, vein infiltration and signal intensity (SI) on native T1-, T2- and dynamic-enhanced T1-weighted images, separately for tumor center and periphery.

Results: Significant differences between HCC (n=55) and benign lesions (n=52) were shown for native T1-, T2- and dynamic-enhanced T1-SI, fat content, and satellite lesions (all P<0.05). Independent predictors for HCC were T1-hypointensity (odds ratio, 4.81), T2-hypo-/hyperintensity (5.07), lack of central tumor enhancement (3.36), and satellite lesions (5.78; all P<0.05). Sensitivity and specificity of HCC were 91% and 75%, respectively, for two out of four independent predictors, whereas specificity reached 98% for all four predictors.

Conclusion: Independent MRI features indicating HCC are T1-hypointensity, T2-hypo- or hyperintensity, lack of central tumor enhancement and presence of satellite lesions. These features may have the potential to improve the diagnosis of HCC in the non-cirrhotic liver.

SS 4.04

Is diffusion-weighted imaging alone sufficient for the detection of colorectal liver metastases?

A. Schulz, E.S. Joelsen-Hatlehol, K.K. Aasand, B. Hanekamp, E. Viktil, J.B. Dormagen; Oslo/NO

Purpose: To evaluate the diagnostic performance of diffusion-weighted imaging (DWI) alone for preoperative detection of colorectal liver metastases (CRLM) compared to magnetic resonance imaging (MRI) including both DWI and dynamic Gd-EOB-DTPA-enhanced sequences.

Material and Methods: Institutional review board approval and written informed consent were obtained. Forty-four consecutive patients with histopathological confirmed colorectal cancer and suspected CRLM underwent prospectively 1.5T liver MRI between September 2011 and January 2013. Three image-sets were provided; each of them was evaluated by two blinded radiologists in consensus. DWI-set and DWI-T2F-set included survey, diffusion-weighted sequences (b values 0, 50, 800s/mm²), ADC map, and biplanar T2-weighted SSH. DWI-T2F-set included additionally respiratory-triggered T2-weighted TSE/SPIR. CE/DWI-set included all sequences from the DWI-sets and Gd-EOB-DTPA-enhanced sequences. Histopathology and follow-up were reference standards.

Results: Reference standard found 308 liver lesions, including 132 CRLM in 40/44 patients. Sensitivity and PPV were for DWI-set 67.4% (58.7%-75.3%) and 95.7% (89.4%-98.8%), for DWI-T2F-set 68.2% (59.5%-76.0%) and 94.7% (88.1%-98.3%) and for CE/DWI-set 88.6% (82.0%-93.5%) and 84.2% (77.0%-89.8%). CE/DWI-set was significantly more sensitive than DWI-set and DWI-T2F-set (p<0.001, McNemar). A tendency towards higher PPV for DWI-set and DWI-T2F-set compared with CE/DWI-set was found.

Conclusion: The diagnostic performance of DWI alone was inferior compared to liver MRI including both DWI and Gd-EOB-DTPA-enhanced sequences. Additional T2-weighted SPIR sequence did not improve sensitivity of DWI. For optimal performance, liver MRI should be based on both DWI and Gd-EOB-DTPA-enhanced sequences.

SS 4.05

A multicenter study on CT texture analysis of the liver: can we predict the presence of occult colorectal metastases?

R. Beckers[1], D.M.J. Lambregts[1], R. Schnerr[1], S.-X. Rao[2], C. Verhoef[3], R.S. Dwarkasing[3], M.-S. Zeng[2], G.L. Beets[1], R.G.H. Beets-Tan[1]; [1]Maastricht/NL, [2]Shanghai/CN, [3]Rotterdam/NL

Purpose: Previous research showed promise for whole-liver CT-texture analysis to discriminate between colorectal cancer (CRC) patients with/without synchronous hepatic metastases. The aim of this multicenter study was to validate these findings and investigate whether CT texture can also predict the development of metachronous metastases before they become visible on CT.

Material and Methods: 180 patients were included, of which a preliminary analysis of n = 67 was performed at the time of writing. Three subgroups were assessed: patients [A] without metastases (n = 27), [B] patients who developed metachronous metastases within 24 months (n = 20) and [C] those with synchronous metastases (n = 20). Whole-liver texture analysis was performed on primary staging portal-phase CT by manual delineation of the non-diseased liver. Mean greylevel intensity (M), entropy (E) and uniformity (U) were derived with different filter values (unfiltered = 0.0, fine = 0.5, medium = 1.5, coarse = 2.5). Univariate logistic regression analysis was performed to identify potentially predictive parameters, which were further evaluated by ROC-curve analysis.

Results: To differentiate between group A/C, all texture parameters (except $E_{0.0}$) showed potential predictive value with AUCs to diagnose synchronous metastasis ranging between 0.60 and 0.92 (for $U_{1.5}$). To differentiate between group A/B, $E_{0.5}$ and $M_{1.5}$ were predictive with AUCs of 0.63 and 0.62 to diagnose patients who will develop metachronous metastases.

Conclusion: Whole-liver CT texture analysis can differentiate between patients with/without metastatic disease and may also hold promise to diagnose patients with occult metastases who will develop metachronous disease.

SS 4.06

Comparison of Tumor Response by Response Evaluation Criteria in Solid Tumors (RECIST) and Choi criteria in patients treated with yttrium-90 radioembolization for intrahepatic cholangiocarcinoma

L. Beuzit, V. Brun, E. Garin, E. Boucher, K. Boudjema, J. Edeline, Y. Rolland; Rennes/FR

Purpose: To determine whether the application of Choi criteria to patients with intrahepatic cholangiocarcinoma (ICC) treated by yttrium90 radioembolization improves prognosis classification compared with Response Evaluation Criteria in Solid Tumors (RECIST).

Material and Methods: The authors retrospectively analyzed 45 patients with locally advanced ICC treated with yttrium90 glass microspheres. Patients must have undergone contrast-enhanced computed tomography before and after treatment. CT scans were analyzed using RECIST 1.1 and the criteria described by Choi in stromal gastro-intestinal tumors.

Results: The rates of objective response (OR), stable disease (SD), and progressive disease (PD) were 11%, 76%, and 13%, respectively, according to RECIST and 82%, 4%, and 13%, respectively, according to Choi criteria. Patients who achieved an OR according to Choi criteria had a longer overall survival (OS) than non-responding patients with SD or PD (median 19.9 months and 5.4 months, respectively (p = .003)), whereas there was no significant difference in the survival of responding and non-responding patients according to RECIST (p = .387). In the 40 non-responding patients according to RECIST, response according to Choi distinguished a significantly different prognosis, with a median overall survival of 19.9 months and 5.4 months in patients who were responding (n = 32) and non-responding (n = 8), respectively (p = .005).

Conclusion: Choi criteria better assessed the prognosis of patients who received yttrium90 microsphere radioembolization for ICC than RECIST.

SS 4.07

withdrawn by the authors

SS 4.08

Diffusion-weighted MRI at 3T: the optimal maximum b value for differential diagnosis of focal solid liver lesions

K. Lomovtseva, G.G. Karmazanovsky, N. Karel'Skaya, V.A. Vishnevsky; Moscow/RU

Purpose: To compare three different b values (600, 800 and 1000 s/mm²) for differentiation between benign and malignant focal solid liver lesions and determine the optimal b value.

Material and Methods: 26 patients with 46 focal solid liver lesions (24 metastases, 5 hepatocellular carcinomas, 10 cholangiocarcinomas, 6 focal nodular hyperplasias, 1 hepatocellular adenoma) underwent respiratory-triggered DWI MRI (3T), using b values 0, 600, 800 and 1000 s/mm². Signal-to-noise ratio (SNR) and contrast-to-noise ratio (CNR) of each lesion for b = 600, 800 and 1000 s/mm² were calculated. Apparent diffusion coefficients (ADC) of lesion were measured on ADC maps, which were automatically created for the following b values: 0-600, 0-800 and 0-1000 s/mm². The ROC analysis was performed and cutoff values of ADC of lesion for differentiation of benign and malignant lesions for every maximum b value were determined.

Results: The mean ADC values of benign solid lesions were significantly higher than malignant solid lesions at all b values of 600, 800 and 1000 s/mm² (p < 0.001). The largest area under the ROC curve was reached by ADC_{lesion} (0.859). The cutoff value of ADC_{600} was 1.180 x 10^{-3} mm²/s, (sensitivity 83.3%, specificity 73.1%). SNR and CNR for b = 600 s/mm² were higher than for b = 800 s/mm² and b = 1000 s/mm².

Conclusion: The diagnostic performance of DWI at b = 600 s/mm² is comparable and even higher than DWI at b values 800 and 1000 s/mm². b = 600 s/mm² may be the optimal maximum b value.

SS 4.09

Superb microvascular imaging technology: initial experience in hepatic tumors

J.Y. Lee, B.I. Choi, J.K. Han, S.H. Kim, S.Y. Kang; Seoul/KR

Purpose: To investigate if superb microvascular imaging (SMI) technology, recently developed to visualize extremely low-velocity flows with high frame rate and high resolution without contrast agents, is helpful for the diagnosis of hepatic tumors.
Material and Methods: Forty hepatic tumors of 28 patients were enrolled in our study. The tumors consisted of hemangiomas (n = 15), focal nodular hyperplasia (FNH) (n = 7), hepatocellular carcinomas (n = 7), and metastasis (n = 11). All lesions were pathologically or radiologically confirmed. Mean tumor was 1.9 cm in diameter (range, 0.9 cm to 5.0 cm). Using SMI technology, all lesions were scanned and categorized into subgroups according to the flow pattern on SMI.
Results: Hemangiomas showed nodular rim pattern in 33% and dot-like pattern in 20%, all of which were very specific findings for the diagnosis of hemangiomas. FNH showed spoke wheel pattern in 43% and radiating vessel pattern in 29%, which were very specific findings for the diagnosis of FNH. Other tumors did not show any specific pattern on SMI.
Conclusion: SMI is a very promising technology for the depiction of very slow flow within hepatic tumors, which may give an additional clue to differentiate hepatic tumors on non-enhanced ultrasound.

SS 4.10

Best diagnostic clue for the diagnosis of biliary hamartomas (von Meyenburg complex)

V. Cappendijk[1], M. Gielens[1], E. Ranschaert[1], F. Bakers[2]; [1]'s-Hertogenbosch/NL, [2]Maastricht/NL

Purpose: Biliary hamartomas (BH) are often misdiagnosed as liver metastases. The characteristics of BH on ultrasound, CT and MRI are well described. However, evaluating available literature, most authors fear to provide a diagnosis with substantial probability. This retrospective study describes the simultaneous use of ultrasound AND CT or MRI information. The purpose is to improve the diagnostic confidence in considering this diagnosis.
Material and Methods: From August 2007 to January 2015, patients with the ultimate diagnosis of BH were evaluated. A preliminary patient evaluation showed typical features on ultrasound (multiple tiny hyperechoic lesions with comettail reflection). CT showed multiple small cysts. Interestingly, the largest cyst on CT of about 1-1,5 cm, which was very accessible by ultrasound, could not be detected on ultrasound. This was hypothesized as the best diagnostic clue (vanishing cyst sign, VCS). With scarce literature support, and in multidisciplinary consensus, this patient was followed with a probable diagnosis of BH. During follow-up, other patients with similar imaging characteristics were recognized and followed.
Results: 16 patients were included (11 f, mean age 56 years). All patients showed the typical modality imaging features of BH. On combining ultrasound with CT or MRI, 15/16 patients showed VCS (1 patient underwent no ultrasound). The mean FU was 23 months. None of the patients developed liver malignancies.
Conclusion: Simultaneous use of ultrasound AND CT or MRI information has potential to improve the diagnostic confidence in considering the diagnosis of biliary hamartoma.

11:00 - 12:30 **Darwin 5**

Scientific Session SS 5

Pancreas: cystic lesions and inflammation

SS 5.01

Evolution of incidental branch-duct type intraductal papillary mucinous neoplasm (bd-IPMN): a study with MRCP

R. Girometti, F. Catapano, L. Cereser, G. Como, C. Zuiani, M. Bazzocchi; Udine/IT

Purpose: To evaluate the evolution over time of incidental bd-IPMN.
Material and Methods: We retrospectively evaluated 77 patients who underwent, over 8 years, a total of 281 MRCPs (mean 3.6) to follow up incidental bd-IPMN found or confirmed at the baseline examination, showing no signs of malignancy. Median follow-up time was 37 months. MRCPs were acquired on 1.5 T/3.0 T systems using 2D and/or 3D technique. Image analysis assessed the per-12-months incidence rate of: (i) changes in the number and size of cysts; (ii) suspicious MRCP findings confirmed to be malignant on endoscopic ultrasound and histological examination after surgery. Cox-proportional-hazard analysis was performed to exploit features associated with bd-IPMN changes.
Results: We found a total of 406 cysts (per-patient mean 5.2) with average size of 8.5 mm (range 5-22 mm). Cysts increased in number (mean 3.5 new cysts) in 5.1% of patients (incidence rate 0.02%), and size (mean increase 5.1 mm) in 23.3% of patients (incidence rate of 0.03%), at median follow-up times of 30 and 16.5 months, respectively. Malignancy developed in 3/77 patients (3.8%) at a median follow-time of 13 months, with an incidence rate of 0.02%. No clinical or initial MRCP features were significantly associated with changes in bd-IPMN appearance.
Conclusion: Incidental bd-IPMN shows a low incidence rate of changes over time. However, there are no definite predictive features of changes, particularly in developing malignancy.

SS 5.02

Radiological criteria to predict malignancy in IPMNs: the introduction of bile duct dilation into current guidelines

A. Strauss, M. Birdsey, B. Schwarz-Bundy, S. Fritz, H.U. Kauczor, M. Klauss, L. Grenacher; Heidelberg/DE

Purpose: Finding radiological predictors of malignancy in IPMNs.
Material and Methods: 384 patients who had preoperative imaging (CT/MRI) and had undergone a pancreatic operation with a confirmed pathological diagnosis of IPMN were included in the study. Images were evaluated retrospectively using a standardized checklist. Descriptive statistics, binary logistic regression and ROC analysis were performed to assess the international consensus guidelines (ICGs) and further radiological predictors of malignancy.
Results: Analysis of current guidelines showed a diagnostic improvement with the addition of bile duct dilation to the ICGs on determining malignancy of IPMNs (2012 ICG: sensitivity 82.2% vs. 86.9%; specificity 62.7% vs. 62.2%). The largest single predictors of malignancy were solid components (OR 3.98) and bile duct dilation (OR 31.26). Over 95% of all cases with cholestasis were malignant IPMNs (PPV 96.4%; NPV 63.1%). Subanalysis of BD-IPMNs also resulted in a diagnostic improvement with the addition of bile duct dilation (sensitivity 28.6% vs. 45.2%; specificity 92.9% vs. 92.1%), which was also the strongest independent predictor for malignancy (OR 29.3). Frequency analysis revealed that even small BD-IPMNs had already undergone malignant transformation (≤1 cm: 15%; 1-2 cm: 26% ; 2-3 cm 20%) with about 10% of those having a dilated bile duct.
Conclusion: A dilated bile duct is a significant positive predictor of malignancy regardless of the size of the lesion. The addition of cholestasis to current guidelines could increase the detection of malignant IMPNs.

SS 5.03

The natural history of non-resected IPMN of the pancreas: a single institution experience

M. Del Chiaro, R. Segersvärd, L. Nilsson, J. Blomberg, E. Rangelova, C. Ansorge, R. Pozzi Mucelli, N. Kartalis, M. Löhr, C. Verbeke; Stockholm/SE

Purpose: To analyze the results of a follow-up program for patients with IPMN.
Material and Methods: From January 2008 to December 2013, 503 patients diagnosed with IPMN were observed. 452 patients were followed-up, while 51 underwent surgery. The patients under follow-up represented the study series population.
Results: The mean follow-up was 932 days. 395 of the patients were under surveillance according to the prevailing guidelines (group 1), whereas 57 patients (group 2) were followed up because of contraindications for surgery. In

group 1, 55 patients (13.9%) required surgery for progression of their IPMN after a median follow-up of 560 days. In 2 patients (0.5%), a synchronous pancreatic cancer developed during follow-up. The 1, 3 and 5 years survival rate for the patient series was 96.5%, 92.4% and 87.1%, respectively. In group 1, 33 patients (8.3%) died under follow-up: 4 (1%) due to IPMN progression, 5 (1.3%) because of extrapancreatic cancer and 24 (6%) due to other causes. The 1, 3 and 5 years survival rate in group 2 was 74.8%, 48.7% and 40.5%, respectively. In this group, 22 patients (38.6%) died due to IPMN progression (10, 17.5%), extrapancreatic cancer (5, 8.8%) or for other reasons (7, 12.3%).
Conclusion: This study confirms the safety of a surveillance program for patients with non-surgical IPMN. The incidence of pancreatic cancer and IPMN-related mortality were low during follow-up.

SS 5.04

MRI criteria to select pancreatic mucinous cystic neoplasm (MCN) candidates for parenchyma-sparing surgery

V. Di Paola, F. Castelli, S. Mehrabi, R. Manfredi, R. Pozzi Mucelli; Verona/IT

Purpose: To identify MRI criteria to detect benign forms of MCNs suitable for parenchyma-sparing surgery to reduce post-surgical morbidity and mortality.
Material and Methods: Inclusion criteria were patients with pathological diagnosis of benign (cystoadenomas) or malignant (cystoadenocarcinomas) MCNs and availability of MR examination. Exclusion criteria were lack of pathological results and/or MR examination. The study population comprised 62 patients (58 females, 4 males, mean age 51 years). A score was assessed giving 1 point for each high-risk malignancy. MRI criteria: mural nodules, septa thickness >5 mm, wall thickness >5 mm, >6 cysts, size >6 cm, T1-hyperintensity, compression of adjacent structures and infiltration of adjacent structures. ROC analysis was performed to find the best cutoff value among the observed scores to discriminate benign from malignant MCNs through comparison with pathological results (Reference Standard).
Results: Pathological findings revealed 45/62 (72,6%) benign MCNs and 17/62 (27,4%) malignant MCNs. The MRI score for benign MCNs was: 0 in 13/45 (29%) cases; 1 in 11/45 (24%) cases; 2 in 12/45 (27%) cases; 3 in 9/45 (20%) cases. The MRI score for malignant MCNs was: 5 in 4/17 (24%) cases; 6 in 6/17 (35%) cases; 7 in 4/17 (23%) cases; 8 in 3/17 (18%) cases. The best cutoff value to discriminate benign from malignant forms of MCNs was 3 pts (AUC = 1, p<0,001), considering as benign MCNs ≤3 pts and as malignant MCNs ≥4 pts.
Conclusion: The presence of ≤3 high-risk criteria allows identification of benign forms of MCNs which could undergo parenchyma-sparing surgery.

SS 5.05

Association of pancreatic fat content with type II diabetes mellitus

C. Nadarajah, K. Sandrasegaran; Indianapolis, IN/US

Purpose: To determine if pancreatic fat content measured by chemical shift MRI differs in patients with and without type II diabetes mellitus (DM).
Material and Methods: A retrospective review of radiology database from January 2004 to December 2013 revealed 63 patients with DM. Patients were excluded if the MRI examination was within 3 months of acute pancreatitis (8), body mass index (BMI) was not available (n = 6) or if they had type I DM (n = 9). The remaining 40 patients were enrolled. Another group of age and gender-matched 114 patients who did not have DM for at least 12 months after MRI were enrolled as the control group. Regions of interest were placed on pancreatic head, body and tail, liver and paraspinal muscles on in- and opposed-phase images.
Results: On logistic regression analysis, there was no difference between DM and control groups for BMI [mean 31.6 (SD 6.5) vs. 29.0 (8.0), p = 0.07], fat content in pancreatic head [7.8 (10.9) vs. 5.6 (8.5), p = 0.74], pancreatic body [7.9 (8.9) vs. 5.1 (7.6), p = 0.84], liver (p = 0.10) and paraspinal muscle (p = 0.43). Pancreatic tail fat was significantly higher in patients with DM [11.0 (10.8) vs. 5.6 (7.0), p = 0.03]. Pancreatic tail fat > 10% had 84% specificity in predicting DM.
Conclusion: Elevated pancreatic tail fat was associated with DM, independently of liver fat or BMI. Assessment of pancreatic tail fat content may help predict patients at risk of diabetes.

SS 5.06

Autoimmune pancreatitis and pancreatic ductal adenocarcinoma: differential diagnosis on the basis of gadoxetic acid-enhanced and diffusion-weighted MR imaging

S.-Y. Choi[1], S.H. Kim[2], K.M. Jang[2], H.J. Park[2], S.J. Lee[2]; [1]Bucheon/KR, [2]Seoul/KR

Purpose: To assess the value of gadoxetic acid-enhanced MR imaging with MR cholangiopancreatography (MRCP) and diffusion-weighted (DW) imaging for differentiating focal autoimmune pancreatitis (AIP) from pancreatic ductal adenocarcinoma (PDAC).
Material and Methods: A retrospective study included 15 patients with mass-forming AIP and 79 patients with PDA with gadoxetic acid-enhanced MR imaging, DW imaging and MRCP. The sensitivity, specificity, diganostic accuracy and odds ratio of significant imaging findings at univariate and multivariate analyses were calculated and those of the combinations were also analyzed. Using ROC analysis, the appropriate cutoff value of ADC corresponding to maximal Youden's index (J) was determined.
Results: In qualitative univariate and multivariate analyses, duct-penetrating sign ($p < 0.001$) and homogenous enhancement ($p = 0.001$) were significantly independent factors for differentiating AIP and PDAC. Mean ADC value ($0.9618 \pm 0.14 \times 10^3$ mm²/s) of AIP was significantly lower than PDAC ($1.1319 \pm 0.23 \times 10^3$ mm²/s) ($p = 0.0201$). The optimal cut point of ADC value for differentiating mass-forming AIP from PDAC was 0.94×10^3 mm²/s. Applying this cutoff value, the sensitivity and specificity for diagnosing AIP was best (66.7% and 81.0%, retrospectively) and the AUC was 0.738 95 [95% CI, 60.7-86.9]. When all three imaging findings with ADC value were satisfied, the sensitivity, specificity and AUC were highest (93.3%, 96.2% and 0.952 [95% CI, 87.1-100.0]).
Conclusion: Gadoxetic acid-enhanced MR imaging with MRCP and DW imaging may be helpful for differentiating AIP from PDAC.

SS 5.07

Useful MR findings for differentiation between autoimmune pancreatitis and pancreatic cancer at 3-T MRI

M. Takahashi, Y. Fujinaga, T. Furukawa, A. Fujita, S. Fujita, S. Yanagisawa, H. Hamano, S. Kawa, M. Kadoya; Matsumoto/JP

Purpose: We aimed to validate previously reported useful MR findings for differentiation between AIP and PC in single institution.
Material and Methods: We retrospectively reviewed MR findings of 37 AIP and 42 PC lesions that were analysed with 3-T MRI including dynamic contrast-enhanced MRI (DCE-MRI). All AIP lesions were diagnosed based on the International Consensus Diagnostic Criteria for autoimmune pancreatitis. All PC lesions were pathologically diagnosed by surgical resection or biopsy. Sensitivity, specificity and accuracy were calculated. In addition, frequencies of MR findings were compared between AIP and PC using Fisher's exact test.
Results: Sensitivity/specificity/accuracy of MR findings such as 1) speckled hyperintensity on fat-suppressed T1-weighted image (FS-T1WI), 2) speckled enhancement on pancreatic phase DCE-MRI, 3) capsule-like rim, 4) homogeneous delayed enhancement, 5) duct-penetrating sign, 6) enhanced duct sign, 7) no main pancreatic duct (MPD) upstream dilatation were as follows in the same order: 1) 100/97.6/98.7%, 2) 97.3/97.6/97.5%, 3) 35.1/100/69.6%, 4) 94.6/85.7/89.9%, 5) 73.0/100/87.3%, 6) 13.5/100/59.5%, 7) 100/64.3/81.0%. Sensitivity, specificity and accuracy of speckled hyperintensity on FS-T1WI and speckled enhancement on pancreatic phase DCE-MEI was over 95%. All findings except for enhanced duct sign was more frequently seen in AIP than in PC ($P < 0.0001$).
Conclusion: Speckled hyperintensity on FS-T1WI and speckled enhancement on pancreatic phase DCE-MRI were most useful in differentiating between AIP and PC at 3-T MRI.

SS 5.08

Magnetic resonance imaging volumetry of the pancreas in autoimmune pancreatitis: evaluation of pancreas volume at diagnosis, post-therapy and follow-up

N. Cardobi, C. Sozzi, R. Manfredi, R. Pozzi Mucelli; Verona/IT

Purpose: To evaluate and quantify the change in volume of the pancreas in autoimmune pancreatitis.
Material and Methods: From 2010 to March 2014, 100 patients with autoimmune pancreatitis were evaluated at our hospital. Inclusion criteria were confirmed clinical and laboratory data and/or biopsy diagnosis of autoimmune pancreatitis and the presence of MRI at least at 3 time points: diagnosis, post-steroid therapy and 1st follow-up. Twenty-five patients were included in the study (20

male, 5 female; 50.1 ± 18.2 years; 15/25 diffuse form, 10/25 focal form). MRI pancreas volume was obtained with Osirix software perfomed on post-contrast injection T1 volume interpolated GRE sequence (TR = 3.5 ms, TE = 1.6 ms, slice thickness = 3 mm, slices = 72, matrix = 512 × 512) sequence in pancreatic phase.
Results: Pancreas volume at diagnosis was 81.4 ± 30.0 mm^3. After steroid therapy (86.2 ± 83.8 days after the 1st exam) the pancreas volume decreased to 51.5 ± 22.4 mm^3 (-35.8%, p <0.01). Further decrease in pancreas volume was found in the 1st follow-up (225.5 ± 160.7 days after the 1st exam) with pancreas volume to 44.5 ± 20.7 mm^3 (-13.1% from the post-steroid examination and -44.5% from the diagnosis, both with p <0.01).
Conclusion: MRI demonstrates the pancreas volumetric reduction in autoimmune pancreatitis. In particular, pancreas volume decreased by a 35.8% after steroid therapy and for a further 13.1% in the next follow-up. Global pancreas volume decrease was 44.5%.

SS 5.09

Secretin-enhanced MRCP findings in patients with pancreatic duct stenosis: signs of benignity and malignancy

E. Boninsegna, R. Manfredi, R. Negrelli, G. Avesani, B. Pedrinolla, S. Mehrabi, R. Pozzi Mucelli; Verona/IT

Purpose: To evaluate MR-cholangiopancreatography (MRCP) findings before and after secretin administration in patients with main pancreatic duct (MPD) stenosis and to define imaging criteria of benignity and malignancy.
Material and Methods: Secretin-enhanced MRCPs of 42 patients were evaluated; 35 presented benign conditions and 7 pancreatic cancer. Image analysis included: presence of solid lesions; site and type of stenosis; presence of upstream dilated side branches; stenosis resolution after secretin administration ("duct-penetrating sign"); number of stenoses; stricture length; upstream MPD diameter.
Results: Between patients with benign condition and those with cancer, there were no statistically significant differences for the presence of solid lesions, site of stenosis and length of MPD stricture (p > 0,1). Cancer caused a higher prevalence of complete stenosis (100% versus 48,6%; p = 0,037), upstream dilated side branches (100% versus 51,4%; p = 0.049) and a considerable lower prevalence of positive duct-penetrating sign (0% versus 88,6%; p < 0.001). The number of stenoses was higher in the presence of benign conditions (1,23 versus 1,00; p < 0,01). Upstream MPD diameter was higher in cancer-induced stenoses compared with non-neoplastic strictures, both in basal conditions (average 3,96 mm versus 2,47 mm; p < 0,01) and after secretin administration (average 4,51 mm versus 2,94 mm; p < 0,001).
Conclusion: Secretin-enhanced MRCP is a useful technique to evaluate MPD stenosis; the presence of a single complete stenosis with upstream dilated side branches and increased MPD caliber, without stenosis resolution after secretin administration, is highly suggestive of malignancy.

SS 5.10

The morphologic evolution of necrotic pancreatic zones in acute pancreatitis: is there a reversible pattern?

E. Kasatkina[1], M. Klauss[1], T. Hackert[1], T. Rieden[2], H.U. Kauczor[1], V.E. Sinitsyn[2], L. Grenacher[1]; [1]Heidelberg/DE, [2]Moscow/RU

Purpose: Necrotizing pancreatitis is a severe form of acute pancreatitis characterized by destruction of pancreatic parenchyma, peripancreatic tissues or both. The accepted CT criteria for diagnosis of pancreatic necrosis are defined as focal or diffuse zones of non-enhanced parenchyma or areas with highly decreased attenuation depicted on the images with contrast administration. The aim was to find whether areas with decreased attenuation in pancreatic parenchyma always correspond to pancreatic necrosis or could be reversible in the setting of acute pancreatitis.
Material and Methods: 25 patients with contrast-enhanced initial and follow-up CT scans were included in the study. Two independent observers analyzed both CT scans retrospectively. The size and change in CT density of hypodense parenchymal areas and other related findings were precisely evaluated on primary and follow-up CT-scans.
Results: In 28% of patients with acute necrotizing pancreatitis, hypodense parenchymal areas on initial CT scan showed increase in HU values in follow-up CT studies. Patients were divided into two groups: those with increased HU values in follow-up studies (Group 1) and those who did not (Group 2). There were statistically significant differences between Group 1 and Group 2 in the size of the primary area and in HU-delta (by size: t-test – p = 0,006, Mann–Whitney U test –p=0,01; by HU-delta: t-test – p = 0,00, Mann–Whitney U test – p = 0,00).
Conclusion: Our results suggest that small hypodense zones in pancreatic parenchyma may not always represent areas of pancreatic necrosis. Reversible pancreatic ischemia and/or decreased perfusion of parenchyma could be considered in cases with small hypodense areas in acute pancreatitis.

11:00 - 12:30 **Leonard de Vinci**

Scientific Session SS 6
Pancreas malignancy and bile ducts

SS 6.01

Does cardiac triggering improve pancreas ADC repeatability?

A. Loureiro[1], T. Metens[2], C. Matos[2]; [1]Lisbon/PT, [2]Brussels/BE

Purpose: To assess if Cardiac Triggering (CT) with individually optimised delay improves repeatability of pancreas ADC measurements; additionally, ADC repeatability after an original filtering correction method is evaluated.
Material and Methods: Six volunteers underwent 3T-DWI, after written informed consent and IRB approval. Respiratory cardiac-triggered (RTCT), breath-hold cardiac-triggered (BHCT) and respiratory-triggered (RTnoCT) DWI sequences with b 0,150,500 s/mm^2 were obtained during two separate sessions at two weeks interval. Four ROIs were drawn in the pancreas tail and body, in identical positions on the three sequences and the two sessions. Average ADC value from the four ROIs, mean and difference between sessions were calculated. Repeatability was assessed with standard deviation of ADC inter-session differences. ADC was recalculated in RTnoCT and RTCT images after artefact elimination by high-pass filtering of signal intensities above the mean signal value for a fixed b.
Results: RTnoCT ADC (1614 $10^{-6}mm^2/s$) tended to be higher than RTCT and BHCT ADC (1413, 1370 $10^{-6}mm^2/s$). After filtering in RTnoCT and RTCT images, ADC=1412,1333 $10^{-6}mm^2/s$ (significantly decreased in RTCT, P=0.03). RTCT and BHCT standard deviation of ADC inter-session differences were significantly lower than in RTnoCT images (64, 98 and 352 10^{-6} mm^2/s, P=0.002, P=0.014; after filtering in RTnoCT, RTCT: 234, 89 $10^{-6}mm^2/s$, P=0,05).
Conclusion: Pancreas ADC repeatability was significantly higher in images acquired with individually optimised CT. After signal filtering, pancreas ADC repeatability remained significantly higher in CT images.

SS 6.02

CT after neoadjuvant FOLFIRINOX chemotherapy for borderline and locally advanced pancreatic adenocarcinoma

M. Wagner[1], C. Antunes[2], D. Pietrasz[1], C. Cassinotto[3], A. Sa Cunha[4], J.-B. Bachet[1], O. Lucidarme[1]; [1]Paris/FR, [2]Coimbra/PT, [3]Pessac/FR, [4]Villejuif/FR

Purpose: To assess computed tomography (CT) modifications after neoadjuvant FOLFIRINOX chemotherapy for borderline (BR) and locally advanced (LA) pancreatic adenocarcinoma (PAC).
Material and Methods: Thirty-six patients with BR and LA PAC who received neoadjuvant FOLFIRINOX chemotherapy and had undergone surgery were retrospectively included. Baseline CT and pre-surgical CT were reviewed by two observers. Largest diameter, product of the 3 diameters (P3D), arterial (superior mesenteric/coeliac/hepatic arteries) and venous (superior mesenteric/portal veins) involvement (score=0-5) and NCCN classification were studied and compared to pathological data.
Results: There were significant decreases of the largest diameter and of P3D (p<0.0001) and a partial response (PR) according to RECIST was found in 17/36 patients (47%). The largest diameter and P3D variations were significantly higher in patients with pathological response (T0-1N0) (p<0.05). A decrease of the arterial or venous involvement was respectively found in 9 (25%) and 8 patients (22%). In the opposite, progression of the vascular involvement was seen in 2 (5%) patients associated with a shorter disease-free survival after the surgery (p<0.05). 31 patients had R0 resection and among them only 4 (13%) exhibited a downstaging according to NCCN classification, while 27 (87%) did not.
Conclusion: Despite a lack of NCCN downstaging during chemotherapy most of BR and LA patients were R0 at surgery suggesting that additional imaging pattern must be found to accurately predict post-chemotherapy resectability.

SS 6.03

Multidetector CT of pancreatic ductal adenocarcinoma: effect of tube voltage and iodine load on image quality, lesion conspicuity and vessel involvement

L. Loizou[1], N. Albiin[1], M.A. Fischer[1], E. Axelsson[1], B. Leidner[1], A. Grigoriadis[1], M. Del Chiaro[1], R. Segersvärd[1], A. Sundin[2], N. Kartalis[1], C. Verbeke[1]; [1]Stockholm/SE, [2]Uppsala/SE

Purpose: To compare a high tube voltage, normal-iodine load (standard) protocol multidetector CT (MDCT) with a low tube voltage, normal- or high-iodine load protocol in patients with pancreatic cancer regarding image quality, tumor conspicuity and vessel involvement.

Material and Methods: In this IRB-approved prospective study, thirty consecutive patients (14 men, mean age 66 years) underwent, preoperatively twice, multiphase 64-channel MDCT examinations according to: (i) standard protocol (SP; 120 kV, 0.75 gI/Kg body weight) and (ii) protocol A (PA; 80 kV, 0.75 gI/kg) or B (PB; 80 kV, 1 gI/kg). In all examinations, two independent readers evaluated blindly the image quality, tumor conspicuity and vessel involvement. A third reader measured the pancreas-to-tumor contrast-to-noise ratio (CNR) in the pancreatic parenchymal (PPP) and portal-venous (PVP) phases. Statistical analysis was performed with Chi-square test.

Results: There was no significant difference between protocols in image quality (p=0.12). Tumor conspicuity was significantly higher in PA and PB compared to PS (both, p<0.05). Vessel involvement between PA and PS coincided in 93% of patients, whereas in only 81% between PB and PS. CNR in PPP was significantly higher in PB compared to PA and SP (both, p<0.05) and in PVP significantly higher in PB compared to SP (p<0.0001).

Conclusion: A low tube voltage and high-iodine load protocol improves tumor conspicuity in patients with pancreatic cancer compared to standard protocol MDCT; however, there might be slight discrepancy between them in assessing vessel involvement.

SS 6.04

Pancreatic metastases from renal neoplasms and neuroendocrine pancreatic tumors: differential diagnoses

F. Lombardo, M.C. Ambrosetti, G.A. Zamboni, T. Sava, A. Malpaga, G. Butturini, R. Pozzi Mucelli; Verona/IT

Purpose: Pancreatic metastases from renal-cell carcinoma (PRCC) and neuroendocrine pancreatic tumors (PNET) are both hypervascular and the differential diagnosis can be difficult. The purpose of this study is to compare the multiphasic MDCT features of these two lesions.

Material and Methods: We retrospectively compared the MDCTs performed on 28 patients with history of clear-cell carcinoma and PRCC with 28 patients with PNET, matched by size. All patients underwent multiphasic CT. In patients with multiple PRCCs, the largest lesion was analyzed. One reader evaluated the site, margins, enhancement intensity and homogeneity (subjective comparison to normal parenchyma) in the arterial and venous phases, vascular invasion and main pancreatic duct (MPD) dilatation.

Results: No significant difference was observed in lesion distribution. All lesions had well-defined margins in both populations. In the arterial phase, 26/28 PRCC and 24/28 PNET were hypervascular, while in the venous phase 17/28 PRCC and 17/28 PNET were hyperattenuating; enhancement was homogeneous in 14/28 PRCC and in 17/28 PNET (all: p = n.s.). Homogeneous PNETs were significantly smaller than inhomogeneous ones (21 ± 4.2 mm vs. 43.18 ± 6.92 mm, p = 0.0073). Vessel invasion was noted in 3/28 PRCC and 6/28 PNET. MPD was dilated in 5/28 cases in both populations.

Conclusion: Both RCC and PNET are well-defined, hypervascular lesions, usually without MPD dilatation or vessel infiltration. We did not find CT features helpful for a differential diagnosis. The best diagnostic clue for PRCC is a history of renal cell carcinoma.

SS 6.05

Pancreatic endocrine tumors (PETs): multimodality imaging features with histopathological correlation

F. Alessandrino, P.E. Humphrey, E. Resnick, A.M. Bellizzi, K.J. Mortele; Boston, NY/US

Purpose: To evaluate the imaging features of pancreatic endocrine tumors (PETs) with histopathological correlation.

Material and Methods: The preoperative imaging (CT: n = 27; MRI: n = 15; ^{111}In-octreotide: n = 12; US: n = 5) of 33 patients (21 female; mean age 55 years) with resected PETs was evaluated for tumor location, size, morphology, echogenicity/attenuation/signal intensity, ^{111}In-octreotide uptake, cystic degeneration, and late arterial phase enhancement. Tissue specimens were assessed for stromal fibrosis, vascular density, and presence of capsule.
Correlation between imaging and histopathology was made using the Fisher–Freeman–Halton test.

Results: PET arose from the pancreatic head/neck (n = 13), body (n = 8), and tail (n = 12). On CT, PET appeared solid (74%), well defined (92.6%), and oval shaped (51.9%). On contrast-enhanced CT, PET appeared hypervascular in 50%. Septations (25.9%) and calcifications (18.5%) were uncommon. On MRI, PET appeared solid (60%), encapsulated (66.6%), oval (75%), hyperintense on T2-WI (75%), and predominantly hypo- or isoenhancing (69%). Cystic PETs (3.0 cm) were not significantly larger than solid (2.3 cm) PETs (CT, p = 0.608; MRI, p = 0.441). ^{111}In-octreotide uptake was demonstrated in 66.6% of cases. By US, PET appeared hypoechoic (60%). By histopathology, PETs were encapsulated (65%); stromal fibrosis comprised <33% of the tumor (71%) with average vascular density (48%). The degree of fibrosis and hypointensity on T2-WI were significantly associated (p = 0.004).

Conclusion: PETs are most commonly oval-shaped, solid, and well-defined/encapsulated masses. Low signal intensity on T2-WI correlates with extensive intratumoral fibrosis. Approximately, 50% of PETs are not hyperenhancing on contrast-enhanced CT/MRI.

SS 6.06

Does diffusion-weighted imaging improve magnetic resonance evaluation of pancreatic neuroendocrine tumors?

R. De Robertis[1], P. Tinazzi Martini[2], G.A. Zamboni[1], M. D'Onofrio[1]; [1]Verona/IT, [2]Peschiera del Garda/IT

Purpose: To assess the diagnostic value of diffusion-weighted imaging (DWI) to evaluate pancreatic neuroendocrine tumors (PNETs) regarding identification, characterization, and staging.

Material and Methods: The MR findings of 30 consecutive patients with surgically resected pancreatic neuroendocrine tumors (PNETs) were retrospectively compared to those of 30 consecutive patients with pancreatic ductal adenocarcinomas (PDACs). T1- and T2-weighted, arterial, portal and delayed phase, b800 and ADC map images were evaluated by two readers in consensus, who performed a quantitative and a qualitative analysis. The latter was completed by a confidence assessment for PNET diagnosis and liver metastases diagnosis by two separate blinded readers.

Results: PDACs had statistically significantly higher mean ADC value compared to PNETs (1.40 vs. 1.19 x 10^{-3}mm^2/s; p = 0.001). b800 images provided the highest lesion conspicuity (p <0.05). On blinded readers' analysis, DWI did not provide significant advantages over other sequences for PNET diagnosis. Regarding liver metastases diagnosis, substantial agreement between readers for DWI and an overall lower diagnostic confidence for conventional sequences vs. DWI were found (both p <0.001). DWI had high AUC values for both readers (0.879 and 0.824) regarding liver metastases diagnosis.

Conclusion: DWI may be of value for the identification of PNETs and for the detection of liver metastases, while it does not seem to provide significant improvements regarding diagnosis. Nevertheless, ADC quantification may be helpful for differential diagnosis.

SS 6.07

Neuroendocrine tumors treated with peptide radionuclide (^{90}Y-DOTATOC) therapy: early whole body diffusion-weighted MRI predicts survival

V. Vandecaveye, S. Van Binnebeek, R. Vanslembrouck, C. Verslype, K. Haustermans, E. Van Cutsem, C. Deroose; Leuven/BE

Purpose: Our aim was to evaluate whole body diffusion-weighted imaging (WB-DWI) for early treatment assessment of peptide receptor radionuclide therapy (PRRT) with Yttrium 90 (^{90}Y) DOTATOC of disseminated neuroendocrine tumours using apparent diffusion coefficient changes at 7 weeks to baseline ($ADC_{ratio7w}$).

Material and Methods: Forty-one patients underwent 3 Tesla WB-DWI using b values of 0-1000 s/mm^2 before and 7 weeks after cycle 1 of ^{90}Y-DOTATOC treatment (full treatment: 4 cycles at 1.85 GBq/m^2/cycle; 8 weeks between cycles). Responses at 7 weeks were assessed with $ADC_{ratio7w}$ at WB-DWI and Response Evaluation Criteria in Solid Tumors (RECIST) at contrast-enhanced magnetic resonance imaging (MRI) Kaplan-Meier and log-rank tests were used to correlate the response variables with progression-free (PFS) and overall survival (OS).

Results: Median PFS was 9 months and median OS 17 months. Survival analyses showed significant effects on PFS by the number of therapy cycles (p=0.026), tumour grade (p=0.024) and $ADC_{ratio7w}$ (p<0.0001) and significant effects on OS by the number of therapy cycles (p=0.006), tumour grade (p=0.0047), nuclear antigen KI67 index (p=0.013) and $ADC_{ratio7w}$ (p<0.0001). After multivariable analysis, the $ADC_{ratio7w}$ remained the only significant predictor of 9 months PFS (p=0.011) and 17 months OS (p=0.001). Seven weeks RECIST did not correlate with outcome.

Conclusion: The $ADC_{ratio7w}$ at WB-DWI was an independent predictor of PFS and OS for disseminated NET treated by ^{90}Y-DOTATOC and may be useful for early treatment assessment.

SS 6.08

Diagnostic performance of transabdominal high-resolution ultrasound for gallbladder cancer and differential diagnosis of neoplastic gallbladder polyps compared with endoscopic ultrasound

J.H. Kim, H.W. Eun, J.Y. Lee, J.K. Han, B.I. Choi, S.J. Ahn; Seoul/KR

Purpose: To compare the diagnostic performance of transabdominal high-resolution ultrasound (HRUS; combined low- and high-MHz transducers) for gallbladder cancer and differential diagnosis of neoplastic polyps compared with endoscopic ultrasound (EUS) and pathology.

Material and Methods: From 125 patients who underwent both HRUS and EUS, our study included 29 pathologically proven gallbladder cancers (T1 = 7, T2 = 19, T3 = 3) including 15 polypoid cancers and 50 surgically proven polyps (neoplastic = 30, non-neoplastic = 20). We reviewed formal report and assessed the diagnostic performance for gallbladder cancer and differential diagnosis of neoplastic gallbladder polyps. Statistical analyses were performed using Chi-square tests.

Results: Sensitivity, specificity, PPV, and NPV for gallbladder cancer were 82.7%, 44.4%, 82.7%, and 44% in HRUS and 86.2%, 22.2%, 78.1%, and 33.3% in EUS. In stage accuracy, HRUS correctly diagnosed tumor stage in 14, overstage in 4, and understage in 11. EUS correctly diagnosed tumor stage in 14, overstage in 3, and understage in 12. Sensitivity, specificity, PPV, and NPV for neoplastic polyp were 80%, 80%, 86%, and 73% in HRUS and 73%, 85%, 88%, and 69% in EUS. Single (8/20 vs. 21/30, p = 0.035) and larger (52.5 + 13.2 vs. 66.1 + 10.3, p = 0.000) polyp were common in the neoplastic polyp, but there was no significant difference in age (52.5 + 13.2 vs. 66.1 + 10.3, p = .079).

Conclusion: Transabdominal HRUS showed comparable performance for the diagnosis of gallbladder cancer and differentiating neoplastic polyps compared with EUS. HRUS is also easy to use following our routine ultrasound examination.

SS 6.09

Adverse biliary events following orthotopic liver transplantation: evaluation with MR cholangiography and MR imaging at 3T

P. Boraschi, F. Donati, R. Gigoni, F. Pacciardi, G. Gherarducci, F. Filipponi, F. Falaschi, C. Bartolozzi; Pisa/IT

Purpose: To assess the diagnostic value of MR cholangiography (MRC) and MR imaging at 3T when evaluating biliary adverse events after orthotopic liver transplantation.

Material and Methods: A series of 116 transplant subjects with suspected biliary complications (impaired liver function tests and/or biliary abnormalities on ultrasound) underwent MRI at 3T (GE-DISCOVERY MR750; GE Healthcare). After the acquisition of axial 3D dual-echo T1-weighted images and T2-weighted sequences (propeller and SS-FSE), MRC was performed through coronal thin-slab 3D-FRFSE and coronal oblique thick-slab SSFSE T2w sequences. DW-MRI of the liver was also performed using an axial spin-echo echo-planar sequence with multiple b values (150, 500, 1000, 1500 sec/mm^2) in all diffusion directions. All MR images were blindly evaluated by two experienced abdominal radiologists in conference to determine the presence of biliary complications, whose final diagnosis was based on direct cholangiography, surgery and integrating clinical follow-up with ultrasound and/or MR findings.

Results: In twenty-four patients no biliary abnormality was observed. The remaining ninety-two subjects were affected by one or more of the following complications: ischemic-type biliary lesions (n=42), anastomotic strictures (n=20), ampullary dysfunction (n=18), anastomotic leakage (n=2), stones, sludge and casts (n=36). The sensitivity, specificity, PPV, NPV and diagnostic accuracy of the reviewers for the detection of all types of biliary complications were 99%, 91%, 98%, 95% and 97%, respectively.

Conclusion: MR cholangiography and MR imaging at 3T are reliable for detecting biliary complications after orthotopic liver transplantation.

11:00 - 12:30 **Goethe**

Scientific Session SS 7
Small bowel

SS 7.01

Contrast-enhanced MRI textural analysis in Crohn's disease is associated with histological markers of hypoxia and angiogenesis

G. Bhatnagar, J. Makanyanga, B. Ganeshan, A. Groves, M. Rodriguez-Justo, S.A. Taylor; London/UK

Purpose: Neoangiogenesis is well described in Crohn's disease (CD). Image textural analysis (TA) is related to angiogenic markers in some cancers. The purpose of the study was to explore TA of contrast-enhanced MRI in CD in comparison to hypoxia and angiogenesis markers.

Material and Methods: Before ileal resection, 7 CD patients (3 male), mean age 38 years (19–75) underwent 3T MR enterography including axial T1 THRIVE 330 s post IV gadolinium. ROIs were placed in bowel destined for resection and subsequently matched to 28 histological section sites using MRI of the resected specimen. Expression of hypoxia (HIF 1alpha) and angiogenesis (VEGF) markers in epithelium and leukocytes was recorded. TA features were acquired using TexRAD software, which utilises an image filtration histogram technique. TA parameters and the presence of histological markers were compared using a Mann–Whitney U test.

Results: At all filter levels, pixel density, SD of pixel density and mean of positive pixels were significantly reduced with VEGF expression (n = 20) vs. nonexpression (n = 8), e.g. median = 211 (filter 0) vs. 298, p = 0.003; median = 132 (filter 6) vs. 216, p = 0.004 and median = 184 (filter 6) vs. 417, p = 0.001, respectively. At the 2 mm filter, kurtosis was significantly increased with leucocyte VEGF expression (n = 13), median = 0.53 vs. median -0.23, p = 0.037; and with leucocyte HIF1alpha expression (n = 12); median 0.42 vs. median -0.19, p = 0.017.

Conclusion: Contrast-enhanced TA features show associations with markers of hypoxia and angiogenesis, raising the possibility of use in disease phenotyping.

SS 7.02

withdrawn by the authors

SS 7.03

Prospective analysis of quantified terminal ileal motility using magnetic resonance enterography as a biomarker of active inflammation in Crohn's disease

A. Plumb[1], A. Menys[1], C. Tutein Nolthenius[2], C.A.J. Puylaert[2], J.A.W. Tielbeek[2], J. Makanyanga[1], G. Bhatnagar[1], E. Gryspeerdt[1], N. Dikaios[1], D. Atkinson[1], J. Stoker[2], S.A. Taylor[1]; [1]London/UK, [2]Amsterdam/NL

Purpose: Retrospective data show a moderate negative correlation between terminal ileal (TI) motility and Crohn's disease (CD) activity. We aimed to confirm this in a larger, multisite prospective cohort.

Material and Methods: 95 patients with CD underwent 3T MR imaging at one of two sites (UK: 39 patients; The Netherlands: 56 patients) following oral 2% mannitol solution. 2D BTFE images were acquired and a polygonal ROI was drawn on the TI by an experienced radiologist blinded to clinical data. A validated optic-flow algorithm was used to quantify TI motility within this ROI. All patients subsequently underwent ileocolonoscopy (median 4 days after MRI) with TI biopsies graded by endoscopic acute inflammatory score (eAIS; 0–6). Spearman rank correlation and receiver-operating characteristic curves were used to examine the association between TI MRI motility and eAIS.

Results: Median eAIS was 1.4 (range 0–4) and motility 0.25 (0.042–0.858), with no significant differences between institutions. There was a statistically significant negative correlation between the eAIS and the motility score (rho = -0.54, p <0.001). The area under the ROC curve for TI motility to classify patients with eAIS ± 1 (i.e. any active inflammation) was 0.83 (95%CI: 0.74-0.93); and the optimal operating point of motility was 83% sensitive and 81% specific for detection of endoscopic inflammation.

Conclusion: MRI-quantified motility is sensitive and specific for histological TI inflammation. Furthermore, the degree of motility disturbance is negatively correlated with the severity of inflammation.

SS 7.04

Abdominal symptoms in Crohn's disease are associated with aberrant global small bowel motility in non-inflamed bowel

A. Plumb, A. Menys, J. Makanyanga, D. Pendse, G. Bhatnagar, D. Atkinson, S.A. Taylor; London/UK

Purpose: Mucosal healing often does not relieve abdominal symptoms in Crohn's disease (CD) and underlying enteric dysmotility has been postulated. This prospective study investigated the relationship between MRI-quantified small bowel (SB) motility and patient symptom burden.
Material and Methods: Fifty-four CD patients (median age 35 years, range 18–56) completed the Harvey Bradshaw Index (HBI) the day before MRI enterography. A coronal steady-state free precession breathhold motility sequence was acquired (1 s temporal resolution, slice thickness 1 cm), repeated to encompass the whole SB volume. An experienced radiologist drew regions of interest (ROI) in each cine block including all morphologically normal SB (i.e. excluding diseased bowel). A validated optic flow registration programme produced quantitative motility maps using the standard deviation of pixel Jacobian determinant. Global SB motility, expressed by mean and variance, correlated the HBI and components (well-being, pain, diarrhoea) using Spearman's rho for non-parametric data.
Results: Mean HBI was 3 (range 0–16) and motility mean and variance were 0.33 (0.18 to 0.51) and 0.01 (0.0014 to 0.034), respectively. There was no association between mean motility and HBI ($p > 0.05$). However motility variance was significantly negatively correlated with total HBI (rho = -0.45, $P < 0.001$), well-being (rho = -0.4, $p = 0.003$), pain (rho = -0.27, $p = 0.05$) and diarrhoea (rho= -0.4, $p = 0.0025$).
Conclusion: Reduced motility variance in morphologically normal small bowel correlates with patient symptoms, supporting underlying symptomatic pan-enteric dysmotility.

SS 7.05

Assessment of bowel wall enhancement for the diagnosis of intestinal ischemia in patients with small bowel obstruction: value of adding unenhanced CT to enhanced CT

A.-M. Chuong, L. Corno, H. Beaussier, I. Boulay Coletta, G. Chatellier, M. Zins; Paris/FR

Purpose: To evaluate the value of adding unenhanced (CT) to enhanced CT to assess decreased bowel-wall enhancement (DBE) for diagnosing intestinal ischemia in a large population with small bowel obstruction (SBO).
Material and Methods: Two gastro-intestinal radiologists (A and B) performed retrospectively independent blinded reviews of 164 unenhanced and enhanced CT scans of 158 consecutive patients admitted for SBO. The diagnosis of ischemia was established either by the surgical and/or the histopathologic findings (80 cases) or the clinical follow-up (84 cases). DBE was assessed according to a three-point confidence scale, using first enhanced CT images alone and one month later both unenhanced and enhanced CT images.
Results: In 41 of 164 (25%) CT scans, ischemia was confirmed at surgery and/or histopathologic finding examination. The sensitivity of DBE was improved between the 2 reviews for both readers A (46.3% [19/41] vs. 65.8% [27/41], p = 0,027) and B (56.1% [23/41] vs. 63.4% [26/41], p = 0.45). The positive likelihood ratio was increased for both readers A (11.4 vs. 13.5) and B (3.6 vs. 11.1). The mean confidence score was significantly ($p < 0.001$) increased: 2.27 vs. 2.88 and 1.70 vs. 2.77 for readers A and B, respectively. The inter-observer agreement improved from fair ($\kappa = 0.48$) to excellent ($\kappa = 0.89$).
Conclusion: Unenhanced CT, in addition to enhanced CT, increases the sensitivity, the positive likelihood ratio, the mean confidence score and the inter-observer agreement of the DBE sign for diagnosing intestinal ischemia complicating SBO.

SS 7.06

Changes in dynamic contrast-enhanced pharmacokinetic parameters reflect response to anti-TNF therapy in Crohn's disease

G. Bhatnagar, D. Prezzi, N. Dikaios, R. Vega, S.A. Taylor; London/UK

Purpose: To determine the utility of dynamic contrast enhancement (DCE) and diffusion-weighted (DWI) MRI in predicting and monitoring response to anti-TNF therapy in Crohn's disease (CD).
Material and Methods: 27 CD patients (mean age 29 years, 11 F) underwent MRI enterography with DCE-MRI (coronal VIBE, 24 measurements/127 s) (n = 21) and DWI-MRI (5 B values 0 to 600) (n = 17) before (median 5 days) and after (median 83 weeks) commencing anti-TNF therapy. An experienced radiologist placed ROIs in the most inflamed bowel segment, matching pre- and post-therapy scans. Tofts modelling derived K^{trans} (min-1), plasma volume v_p and extracellular extra vascular volume v_e. ADC was calculated. A gastroenterologist blinded to MRI defined patients as responders or non-responders at the time of follow-up MRI using physician global assessment (composite of clinical, biochemical, imaging and endoscopic parameters). Baseline MRI parameters and post-treatment changes were compared using Mann–Whitney test according to therapeutic response.
Results: Baseline K^{trans} was not significantly different between responders (n = 15, median 0.26) and non-responders (n = 6), median 0.12, $p = 0.38$. However there was a significant difference between K^{trans} change (median 52% fall in responders vs. median 165% increase in non-responders), $p = 0.038$. The remaining DCE parameters and ADC did not demonstrate any difference between responders and non-responders ($p > 0.05$).
Conclusion: DCE parameters nor ADC predict response to anti-TNF therapy. However responders show a significant fall in K^{trans} compared to non-responders suggesting enteric perfusion reflects therapeutic response.

SS 7.07

Histological validation of ultrasonic features of acute and chronic inflammation in enteric Crohn's disease using surgical resection specimens

G. Bhatnagar[1], S. Singh[1], A. Higginson[2], A. Windsor[1], M. Rodriguez-Justo[1], S.A. Taylor[1]; [1]London/UK, [2]Portsmouth/UK

Purpose: To explore the relationship between ultrasonic small bowel (SBUS) morphological observations in Crohn's disease (CD) and histopathological inflammation.
Material and Methods: SBUS was performed in 10 CD patients (mean age 34 years (17-69), 6 males, 4 females) immediately prior to small bowel resection. Ultrasound characteristics including mural, mucosal and submucosal thickness; submucosal echogenicity (1 = reduced, 2 = increased, 3 = increased with bands) and clarity (0 = normal,1 = ill defined); mesenteric echogenicity (increased with (1) or without (2) fat wrap, 3 = stratified, 4 = reduced) and clarity (1 = well defined, 2 = ill defined, 3 = focal ill defined); Doppler signal (1 = increased focal, 2 = increased general) were scored in 41 sections by an experienced radiologist. Matching with histological sampling was made via scanning of the resected specimen. Parameters of acute (neutrophil number, depth, cryptitis and destruction, ulceration) and chronic (chronic inflammatory cell number, transmural lymphoid aggregates and depth, perineural inflammation) inflammation were scored by a histopathologist. Ultrasound and histological parameters were correlated using Pearson's correlation coeffecient.
Results: Wall thickening, mesenteric fat echogenicity, and submucosal echogenicity correlated with acute and chronic inflammation ($R = 0.55$, $p = 0.01$, $R = 0.44$, $p = 0.01$ and $R = 0.40$, $p = 0.01$), respectively. Wall and mucosal thickening correlated with cryptitis ($R = 0.32$, $p = 0.05$, $R = 0.57$, $p = 0.01$ respectively). Wall thickness, submucosal echogenicity, submucosal thickness and mesenteric fat echogenicity correlated with crypt destruction ($R = 0.70$, $p = 0.01$, $R = 0.52$, $p = 0.01$, $R = 0.39$, $p = 0.05$ and $R = 0.50$, $p = 0.01$, respectively) and ulceration ($R = 0.70$, $p = 0.01$, $R = 0.55$, $p = 0.01$, $R = 0.38$, $p = 0.01$ and $R = 0.58$, $p = 0.01$, respectively).
Conclusion: Morphological SBUS observations appear predictive of both active and chronic inflammation, with some overlap between the two.

SS 7.08

Clinical significance of pneumatosis intestinalis: correlation of MDCT findings with patients' management and outcome

S. Schmidt Kobbe, J.-F. Knebel, R. Meuli, M.-O. Treyvaud; Lausanne/CH

Purpose: To evaluate the clinical significance of pneumatosis intestinalis (PI) including the influence on patients' management and outcome
Material and Methods: Two radiologists in consensus reviewed CT examinations of 149 consecutive emergency patients (53 women, mean age 64 years) with PI of the stomach (n = 4), small (n = 68) and/or large bowel wall (n = 96). The extent of PI and possibly associated portomesenteric venous gas (PMVG) were correlated with other radiological and clinical findings, management, and final diagnosis.
Results: The most frequent cause of PI (n = 80,53.7%) is bowel ischemia, followed by infection (n = 18, 12.1%), obstructive (n = 12,8.1%) and non-obstructive (n = 10, 6.7%) bowel dilatation, unknown aetiologies (n = 8,5.4%), drugs (n = 8,5.4%), inflammation (n = 7,4.7%), and others (n = 6,4%). The overall mortality was 41.6% (n = 62), mostly occurring with ischemia (n = 39, 54.2%) despite surgery in 51 patients (63.8%). The association of PMVG with PI significantly correlated with underlying ischemia ($p = 0.001$), like distribution of PMVG ($p = 0.004$). Absent bowel wall contrast enhancement was the only MDCT feature significantly associated with ischemia ($p = 7.484 \times 10^{-6}$), unlike other MDCT findings. The degree of calcified atherosclerosis, evaluated on MDCT, significantly correlated with underlying ischemia ($p = 0.024$), unlike other cardiovascular risk factors ($p = 0.723$). Patients with PI due to ischemia had a significantly higher fatal outcome ($p = 0.003$), regardless of their age.
Conclusion: In emergency patients, PI is caused by various intestinal disorders. Ischemia remains the most common aetiology with the highest mortality despite frequent surgery. PI with associated PMVG should alert the radiologist to think of ischemia.

SS 7.09

To operate or not to operate: the contribution of CT findings in small bowel obstruction in the determination of the need for surgery

D. Oncel, B. Polat; Izmir/TR

Purpose: To evalute the contribution of CT findings in small bowel obstruction in determining the need for surgery or conservative therapy.

Material and Methods: We evaluated retrospectively a total of 110 patients (62 males, 48 females, mean age 62 years) who were admitted to the Emergency Department between January 2012 and October 2014 and diagnosed with small bowel obstruction with CT findings and clinical evaluation. The significance of CT findings, such as transition zone, faeces sign, mesenteric edema, free peritoneal fluid, strangulation, closed loop obstruction and air in portal vein, in determining the need for surgical treatment were evaluated statistically.

Results: The patients were seperated into two groups as patients treated surgically (67 patients) and patients treated conservatively (43 patients). The transition zone sign, when observed alone, was not statistically significant in determining the need for surgery. But when observed together with at least one of the findings such as mesenteric edema or free peritoneal fluid, it had a higher specificity and was found to be statistically significant. Most of the patients with faeces sign were treated conservatively. However; strangulation, closed loop obstruction and air in the portal vein were considered as indications for surgery even if they were observed alone and found to be statistically significant.

Conclusion: CT provides an important contribution to the diagnosis of small bowel obstruction and also in the guidance of appropriate treatment.

SS 7.10

Closed-loop small-bowel obstruction: precise diagnosis with multiplanar MDCT imaging with specific signs

K. Hekimoglu, S. Arslan, M. Kirnap, M. Coskun; Ankara/TR

Purpose: Closed-loop obstruction (CLO) is an uncommon clinical entity. The length of the CLO is variable, ranging from a short segment to several loops. Early diagnosis of this abnormality remains crucial in the decision whether to use surgical or medical management. Multidetector computed tomography (MDCT) has been shown to be useful in revealing the site and the cause of the obstruction with multiplanar imaging capability. The purpose of this study was to determine the diagnostic impact of multiplanar evaluation of MDCT in patients with CLO.

Material and Methods: The MDCT findings of 53 patients with clinically suspected CLO were evaluated prospectively. MDCT exams were performed with 16 slices scanner with 3-dimensional reformatting at Workstation for multiplanar evaluation of CLO with specific MDCT findings.The diagnosis was correlated with the surgery.

Results: Thirty-one patients were diagnosed with CLO with specific signs. All of them had dilated U/C- shaped bowel loops. Twenty patients had beak sign, ten had radial vessels distribution, eight had pneumatosis, four of them had whirl sign, and three patients had internal hernia which were demonstrated on coronal and sagittal multiplanar imaging. Twenty-five of the 31 patients underwent surgery. Adhesions were demonstrated to be the most important reasons for the CLO by surgery. Multiplanar MDCT had 94% sensitivity, 90% specificity, and 95% accuracy for the correct diagnosis of CLO.

Conclusion: Multiplanar MDCT imaging is a valuable method for demonstrating the specific signs and precise diagnosis of CLO.

11:00 - 12:30 **Darwin 3**

Scientific Session SS 8

Rectum and pelvic floor disorders

SS 8.01

Magnetization transfer imaging as a tool to quantify post-chemoradiation fibrosis in rectal cancer: does it help in the assessment of tumor response?

M.H. Martens[1], D.M.J. Lambregts[1], N. Papanikolaou[2], S. Alefantinou[2], M. Maas[1], K. Marias[2], G.C. Manikis[2], R.G. Riedl[1], G.L. Beets[1], R.G.H. Beets-Tan[1]; [1]Maastricht/NL, [2]Heraklion/GR

Purpose: Single-slice magnetization transfer (MT) imaging has shown promising results to quantify post-radiation fibrosis. The aim of the study was to evaluate the value of multislice MT imaging (including histogram data analysis) of the whole tumor volume to assess tumor response after chemoradiotherapy by comparing the magnetization transfer ratio (MTR) with the tumor regression grade (TRG) assessed at histopathology.

Material and Methods: 30 patients with locally advanced rectal cancer underwent a restaging MRI (1.5 T) ±8 weeks post-chemoradiotherapy. MRI included a multislice MT sequence, covering the entire tumor bed. Two independent readers (R1; R2) delineated regions of interest on the MTR map, covering all potential remaining tumor and fibrotic areas. Diagnostic performance was calculated using ROC curves for the mean MTR and corresponding histogram parameters (minimum, maximum, median, standard deviation, skewness, kurtosis, and 5–30–70–95th percentiles), using histological TRG 1–2 (good response) versus TRG 3–5 (poor response) as the reference standard.

Results: Mean MTR rendered AUCs of 0.65 (R1) and 0.87 (R2) to differentiate between TRG1-2 and TRG3-5. The best results were obtained for the 95th percentile (AUC 0.75 (R1) and 0.88 (R2)). Interobserver agreement was moderate (ICC 0.50) for mean MTR and good (ICC 0.80) for the 95th percentile.

Conclusion: Magnetization transfer imaging is a promising tool to quantify post-chemoradiation fibrosis in rectal cancer. Particularly, the 95th percentile of the histogram results in AUCs up to 0.88 to discriminate patients with a good tumor response.

SS 8.02

MR relative mean T2-signal intensity as a possible marker of response to neoadjuvant therapy and distant recurrence in moderate- to high-risk rectal cancer

I. Santiago, R. Rocha, R. Theias, A. Gomes, A. Costa, T. Fiuza, V. Nunes; Amadora/PT

Purpose: To evaluate the relation between staging MR T2-signal intensity-derived parameters, response to neoadjuvant therapy and long-term patient outcome in moderate-/high-risk rectal cancer patients.

Material and Methods: All rectal cancer patients with a preoperative staging pelvic MR who underwent long-course chemoradiotherapy (CRT) followed by total mesorectal excision (TME), diagnosed at our Institution between 01-01-2004 and 02-17-2014, were included, totaling 47 patients (64.8 ± 13.2years, 30 males). Staging MR high-resolution T2-weighted images were retrospectively evaluated by a single radiologist with 5 years of experience in pelvic MR. Signal intensity distribution was analyzed using representative regions of interest with a minimum area of 50 mm^2 (ROI50) (TROI50) and total tumor volume (TV); ROI50 of dense skeletal muscle was used as reference. Relative minimum, maximum and mean signal intensity values were calculated both for TROI50 and TV. Histopathologic and patient long-term outcome variables were analyzed.

Results: A significant association between relative mean signal intensity using both TROI50 (2.43 ± 0.96 vs. 3.13 ± 0.97; p = 0.029) and TV (2,50 ± 1,17 vs. 3.37 ± 0.95; p = 0.009) on staging MR and distant disease recurrence was found. Relative mean signal intensities using both TROI50 and TV were significantly correlated to post-CRT tumor differentiation (r = -0.310, p = 0,037; r = -0.454, p = 0.002, respectively). Post-CRT tumor differentiation grade was higher in patients with distant recurrence (p = 0.012).

Conclusion: Staging MR T2-derived relative mean tumor signal intensity may be an important marker of response to CRT and distant recurrence in moderate- to high-risk rectal cancer patients.

SS 8.03

Is diffusion-weighted imaging helpful in evaluating extramural tumor invasion in primary rectal cancer?

S.H. Kim, J.-H. Yoon, Y. Lee; Busan/KR

Purpose: To evaluate the added value of diffusion-weighted imaging (DWI) to T2-weighted images (T2WI) for evaluating extramural tumor invasion in patients with primary rectal cancer.

Material and Methods: The institutional review board approved this retrospective study and waived the informed consent from patients. Seventy-two patients who underwent 1.5-T MRI including DWI (b = 0, 1000 s/mm^2) and subsequent surgery were included in this study. To evaluate the additional value of DWI, two blinded radiologists independently read the T2WI first, and then the combined set of T2WI and DWI. They recorded their confidence level using a 5-point scale regarding extramural tumor invasion. The diagnostic accuracy was calculated for each reviewer using a receiver operating characteristic (ROC) curve analysis. To evaluate the added value of DWI to T2WI for extramural tumor invasion, a pairwise comparison of ROC curves was used. Histopathologic results served as the reference standard for extramural tumor invasion.

Results: The study population consisted of T1 (n = 11), T2 (n = 15), T3 (n = 43) and T4 (n = 3). The area under the ROC curve did not significantly increase after adding DWI to T2WI (for reader 1, from 0.961 to 0.982, P = 0.2118; for reader 2, from 0.931 to 0.929, P = 0.8770).

Conclusion: Adding DWI to T2WI showed no additional diagnostic benefit for evaluating extramural tumor invasion in patients with primary rectal cancer.

SS 8.04

Follow-up with MRI of rectal cancer treated by TEM: recurrence detection and inter-observer reproducibility

M. Maas[1], M.H. Martens[1], C. Van Berlo[1], W. Deserno[2], J. Leijtens[2], G.L. Beets[1], R.G.H. Beets-Tan[1]; [1]Maastricht/NL, [2]Roermond/NL

Purpose: Small rectal cancers can be treated with transanal endoscopic microsurgery (TEM). Post-operative changes make follow-up with MRI challenging. The aim of the study was to evaluate post-TEM-MRI at different time points for recurrence detection and assess interobserver reproducibility.

Material and Methods: 38 patients underwent TEM (8 after CRT). MRI was performed every 3-4 months during follow-up and consisted of T2W-MRI ± DWI. 122 MRIs were performed with a mean of 3 MRI per patient. Seven patients recurred. MRIs were evaluated by 2 readers with different experience by confidence level (CL), scoring for recurrence, and reproducibility was evaluated with weighted-κ-statistics.

Results: For all MRIs AUC for recurrence detection was 0.79 and 0.73 for T2W-MRI and 0.69 and 0.76 for DWI. During follow-up, AUC increased from 0.55 to 0.67 at T2W-MRI and from 0.57 to 0.73 for the expert. Interobserver reproducibility increased during follow-up for T2W-MRI from κ0.127 to 0.429. For DWI, reproducibility was fair (κ0.38–0.40). Nodal staging had stable moderate reproducibility (κ0 .53). At the first post-TEM-MRI higher CL scores were given at DWI than at T2W-MRI, and this difference disappeared from the second MRI. The number of equivocal scores decreased during follow-up. Isointensity in bowel wall and/or mesorectal fat was predictive for recurrence.

Conclusion: The first post-TEM-MRI is difficult to assess. During follow-up, the accuracy for recurrence detection increases, because of comparison with earlier studies. There is a learning curve during follow-up that leads to more certainty. Reproducibility is fair–moderate, but increases during follow-up. Isointensity in bowel wall and/or mesorectal fat was predictive of recurrence.

SS 8.05

Automated and semi-automated diffusion-weighted MRI tumour volumetry to assess response to neoadjuvant therapy in rectal cancer

M.M. Van Heeswijk[1], D.M.J. Lambregts[1], S. Oei[1], S.-X. Rao[2], C. De Graaff[1], G.L. Beets[1], R.A. Vliegen[3], R.G.H. Beets-Tan[1]; [1]Maastricht/NL, [2]Shanghai/CN, [3]Heerlen/NL

Purpose: DWI tumour volumetry using manual tumour delineation has shown promise to assess tumour response to chemoradiotherapy (CRT). Manual delineation is, however, time consuming and thus unpractical in clinics. The aim of the study was to assess the validity and reproducibility of automated and semi-automated DWI tumour volumetry compared to manual measurements.

Material and Methods: Seventy-nine rectal cancer patients underwent pre- and post-CRT DWI at 1.5T (highest b-value b1000–1100). Volumes were measured in threefold by 2 observers: [1] manual delineation, [2] automated using a "region-growing" model, [3] semi-automated by manual adjustment of method 2. Volumes (+ time to complete measurements) were compared between the different methods/observers.

Results: Mean volumes (+ measurement time) pre-CRT were: 27.4 cm^3 (110 s) for manual delineation, 27.0 cm^3 for automated measurements and 25.9 cm^3(77 s) for semi-automated measurements. After CRT, the numbers were 3.3 cm^3(86 s), 3.4 cm^{3}and 3.7 cm^3(77 s). Compared to manual delineation, intraclass correlation coefficient (ICC) for the automated method was 0.93 pre-CRT and 0.61 post-CRT. For the semi-automated method ICCs (compared to manual delineation) were 0.96 pre-CRT and 0.86 post-CRT. ICC between the two observers pre-CRT/post-CRT was 0.86/0.71 for manual delineation, 0.82/0.60 for automated measurements and 0.91/0.73 for semi-automated measurements.

Conclusion: Considering its reproducibility compared to manual delineation as well as between observers, semi-automated DWI tumour volumetry is a promising and time-saving alternative to manual tumour delineation.

SS 8.06

Dynamic contrast enhancement MRI combined with diffusion-weighted imaging for rectal cancer response assessment after neo-adjuvant chemoradiation

P.P. Arcuri[1], S. Roccia[2], P. Castaldo[1], A. Pingitore[3], S. Molica[1], G. Fodero[1]; [1]Catanzaro/IT, [2]Lamezia Terme/IT, [3]London/UK

Purpose: This study retrospectively assessed the predictive potential of DCE-MRI combined with DWI for selecting patients with a favourable pathological response in rectal cancer after neo-adjuvant CRT.

Material and Methods: We studied retrospectively 35 patients affected by locally advanced rectal cancer. The study consisted of two MRI exams, one pre-CRT and the other pre-surgery. MR imaging pre-contrast included T1-W TSE, T2-W TS and DWI using b-values of 0, 600 and 1000 s/mm^2. Dynamic images were obtained by axial fat-sat THRIVE sequence. Fifteen dynamic series were acquired at 0–240th s. Surgery was performed in all patients. Histopathology was considered as standard of reference for statistical evaluation. Quantitative evaluation of DCE-MRI was performed by SI–time curves, calculating the wash-in rate (WIR), maximum relative enhancement (RME), time-to-peak enhancement (TTP) and wash-out rate (WOR). For the quantitative analysis of DWI, ADC values of the tumor were calculated and correlated with histologic grade. The values were compared using the Mann–Whitney U test.

Results: Agreement between DWI and pathology was found in 21/35 patients (60%). 9 cases were understaged and 5 were overstaged. Agreement between post-contrast and pathology was found in 23/35 patients (66%). 5 cases were understaged and 7 were overstaged. DWI obtained sensitivity 74%, specificity 69%, PPV 41%, NPV 85% and accuracy 61%. Post-contrast obtained sensitivity 98%, specificity 81%, PPV=58, NPV=94 and accuracy 83%.

Conclusion: In conclusion, this study shows that the addition of DWI to a DCE-MRI improves the performance and confidence of radiologists in selecting patients with a pathological complete tumor response after chemoradiation for locally advanced rectal cancer.

SS 8.07

Which images are clinically significant findings in constipated patients with pelvic floor dyssynergia? A guide to surgery

H.J. Jeon, M.K. Seong, U.C. Park, Y.J. Kim, M.H. Yu, S.I. Jung, S.W. Park; Seoul/KR

Purpose: The current study was designed to assess the defecographic characteristics and clinical significance of pelvic floor dyssynergia (PFD). Moreover, the standardized parameters for the diagnosis of PFD were analysed.

Material and Methods: Studies included defecography and cinedefecography (n = 553), anal manometry (n = 237), and colonic transit time study (n = 85). 317 patients (57.1%) were found to have pelvic outlet obstruction. Diagnostic criteria were based on 3 factors: 1) persistent angulation of the posterior rectal wall, 2) poor emptying of the rectum, 3) poor opening of the anal canal. PFD was evaluated by 3 different doctors. Cronbach's α test for reliability was used to define the internal consistency of the findings. Cohen's k test was used to define agreements between each of the defecographic findings and results of other tests.

Results: Findings were categorized into three factors: 1) persistent angulation of the posterior rectal wall in 33 (34%); 2) poor emptying of the rectum in 61 (63%); 3) poor opening of the anal canal in 33 (34%). Internal consistency of defecographic three factors was good (α = 0.78). Agreements between each defecographic findings and each result of other tests were all poor. Defecography as imaging test has been considered to be a sensitive and specific measurement of PFD when it documents the three diagnostic factors.

Conclusion: The present series provided different anatomical, functional and clinical profiles of patients with PFD. Parameters to define the internal consistency of defecographic findings were useful for the diagnosis of PFD.

SS 8.08
Role of conventional evacuation proctography in the evaluation of faecal evacuation disorder with anorectal manometric correlation
A. Chatterjee, S. Kumar; Lucknow/IN

Purpose: To evaluate the role of conventional evacuation proctography (EP) in the evaluation of faecal evacuation disorder (FED) and to find any correlation with the findings of anorectal manometry.
Material and Methods: Conventional EP was performed in consecutive 36 patients with clinical diagnosis of faecal evacuation disorders. Anorectal angle (ARA) and the distance between the anorectal junction and pubococcygeal line were recorded at rest and during squeezing, straining and defecation. Anorectal manometry and balloon evacuation test (BET) were done in 28 patients and the findings recorded.
Results: Percentage change in ARA from rest to defecation was lower in patients with manometric diagnosis of anismus and abnormal BET (average 16%, range: 0–41%) than in patients without the diagnosis (average 23%, range: 5–84%). In the first group, 3 patients had paradoxical increase in ARA during straining. There was mild positive correlation (correlation co-efficient 0.3) between the squeeze pressure of the external sphincter and percentage of decrease in ARA from rest to squeeze. No correlation was obtained between resting ARA and basal sphincter pressure. Additional diagnoses made in EP were rectal descent (n = 18), anterior rectocele (n = 5) and intussusception (n = 4). Among patients with rectal descent, 3 patients (16.7%) had a descent only during straining or defecation.
Conclusion: Conventional EP has good correlation with anorectal manometry in the evaluation of FED and also demonstrates additional findings such as rectal descent, rectocele and intussusception.

SS 8.09
Comparison between two different magnetic resonance defecography techniques for evaluating pelvic floor disorders: air-balloon versus gel rectal filling
F. Maccioni, V. Buonocore, N. Al Ansari, C. Catalano; Rome/IT

Purpose: To compare 2 different functional MRI techniques, based on different rectal filling techniques, for evaluation of pelvic floor disorders.
Material and Methods: 26 patients with pelvic floor dysfunctions underwent 2 different rectal filling techniques during the same procedure at 1.5 T. The first MRI technique, the "air-balloon" technique (AB-DPF MRI) is based on the distension of the rectum with room air (Foley catheter); the other one, the gel-filling technique (GF-DPF MRI) is based on the use of ultrasound gel for rectal filling. Images were acquired at rest, during prolonged contraction and straining with balanced or T2-weighted sequences on different planes. For both MR techniques, rectal prolapse, rectocele, cystocele and colpocele were evaluated in all patients by 2 radiologists and graded. For intussusception and enterocele, only the presence or the absence was reported.
Results: GF-DPF MR showed 25 rectal prolapses, 21 rectoceles, 20 cystoceles, 8 colpoceles, 21 intussusceptions and 7 enteroceles. AB-DPF MRI showed 24 rectal prolapses, 23 rectoceles, 20 cystoceles, 10 colpoceles, 18 intussusceptions and 11 enteroceles. The air-balloon technique missed 1 rectal prolapse; a higher number of rectoceles, colpoceles and enteroceles were depicted with AB-DPF MRI. The capability of the 2 techniques for intussusception was not statistically different (p = 0,12).
Conclusion: In our experience, both techniques are valuable and show favorable and unfavorable aspects; they may be associated in the same imaging session to reach maximal accuracy.

SS 8.10
The relationship between the severity of venous calcifications and clinical symptoms of phlebosclerotic colitis
C.S. Yen, C.A. Liu, N.-C. Chiu, Y.-Y. Chiou, Y.-H. Chou, C.-Y. Chang; Taipei/TW

Purpose: To investigate the correlation between the severity of venous calcifications and clinical symptoms of phlebosclerotic colitis.
Material and Methods: This is a retrospective study. The data, including the numbers of episodes of active disease, were collected from medical records in Taipei Veterans General hospital and Wei Gong Memorial hospital in Taiwan between January 2005 and December 2014. The severity of calcifications at tributaries of portal vein was measured by a Scoring System of Calcification of Phlebosclerotic colitis.
Results: From 2005 to 2014, 12 patients with a mean age 61.8 ± 11.5 years were enrolled with imaging features of phlebosclerotic colitis at Taipei Veterans General hospital and Wei Gong Memorial hospital. The episodes of active disease ranged from 0 to 27 (1 ± 1.75, median ± interquartile). The calculated scores using the scoring system ranged from 9 to 33 (18 ± 13, median ± interquartile). The Spearman's correlation revealed that the numbers of episodes of active disease of phlebosclerotic colitis had significantly positive correlation with the severity of the calcifications of mesenteric veins (rho = 0.619, P < 0.05).
Conclusion: The extent of mesenteric venous calcifications has positive relationship with the frequency of clinical symptoms of active disease in the patients with phlebosclerotic colitis.

11:00 - 12:30 **Darwin 4**

Scientific Session SS 9
Bile ducts: diagnosis and intervention

SS 9.01
MRI findings of cystic fibrosis-associated liver disease: preliminary results
S. Poetter-Lang, D. Muin, N. Bastati-Huber, D. Tamandl, J. Hodge, A. Ba-Ssalamah; Vienna/AT

Purpose: To evaluate the early morphologic features in patients with cystic fibrosis (CF)-associated liver disease (CFLD) using gadoxetic acid-enhanced MRI.
Material and Methods: Twenty-two CF patients, 12 females and 10 males (mean age 30.8 years), who underwent gadoxetic acid-enhanced MRI, were included. Two radiologists assessed in consensus the MRI findings including the presence of fatty infiltration, liver fibrosis or cirrhosis, splenomegaly, and gallbladder and bile duct alterations. Furthermore, the degree of liver enhancement and homogeneity after contrast medium injection as well as the excretion was scored. These findings were compared to that of a control group, consisting of 20 patients matched in age and gender. Additionally, laboratory tests as well as clinical data and histopathological results, when available, were correlated with the MRI findings.
Results: The splenic volume was significantly higher in the CF group compared to the control group (p <0.05), while the liver volume did not differ significantly. The degree of hepatic steatosis as well as periportal fat deposition was higher in the CF group (p <0.05). Additionally, periportal tracking and bile duct abnormalities were detected significantly more often in the CF group (p <0.05). Furthermore, the number of gallbladder abnormalities was significantly higher in the CF group. However, the degree of hepatobiliary uptake and excretion of gadoxetic acid as well as the laboratory parameters were not significantly different between the groups.
Conclusion: Gadoxetic acid-enhanced MRI is an emerging tool to detect early hepatobiliary involvement in cystic fibrosis patients.

SS 9.02
Introducing a pathway for suspected obstructive jaundice to a district general hospital with MRCP as the first investigation
J.V. Macpherson[1], D. Shetty[2], M. Meller[1], A. Sanderson[1]; [1]Barnstaple Devon/UK, [2]Truro/UK

Purpose: To evaluate the introduction of a pathway for suspected obstructive jaundice, with magnetic resonance cholangiopancreatography (MRCP) as the first test. The aim of the jaundice pathway was to streamline the imaging pathway for patients, whether they were inpatients or outpatients, and to reduce time from referral to relief of biliary obstruction.
Material and Methods: Patients with jaundice, taken to be a bilirubin of greater than 50 µmol/L, undergoing endoscopic retrograde cholangiopancreatography (ERCP) or percutaneous transhepatic cholangiography (PTC) were evaluated before and after the pathway was introduced. A standard of the pathway was that MRCPs should be performed within 2 working days. Day 0 was the first date a request for imaging was made. The time in days to ERCP/PTC in 2009 was compared with that in 2013.
Results: The study population consisted of 55 patients in 2009 and 45 in 2013. Of the patients who underwent an MRCP, the scan was performed within 2 working days of request in 33/37 (89%) patients in 2009 and 37/37 (100%) patients in 2013. The time to first ERCP/PTC from day 0 was a mean and median of 9.7 days and 3 days in 2009 and 3.9 days and 2 days in 2013.
Conclusion: The introduction of the jaundice pathway has reduced the time to first biliary drainage procedure. 18/55 (32%) in 2009 waited more than a week for their ERCP/PTC compared with 5/45 (11%) in 2013.

SS 9.03
Value and accuracy of multidetector computed tomography in obstructive jaundice
R.P. Mathew, M. Abdunnisar, H.B. Suresh; Mangalore/IN

Purpose: To find out the role of multidetector computed tomography in the evaluation of obstructive jaundice with respect to: a. cause of the obstruction and b. level of the obstruction.
Material and Methods: This was a prospective study conducted over a period of one year from August 2013 to August 2014. Data were collected from 50 patients with clinically suspected obstructive jaundice who were evaluated with MDCT (GE BRIGHT SPEED 16 SLICE). CT findings were correlated with histopathology/surgical findings/ERCP findings as applicable. Patients with non-obstructive jaundice and with contrast hypersensitivity were excluded from the study. Statistical analysis included sensitivity, specificity, positive predictive value, negative predictive value, and kappa statistics.

Results: Majority of the patients fell into the age group of 41–60 years. The major cause for obstructive jaundice was choledocholithiasis. There was 100% correlation between the CT diagnosis and the final diagnosis regarding the level and type of obstruction. MDCT was able to determine the cause of obstruction with an accuracy of 96%. The sensitivity for diagnosing cholangiocarcinoma was 88.9% and the diagnosis of choledocholithiasis gave a sensitivity of 100% and specificity of 97.4%. There was 100% sensitivity and specificity in diagnosing pancreatic head mass as cause for biliary obstruction.
Conclusion: MDCT with good reformatting techniques has excellent accuracy in the evaluation obstructive jaundice with regards to level and cause of obstruction.

SS 9.04

Usefulness of virtual non-enhanced image derived from dual-energy computed tomography in evaluation of gallstone diseases

Y.H. Lee, H.A. Lee, K.H. Yoon, Y. Cha; Iksan/KR

Purpose: To compare virtual non-enhanced (VNE) images using dual-energy computed tomography (DECT) with true non-enhanced (TNE) images in the detection of gallstones.
Material and Methods: We enrolled 112 patients (70 men, 42 women; mean age, 62 years) with clinically suspected acute cholecystitis or gallstone, who underwent DECT. Semi-quantitative infrared spectroscopy (FTIR) was performed to confirm the chemical composition of gallstones. The following parameters were evaluated on VNE and TNE images: mean attenuation values of liver, gallbladder, gallstone; stone size; contrast-to-noise ratio (CNR) of gallstone to bile; effective radiation dose; visibility, number, density of gallstones; image quality. The acceptability of VNE images as a replacement for TNE images was determined.
Results: FTIR identified 40 cholesterol gallstones (21 patients) and 43 calcium gallstones (24 patients). Both types of stones were smaller on VNE than TNE images. The mean CNR of cholesterol stones was 5.24 ± 4.47 and 3.46 ± 2.45 ($p = 0.001$), and mean CNR of calcium stones was 21.18 ± 12.93 and 25.92 ± 16.11 ($p < 0.001$) on VNE and TNE images, respectively. The visibility of cholesterol stones was higher on VNE images, and despite more image noise acceptability scores were high. The estimated effective radiation dose reduction was 34.87% and 48.85% on triple and dual phase, respectively.
Conclusion: VNE images allow better visualization of cholesterol gallstones with reasonable image quality and low radiation exposure.

SS 9.05

Review of clinical indication and findings based on Magnetic Resonance Cholangiopancreatography with comparative assessment of the diagnostic accuracy of ultrasound

K. Mullin, R. Singh; Derby/UK

Purpose: The use of Magnetic Resonance Cholangiopancreatography (MRCP) has steadily increased in the investigation of biliary disease and in some cases has become the first-line investigation. The aim of this study is to assess the diagnostic accuracy of ultrasound in comparison to MRCP findings and review the referral criteria for MRCP to identify if there is a need for formal guidelines to be introduced.
Material and Methods: We performed a retrospective study of MRCP examinations (n=595) performed in 2013 at Royal Derby Hospital using electronic records. The MRCP findings were correlated with recent abdominal ultrasound (within 6 weeks). Clinical referral details for all MRCP studies were reviewed.
Results: In cases where both MRCP and ultrasound were performed, 11% of both reported normal findings with 47% of subsequent MRCP studies yielding no clinically significant additional information. Ultrasound was shown to have a sensitivity of 59% and specificity of 78% in the detection of biliary dilatation. 303 MRCP cases did not have a recent ultrasound, with 40% reported as normal and 25% demonstrating gallstone disease. A wide range of referral details were identified.
Conclusion: Ultrasound should still be considered a first-line investigation in the detection of biliary tree dilatation and routine MRCP should not be used to detect the presence of gallstones.The introduction of referral guidelines may enable a more consistent imaging pathway for investigation of biliary disease.

SS 9.06

Role of magnetic resonance cholangiopancreatography in the evaluation of patients with post-cholecystectomy syndrome

D.E. Geylan, A.C. Yalçin, M. Uçar, F. Öncü, N. Tokgoz; Ankara/TR

Purpose: The aim of this study was to assess the role of magnetic resonance cholangiopancreatography (MRCP) in the evaluation of patients with post-cholescystectomy syndrome (PCS).
Material and Methods: A retrospective study over a period of 3 years (between January 2011 and November 2014) was performed with 153 patients who have cholecystectomy history and recurrent upper abdominal symptoms. The clinical data from hospital's electronic medical record system and MRCP images of patients were retrieved and evaluated. The definitive diagnosis was confirmed by patient history, physical examination, laboratory tests, US, MRCP and ERCP all together and it was compared to MRCP findings to assess accuracy of MRCP alone in PCS.
Results: The patient group consisted of 24 early PCS and 129 late PCS. 34 of patients had extrabiliary causes (gastroesophageal reflux, peptic ulcer disease etc), 119 of patients had biliary causes (choledocolithiasis, cystic duct stump, sphincter dysfunction, strictures, malignancy, etc). MRCP yielded an overall sensitivity of 98%, specificity of 92%, accuracy of 94% for the diagnosis of causes of PCS.
Conclusion: MRCP is useful and reliable method in the diagnosis of causes of PCS and should be recommended for a better management of these patients.

SS 9.07

Evaluating the effectiveness of percutaneous image-guided drainage in patients with perforation of the gall bladder

K. Chokkappan, S. Srinivasan, H.S. Teh, R. Lohan, T.H. Khai, R. Chung, S.B. Babu; Singapore/SG

Purpose: To assess the effectiveness of image-guided percutaneous drainage in patients with perforation of the gall bladder.
Material and Methods: From 2011 to 2013, 16 patients who presented with perforated gall bladder underwent percutaneous drainage for the treatment. Twelve patients underwent (transhepatic/transperitoneal) percutaneous cholecystostomy and 4 patients underwent drainage of the collection which was communicating with the perforated gall bladder. Procedure was done with ultrasonography (US) or US and fluoroscopic guidance. Clinical follow-up was done.
Results: Patients age ranged from 41 to 88 years (mean 69 years). 14 patients (87.5%, 14/16) were males. Among them, type 2 perforation was seen in 14 (87.5%, 14/16) patients. Technical success was achieved in all sixteen patients (100%, 16/16) and all patients had resolution of acute symptoms. There were no procedure-related complications. Four patients (22%, 4/18) later underwent interval cholecystectomy. There was no procedure-related mortality. Two patients (2/18, 11%) died due to unrelated illness (one with metastatic gastric carcinoma and the other patient with recurrent sepsis on subsequent admission). The limitation of the study is that we do have age-matched control of patients who had laparotomy or laparoscopic treatments for comparison.
Conclusion: Percutaneous image-guided drainage is a safe and effective treatment option for patients with perforated gall bladder and should be considered as a first-line treatment. If needed, cholecystectomy can be planned after the resolution of the acute episode.

SS 9.08

Pre-operative percutaneous transhepatic biliary drainage in choledochal cysts

S. Kumar, A. Gupta, A. Chatterji; Lucknown/IN

Purpose: To evaluate the role of percutaneous transhepatic biliary drainage (PTBD) in the perioperative management of choledochal cysts.
Material and Methods: Retrospective evaluation of the records of 10 consecutive patients with choledochal cysts were performed who were treated with PTBD in the pre-operative period.
Results: 6 patients had type 1 and 4 patients had type IVA choledochal cysts. Age of the patients varied from 5 to 60 years. Indication of drainage was cholangitis in 5 patients and reduction of hyperbilirubinemia (average 14 mg/dL, range 9–21 mg/dL) in 5 patients. In all cases, 8–10 F Malecot catheters were inserted under ultrasound and fluoroscopic guidance using Seldinger technique. All procedures were done in local anaesthesia and conscious sedation. In 8 patients, segment 3 hepatic duct was drained and in one case, segment 8 duct was drained. In 2 patients, internalisation using ring biliary catheter (8F) was done prior to surgery. 2 patients were lost to follow-up. Definitive surgery was done in 8 patients after an average time period of 36.75 days (range 20–91 days) after the cholangitis subsided or hyperbilirubinemia is controlled. Catheter dislodgement occurred in 1 patient and self-resolving hemorrhage occurred in 1 patient.
Conclusion: Patients with choledochal cysts presenting with cholangitis and/or very high bilirubin levels may be safely and effectively managed by PTBD with or without internalisation using ring biliary catheters.

SS 9.09

Feasibility and safety of intraoperative electrochemotherapy in locally advanced pancreatic tumor: a preliminary experience

V. Granata, R. Fusco, S. Filice, R. Palaia, F. Izzo, A. Petrillo; Naples/IT

Purpose: Electrochemotherapy (ECT) is an effective treatment for various cutaneous tumors and could be translated into treatment of deep-seated tumors. With this aim, a prospective clinical phase I/II study was conducted to evaluate feasibility and safety of intraoperative ECT in locally advanced pancreatic adenocarcinoma: the preliminary results were reported in this study. The secondary endpoint was to assess treatment response in terms of morphological and functional criteria based on Magnetic Resonance Imaging.
Material and Methods: Eleven consecutive patients were enrolled, recruited in a clinical phase I/II study approved by Ethical Committee of National Cancer Institute G. Pascale Foundation—IRCCS of Naples. Electrochemotherapy with bleomycin was performed during open surgery. All patients underwent MR and CT scan, before and after ECT treatment, using morphological and functional imaging. RECIST criteria were used to evaluate ECT response on CT and MR images. Functional parameters were also used to evaluate ECT response on MR images.
Results: No acute and/or post-operative serious adverse events related to ECT were observed. All patients showed significant changes in the values of wash-in, wash-out, ADC and D * a decrease of at least 30% of the value of the parameter. The perfusion was the only parameter to show a decrease with a lower average value of 20%.
Conclusion: ECT proved to be feasible and safe treatment. DCE-MRI is more suitable to assess treatment response than CT.

11:00 - 12:30 **Darwin 5**

Scientific Session SS 10

Diffuse liver disease II

SS 10.01

withdrawn by the authors

SS 10.02

MR magnetization transfer in liver imaging: influence of liver steatosis and fibrosis

L. Tselikas[1], M. Roux[1], R. Amathieu[1], B. Robert[2], I. Leclercq[3], S. Lotersztajn[4], F. Pigneur[1], J. Calderaro[1], M. Djabbari[1], A. Mallat[1], A. Rahmouni[1], A. Luciani[1]; [1]Creteil/FR, [2]Saint Denis/FR, [3]Woluwe-Saint Lambert/BE, [4]Paris/FR

Purpose: To develop and optimize a Magnetization Transfer (MT) sequence designed to be applied ex vivo, on a murine model and in humans, to assess the influence of liver steatosis and fibrosis on the MT Ratio (MTR).
Material and Methods: A MT sequence was tested at 1.5T and 3T in 3 distinct ex vivo samples—including fresh liver, fat liver and muscle—as well as in a murine model of liver steatosis (Foz/foz obese mice and controls), and in 100 patients with documented liver cirrhosis as well as in 161 control patients. Liver fat was determined by T2* and T1-corrected 1H spectroscopy. The MTR was assessed and compared in between tissues (Mann–Whitney, Anova or Kruskal–Wallis when appropriate). The influence of the B0 field and offset, liver steatosis and fibrosis were assessed in sub-group analysis.
Results: Ex vivo, the MTR in fresh muscle was significantly superior to that of fresh liver and to that of fat liver ($p<0.02$). The MTR significantly increased with reduced offset and with increased B0. Steatotic foz/foz mice showed significantly reduced MTR compared to controls ($p<0.01$). In humans, neither fibrosis nor the levels of steatosis had an influence on MTR.
Conclusion: Although liver fat significantly reduces MTR in high-grade fatty liver observed in animal models of obesity, the levels of liver fat and fibrosis observed in humans have no impact on MTR.

SS 10.03

Assessment of an Hi SNR C-MRI sequence for use in determination of low hepatic proton density fat fraction (PDFF) in adults

C.A. Hooker, W.M. Haufe, R. Loomba, M.S. Middleton, C. Sirlin, G. Hamilton; San Diego, CA/US

Purpose: To assess in adults the accuracy of complex-MRI (C-MRI) and high-SNR (Hi-SNR) C-MRI to determine hepatic proton density fat fraction (PDFF), at PDFF <10%.
Material and Methods: In this prospective study, an Hi-SNR C-MRI sequence was developed by increasing slice thickness from 8 to 10 mm, and decreasing matrix from 224x128 to 128x92. Adult subjects with known or suspected non-alcoholic fatty liver disease (NAFLD) underwent 3T MRIs including C-MRI and magnetic resonance spectroscopy (MRS). C-MRI PDFF values were determined by averaging the observed value in three regions of interest placed on C-MRIs co-localized to the MRS voxel location, one slice above and below that location. Linear regression models were used to assess accuracy of C-MRI PDFF using MRS PDFF as reference.
Results: 56 adults enrolled (25 M, 30 F; age 51.3 ± 12.6 yrs). Regression analysis of Hi SNR C-MRI using MRS as reference had a slope, y-intercept and R^2 value, respectively, of 0.936, 0.307% and 0.984 for all subjects; and 0.985, -0.231% and 0.942 for 22 subjects with PDFF <10%. Those values for C-MRI were 0.978, -0.055% and 0.983 for all subjects; and 0.914, 0.051% and 0.681 for 22 subjects with PDFF <10%.
Conclusion: In adults with known or suspected NAFLD, correlation of Hi-SNR C-MRI PDFF with MRS was higher than that for just C-MRI, for PDFF values <10%.

SS 10.04

Accuracy of PDFF estimation by M-MRI and C-MRI in children with known or suspected non-alcoholic fatty liver disease

W.M. Haufe, T. Wolfson, G. Hamilton, M.S. Middleton, J. Schwimmer, C. Behling, K. Newton, H.I. Awai, J. Durelle, M.N. Paiz, J.E. Angeles, D. De La Pena, C. Sirlin; San Diego, CA/US

Purpose: To compare accuracy of magnitude-based MRI (M-MRI) and complex-based MRI (C-MRI) in estimating hepatic proton density fat fraction (PDFF) in children with known or suspected non-alcoholic fatty liver disease (NAFLD), using magnetic resonance spectroscopy (MRS) as reference.

Material and Methods: In this prospective, cross-sectional study, 200 children (ages 8–18 years) underwent 3T MR examinations which included M-MRI, C-MRI, and T1-independent, T2-corrected, single-voxel, STEAM MRS. Both MRI methods acquired 6 echoes at low flip angles. T2* corrected PDFF parametric maps were generated. PDFF values were recorded from regions of interest drawn on the maps and co-localized to the MRS voxel location. PDFF values estimated by M-MRI and C-MRI were plotted against MRS-measured PDFF values. Regression analyses were performed. Regression accuracy indices and 95% confidence intervals (CIs) were computed.
Results: Mean MRS-measured PDFF was 13.4% (range 0.9–41.9%). C-MRI PDFF estimation was highly accurate (regression slope 0.981 ± 0.024; intercept -0.017 ± 0.396%; R^2 0.972). The 95% CIs for slope and intercept included 1 and 0, respectively. M-MRI PDFF was also highly accurate (slope 0.991 ± 0.022; intercept 0.729 ± 0.359%; R^2 0.976). The 95% CI for slope included 1, but the 95% CI for intercept did not include 0, indicating small systematic underestimation by M-MRI.
Conclusion: Both M-MRI and C-MRI accurately measure PDFF in children. Although both techniques were accurate with MRS as reference, M-MRI showed small, systematic underestimation.

SS 10.05

Association of hepatic histologic features with MR spectroscopy-derived hepatic fat and water T1 and T2 estimates in adults with non-alcoholic fatty liver disease

A. Schlein, P. Manning, C. Sirlin, M.S. Middleton, T. Wolfson, G. Hamilton; San Diego, CA/US

Purpose: To assess possible associations between hepatic histologic features of non-alcoholic fatty liver disease (NAFLD) and magnetic resonance spectroscopic (MRS)-derived T1 and T2 fat and water estimates in adults.
Material and Methods: Enrolled subjects receiving standard-of-care liver biopsy for evaluation of NAFLD were consented for 3T liver MR examinations. Their biopsies were scored based on NASH CRN criteria. A custom MRS sequence that acquired 32 spectra across a range of TR and TE in a 21 s breath hold was used to estimate the T1 and T2 of liver fat and water. Spectra were analyzed offline using jMRUI. Fat and water T1 and T2 were estimated by non-linearly fitting the standard MR decay function to the fat and water peak areas. The relationship between T1 and T2 values of fat and water, and histologically determined steatosis, inflammation, ballooning, and fibrosis were examined using Spearman's correlation with Bonferroni correction.
Results: 101 adults were enrolled in this study. Water T1 and T2 showed a positive association with fibrosis (rho = 0.35 and 0.39, $p < 0.0005$ and 0.0001, respectively; significant after Bonferroni correction). Fat T2 showed a positive association with steatosis (rho = 0.478, $p < 0.0001$). There were no other statistically significant associations.
Conclusion: In adults with NAFLD, hepatic fibrosis shows association with MRS-estimated water T1 and T2 and steatosis with fat T2. This may contribute to non-invasive detection and monitoring of NALFD.

SS 10.06

Volumetric estimation of liver function based on Gd-EOB-DTPA-enhanced MR-relaxometry

M. Haimerl[1], N. Verloh[1], C. Fellner[1], D. Nickel[2], C. Stroszczynski[1], P. Wiggermann[1]; [1]Regensburg/DE, [2]Erlangen/DE

Purpose: To determine whether liver function expressed by the indocyanine green clearance (ICG) could be estimated quantitatively from hepatic magnetic resonance (MR)-relaxometry with Gd-EOB-DTPA.
Material and Methods: 113 consecutive patients underwent an ICG clearance test and Gd-EOB-DTPA-enhanced MR including MR-relaxometry. After acquisition of a B1 map for inline correction of B1 inhomogeneities a prototypical transverse 3D VIBE sequence with inline T1 calculation was acquired prior and 20 minutes post-Gd-EOB-DTPA administration. The reduction rate of T1 relaxation time (rrT1) between pre- and post-contrast images and the liver volume-assisted index of T1 reduction rate (LVrrT1) were evaluated. The plasma disappearance rate of ICG (ICG-PDR) was correlated with the liver volume (LV), rrT1 and LVrrT1, providing an MRI-based estimated ICG-PDR value ($ICG\text{-}PDR_{est}$).
Results: Simple linear regression model showed a significant correlation of ICG-PDR with LV (r=0.31; p=0.001), $T1_{post}$ (r=0.63; p<0.001) and rrT1 (r =0.84; p<0.001). Assessment of LV and consecutive evaluation of multiple linear regression model revealed a stronger correlation of ICG-PDR with LVrrT1 (r=0.90; p<0.001), allowing for the calculation of $ICG\text{-}PDR_{est}$.
Conclusion: Liver function as determined using ICG-PDR can be estimated quantitatively from Gd-EOB-DTPA-enhanced MR-relaxometry. Volume-assisted MR-relaxometry has a stronger correlation with liver function than does MR-relaxometry. Global and regional liver function may be visualized by Gd-EOB-DTPA-enhanced MRI, which might be of importance for planning liver resections.

SS 10.07

Liver histology and diffusion-weighted MRI measurements in children with non-alcoholic fatty liver disease: a MAGNET study

P. Manning, P. Murphy, K. Wang, J.C. Hooker, T. Wolfson, M.S. Middleton, K. Newton, C. Behling, H.I. Awai, J. Durelle, M.N. Paiz, J.E. Angeles, D. De La Pena, J. Schwimmer, C. Sirlin; San Diego, CA/US

Purpose: To determine relationships between histologic features of non-alcoholic fatty liver disease (NAFLD) and magnetic resonance diffusion-weighted imaging (DWI) measurements in children.
Material and Methods: This prospective, cross-sectional study was performed as part of the Magnetic resonance Assessment Guiding NAFLD Evaluation and Treatment (MAGNET) ancillary study to the Non-alcoholic Steatohepatitis Clinical Research Network (NASH CRN). Enrolled subjects underwent 3T DWI (b-values: 0, 100, and 500 s/mm^2). Images were reconstructed using an advanced method based on the BetaLogNormal distribution to reduce bulk motion artifact confounding effects. Three parameters were measured in the right hepatic lobe: apparent diffusion coefficient (ADC) assuming exponential decay, and diffusivity (D) and perfusion fraction (F), assuming bi-exponential intra-voxel incoherent motion. Biopsies were scored using NASH CRN criteria. Associations between histologic features and DWI-measured parameters were tested using multivariable linear regression.
Results: Sixty-three children (45 boys, mean age 12 yrs, range 9–17 yrs) with biopsy-proven NAFLD were enrolled in this study. The estimated means ± standard deviations (and ranges) were: ADC 1.3 ± 0.2 (0.9 – 1.8) x 10^{-3} mm^2/s; D: 0.8 ± 0.1 (0.6 – 1.0) x 10^{-3} mm^2/s; and F: 17 ± 5 (6 - 28)%. Multivariable analyses showed that ADC and D decreased with steatosis and F decreased with fibrosis ($p < 0.05$).
Conclusion: In children with NAFLD, steatosis and fibrosis have independent effects on DWI-measured parameters ADC, D and F. Further research is needed to determine the underlying mechanisms and clinical implications of these effects.

SS 10.08

Compartment model analysis of dynamic CT in splenic hemodynamics: a comparison with the degree of liver fibrosis and splenomegaly

T. Suzuki, A. Yamada, D. Komatsu, M. Kurozumi, Y. Fujinaga, K. Ueda, S. Miyagawa, M. Kadoya; Matsumoto/JP

Purpose: To evaluate splenic hemodynamics quantitatively according to the degree of liver fibrosis and splenomegaly using compartment model analysis of intravenous contrast-enhanced dynamic CT.
Material and Methods: One hundred and thirty-three consecutive patients with histologically proven fibrosis stage of the liver (F stage) who underwent multiphasic intravenous contrast-enhanced dynamic CT were included in this study. Hemodynamic parameters of the spleen (inflow blood velocity constant [K_1], mean transit time [$1/k_2$] and the distribution volume [K_1/k_2]) were quantitatively evaluated by compartment model analysis of dynamic CT. The correlation between F stages and each of these hemodynamic parameters, plus the diameter of the spleen (R), was evaluated statistically.
Results: Analysis of variance revealed that there were significant differences in R ($P < 0.01$), K_1 ($P < 0.01$) and $1/k_2$ ($P < 0.01$) according to F stage. As a result of stepwise regression analysis, R and 1/k2 were found to be independent explanatory variables on F stage (F = 0.033 [R (mm)] + 0.035 [$1/k_2$ (s)] – 2.62). $1/k_2$ was significantly longer in the patient with cirrhosis (43.5 s) compared to the other F stages (F0: 30.1 s, F1: 33.6 s, F2: 32.1 s, F3: 34.8 s).
Conclusion: $1/k_2$ of the spleen can be longer with progression of liver fibrosis; therefore, $1/k_2$ of the spleen can be a significant predictor for cirrhosis, independent of splenomegaly.

SS 10.09

Validation and reproducibility of a novel method to measure total liver and hepatic arterial blood flow using phase-contrast MRI

M. Chouhan, A. Bainbridge, N. Davies, R. Jalan, S. Walker-Samuel, M. Lythgoe, R. Mookerjee, S. Punwani, S.A. Taylor; London/UK

Purpose: Non-invasive measurements of total liver blood flow (TLBF) and hepatic arterial flow (HAF) would be valuable in the assessment of portal hypertension. The purpose of this study was to validate and test the reproducibility of a novel method using phase-contrast MRI (PCMRI) measurements of the inferior vena cava (IVC) and portal vein (PV) to estimate TLBF and HAF.

Material and Methods: Fasted healthy volunteers (n = 13) underwent PV, HA, proximal and distal IVC breath-hold,cardiac-gated 2D cine-PCMRI (5 mm slice thickness, α = 10°, 256 x 256 (FE x PE)) at 3 T, with velocity encoding settings of 40, 60 and 80 cm/s. TLBF was estimated by subtracting proximal IVC flow (above renal, but below hepatic venous inlets) from distal IVC flow (above hepatic venous inlets, but below the IVC-right atrial junction). HAF was estimated by subtracting PV flow from estimated TLBF. Estimated flow measurements were validated with direct PCMRI measurements of PV and HA inflow. Reproducibility scans were conducted after 1 week (n = 11).
Results: Significant correlations between estimated TLBF ($r = 0.8967$; $p < 0.0001$), estimated HAF ($r = 0.5998$; $p = 0.0019$) and estimated HA fraction ($r = 0.5713$; $p = 0.0035$) and their directly measured counterparts were observed. No significant differences between the mean estimated and directly measured TLBF (85.66 ± 5.702 vs. 89.97 ± 5.669 ml/min/100 g; $p = 0.1087$), HAF (7.502 ± 3.214 vs. 11.82 ± 1.669 ml/min/100g; $p = 0.1087$) and HA fraction (7.466 ± 4.201 vs. 14.08 ± 2.082%; $p = 0.0686$) were observed. The coefficients of reproducibility for estimated TLBF were comparable to directly measured TLBF (31.60 vs. 29.56 ml/min/100g), but larger for estimated HAF (28.77 vs. 19.53 ml/min/100g) and estimated HA fraction (45.13 vs. 21.76%) relative to directly measured counterparts.
Conclusion: Our methods can successfully estimate TLBF and HAF. Measurements validate with direct inflow measurements, but the reproducibility of the estimated HAF and fraction is compromised by error propagation.

SS 10.10

Incremental flip angle during hepatocyte phase of gadobenate dimeglumine-enhanced MRI in patients with cirrhosis: quantitative analysis

D.J. Kim; Seongnam-si/KR

Purpose: To evaluate the effects on hepatocyte phase using gadobenate dimeglumine (BOPTA)-enhanced MRI when increasing the flip angle (FA).
Material and Methods: A total of sixty-three patients with liver cirrhosis and 63 focal liver lesions underwent BOPTA-enhanced MRI during the hepatocyte phase at 90 min, with 10°, 20° and 30° FAs. The relative enhancement (RE) and the signal to noise ratio (SNR) of liver parenchyma at hepatocyte phase with FAs were calculated. The liver-to-lesion contrast to noise ratio (CNR) and SNR of lesion at hepatocyte phase with FAs were calculated. Analysis of variance with the Sheffe method was used to evaluate the statistical significance of the differences in RE, SNR and CNR values, according to the FAs.
Results: The RE values of hepatic parenchyma were significantly different in FAs (10°, mean of RE = 0.69; 20°, mean of RE = 0.63; 30°, mean of RE = 0.49; $p = 0.043$). The SNR of hepatic parenchyma was significantly different in FAs (10°, mean of SNR = 26.2; 20°, mean of SNR = 25.3; 30°, mean of SNR = 22.8; $p = 0.004$). The CNR of lesions was not significantly different in FAs (10°, mean of CNR = 7.5; 20°, mean of CNR = 10.2; 30°, mean of CNR = 10.1; $p = 0.051$). The SNR of lesions was significantly different in FAs (10°, mean of SNR = 18.2; 20°, mean of SNR = 15.0; 30°, mean of SNR = 13.0; $p = 0.000$).
Conclusion: In patients with liver cirrhosis, increasing FA on hepatocyte phase BOPTA-enhanced MRI decreases hepatic parenchyma enhancement and does not improve lesion CNR.

11:00 - 12:30 **Dickens 1+2**

Scientific Session SS 11
Liver and pancreas intervention

SS 11.01

Feasibility and efficacy of chemoembolization for subcentimeter-sized hepatocellular carcinoma

H.-C. Kim; Seoul/KR

Purpose: To address the feasibiity and efficacy of chemoembolization for subcentimeter-sized hepatocellular carcinoma.
Material and Methods: From July 2006 to December 2013, 49 patients who had subcentimeter-sized single nodule were treated with conventional chemoembolization. Inclusion criteria were: 1) single nodule less than 1 cm, 2) enhancement on arterial phase of CT or MRI, 3) wash-out on portal venous phase, delayed phase, or equilibrium phase of CT or MRI, 4) no previous chemoembolization, 5) treatment by using Lipiodol. Superselective chemoembolization was performed by using 2.0Fr microcatheter and Lipiodol/doxorubicin emulsion. Diagnosis of HCC was rendered when dense accumulation of Lipiodol was noted on follow-up CT scan. Local tumor recurrence was measured by Kaplan–Meier method.
Results: 42 nodules had dense accumulation of Lipiodol on follow-up CT scan, and 7 showed faint accumulation of Lipiodol. Among 7 nodules with faint accumulation of Lipiodol, 4 were concluded as benign because they were persistent without size change on follow-up CT scan. 3 nodules were inconclusive because of subsequent radiofrequency ablation without tissue diagnosis. Among the 42 nodules with dense accumulation of Lipiodol, cumulative local recurrence rates were 2.4%, 12.8%, and 18.6% at 6 months, 1 year, and 2 years, respectively.
Conclusion: Subcentimeter-sized nodules with enhancement on arterial phase and wash-out on delayed phase can be frequently diagnosed and treated by chemoembolization using Lipiodol.

SS 11.02

Hepatic vein embolization after portal vein embolization for optimizing liver hypertrophy in about 10 cases

G. Baudin[1], G. Piana[2], L. Avril[1], A. Sarran[2], J.R. Delpero[2], J. Gugenheim[1], P. Chevallier[1]; [1]Nice/FR, [2]Marseille/FR

Purpose: To evaluate the effect and safety of embolization of one or more hepatic veins (HV) after portal vein embolization (PVE) on hepatic hypertrophy before complex hepatic resection.
Material and Methods: Preoperative hepatic vein embolization (HVE) was performed in 10 patients who had an inadequate liver hypertrophy after portal vein embolization (PVE). The right and/or medial HV was/were embolized using Amplatzer vascular plugs.
Results: Of the 10 patients, 8 had secondary lesions of colorectal cancer, 1 had cirrhosis with hepatocellular carcinoma and the last one had a hilar cholangiocarcinoma. The ratio between the future remnant liver volume and non-tumoral liver total volume was 23.8% ± 9% before PVE, 30% ± 7% 4 weeks after PVE, and 37.4% ± 7% 4 weeks after HVE. The patients underwent HVE on average 54 ± 15 days after PVE. Surgery could be performed in 5 patients 122 ± 22 days after PVE. No complications related to HVE have been reported. Of the 5 patients who underwent surgery, 1 died of post-operative liver failure. The other 5 patients were not operated because of major tumor progression.
Conclusion: Preoperative HVE in addition to PVE seems to be a safe and effective technique to increase hypertrophy of the future remnant liver and can make some selected patients eligible for major hepatic surgery.

SS 11.03

Comparison between radiofrequency ablation and surgical resection using propensity score matching for hepatocellular carcinoma within Milan criteria

A. Hocquelet[1], P. Balageas[1], C. Laurent[1], C. Cassinotto[2], N. Frulio[1], C. Salut[1], M. Bouzgarrou[1], P.-H. Bernard[1], J.-F. Blanc[1], H. Trillaud[1]; [1]Bordeaux/FR, [2]Pessac/FR

Purpose: To compare survival between radiofrequency ablation (RFA) and surgical resection (SR) in patients with hepatocellular carcinoma (HCC) within Milan criteria (WMC).
Material and Methods: From January 2005 to December 2013, we consecutively included all patients with first occurrence of HCC WMC receiving SR or RFA as first-line treatment. The cumulative overall survival (OS), disease-free survival (DFS) and survival WMC at the first recurrence were compared after propensity score matching. Variables included in the propensity model were age, sex, tobacco abuse, body mass index, dyslipidaemia, tumor number, tumor size, alanine aminotransferase level, platelet count, Creatinine, bilirubin, albumin, INR, alpha-fetoprotein level, liver function reserve (Child-Pugh) and cirrhosis' aetiologies.

Results: A total of 285 patients (RFA: 188; SR: 97) were enrolled. After matching, 128 patients (64 per treatment arms) were retained for analysis. Matching variables were not significantly different between groups. The respective 1- 3- and 5-year OS for SR and RFA group were 92.9%, 79.1%, 59.9% and 95.2%, 62.3%, 54.5%, p=0.209. The respective 1-, 3- and 5-year DFS for SR and RFA group were 69%, 44.1%, 17% and 64.5%, 40.1%, 24.5%, p=757. The respective 1-, 3- and 5-year WMC for SR and RFA group were 88.2%, 66.9%, 54.1% and 86.1%, 81% and 81%, p=0.307.
Conclusion: This propensity score matching study shown that RFA and SR had similar overall and disease-free survival for HCC WMC.

SS 11.04

withdrawn by the authors

SS 11.05

Hepatocellular carcinoma within Milan criteria: comparison of radiofrequency ablation, surgical resection and trans-arterial chemoembolization using stabilized inverse probability weighting

A. Hocquelet, P. Balageas, C. Laurent, J.-F. Blanc, N. Frulio, C. Salut, M. Montaudon, J. Hoareau, H. Trillaud; Bordeaux/FR

Purpose: To compare survival after radiofrequency ablation (RFA), surgical resection (SR) or trans-arterial chemo-embolization (TACE) in patients with hepatocellular carcinoma (HCC) within Milan criteria.
Material and Methods: We retrospectively and consecutively included all patients with first occurrence of HCC within Milan criteria receiving either SR or RFA or TACE as first-line treatment from January 2004 to December 2013 in one French centre. The cumulative overall survival (OS) was compared using stabilized inverse probability of treatment weighting to reduce selection bias effects.
Results: 417 patients were included (98 SR, 208 RFA and 111 TACE). After weighting, only bilirubin level still differed between the three groups (p = 0.013). Mean follow-up was 3 (95% CI: 2.8–3.2) years. Five-year OS values were not different between RFA (46%), SR (48%) and TACE (30%) groups, p = 0.168. Hazard ratios were 0.91, 0.94 and 1.33 for RFA, SR and TACE, respectively.
Conclusion: SR, RFA and TACE offer similar 5-years overall survival for hepatocellular carcinoma within Milan criteria.

SS 11.06

^{90}Y Glass microsphere radioembolization as treatment of unresectable intrahepatic cholangiocarcinoma: a retrospective study with chemotherapy alone

L. Beuzit, V. Brun, E. Garin, E. Boucher, K. Boudjema, Y. Rolland, J. Edeline; Rennes/FR

Purpose: To study the efficacy of ^{90}Y glass microsphere radioembolization as a treatment of unresectable intrahepatic cholangiocarcinoma, with or without chemotherapy, and compare it with the results of chemotherapy alone.
Material and Methods: We retrospectively analyzed data from patients treated at our institution with ^{90}Y-radioembolization for unresectable intrahepatic cholangiocarcinoma without extrahepatic spread. We compared the results with those of the patients with locally advanced non-extrahepatic cholangiocarcinoma treated at our institution with chemotherapy before ^{90}Y-radioembolization was available. The response was evaluated by CT scan, using RECIST1.1. Toxicity was retrospectively graded using NCI-CTCAE v4. Survival data were analyzed using the Kaplan–Meier method with the log-rank test.
Results: Thirty patients treated with ^{90}Y-radioembolization between 2010 and 2013 and 34 patients who received only chemotherapy between 2005 and 2009 were included. Most patients treated with radioembolization also received chemotherapy (27 in 30). Median overall survival after radioembolization was 17.6 months versus 8.5 months for patients treated with chemotherapy alone (p = 0.001). Median progression-free survival after radioembolization was 10.0 months versus 6.5 months for patients treated solely with chemotherapy (p = 0.05). Six patients treated with ^{90}Y-radiembolization went to surgery (20%) and grade 3 adverse events were reported in 3 (10%).
Conclusion: A strategy including ^{90}Y-radioembolization seems to significantly improve survival in patients with unresectable intrahepatic cholangiocarcinoma, compared to chemotherapy alone.

SS 11.07

Radiofrequency ablation of hepatocellular carcinoma: mono- or multipolar?

V. Cartier, J. Boursier, J. Lebigot, F. Oberti, I. Fouchard, C. Aubé; Angers/FR

Purpose: Thermo-ablation by radiofrequency is recognized as a curative treatment for early-stage hepatocellular carcinoma (HCC). However, local recurrence may occur because of incomplete peripheral tumor destruction. Multipolar radiofrequency has been developed to increase the size of the maximal ablation zone. We aimed to compare efficacy of monopolar and multipolar radiofrequency for the treatment of HCC and determine factors predicting failure.
Material and Methods: 171 consecutive patients with 214 HCCs were retrospectively included. 158 tumors were treated with an expandable monopolar electrode and 56 with a multipolar technique using several linear bipolar electrodes. Imaging studies at 6 weeks after treatment, then every 3 months, assessed local effectiveness. Radiofrequency failure was defined as persistent residual tumor after 2 sessions (primary radiofrequency failure) or local tumor recurrence during follow-up.
Results: Imaging showed complete tumor ablation in 207 of 214 lesions after the first session of radiofrequency. After a second session, 2 cases of residual viable tumor were observed. During follow-up, 46 local tumor recurrences occured. Thus, radiofrequency failure occurred in 48/214 (22.4%) cases. By multivariate analysis, technique (p<0.001) and tumor size (p=0.023) were independent predictors of radiofrequency failure. Failure rate was lower with the multipolar technique for tumors <25mm (p=0.023) and for tumors between 25 and 45 mm (p=0.082). There was no difference for tumors ≥45mm (p=0.552).
Conclusion: Compared to monopolar radiofrequency, multipolar radiofrequency improves tumor ablation with a subsequent lower rate of local tumor recurrence.

SS 11.08

Percutaneous radiofrequency ablation of hepatocellular carcinoma: a comparison of fusion imaging guidance to conventional sonography guidance

C.A. Liu, N.-C. Chiou, Y.-Y. Chiou; Taipei/TW

Purpose: To review our experience with percutaneous radiofrequency ablation (RFA) of hepatocellular carcinoma (HCC) and evaluate the guided method as a predictor of the ability to achieve complete necrosis by imaging criteria.
Material and Methods: Over a 2-year period, 146 patients with HCC who underwent percutaneous RFA were randomly assigned to fusion imaging and conventional sonography-guided ablation group.The contrast enhancement on CT was interpreted as complete coagulation necrosis. The relationship between guided methods (fusion imaging and conventional sonography-guided ablation) and the tumor location (peripheral and nonperipheral lesion) was identified using Chi-squared analysis. A logistic regression analysis was used to pick up the factors statistically correlated with technical success.
Results: All 138 tumors underwent complete necrosis. A significant technical successful rate showed when comparing imaging fusion and conventional sonography-guided ablation on the tumors in peripheral lesion. A guided method also was a significant predictor (p = 0.024) toward predicting getting technical success (odds ratio: 3.270; 95% CI, 1.172-9.118), whereas the location showed a nonsignificant result (p = 0.471) of complete necrosis.
Conclusion: Fusion imaging is a promising predictor for HCC in patients who are candidates for percutaneous RFA. There is a significant technical success on the tumors in peripheral lesion when using fusion imaging.

SS 11.09

Endovascular management of postpancreatectomy hemorrhage

M. Ronot, E. Pottier, S. Gaujoux, L. Barbier, M.-P. Vullierme, A. Sauvanet, V. Vilgrain; Clichy/FR

Purpose: To evaluate the efficacy of endovascular management of post-pancreatectomy hemorrhage (PPH).
Material and Methods: Between 2005 and 2013, patients referred for endovascular treatment of PPH were included. Pretreatment CT scans were reviewed. Active bleeding, pseudo-aneurysm, arterial stenosis, and culprit artery were recorded. Endovascular procedures were classified as successful (bleeding origin identified and treated), failure (bleeding incompletely treated), and no-treatment (no vascular abnormality, no treatment performed). Factors associated with rebleeding were analyzed by uni- and multivariate analysis.
Results: 69 patients (53 men, mean 58.5 years (32-75)) were included. CT showed 27 (39%) active bleeding, 25 (36%) pseudo-aneurysms, 2 (3%) arterial stenosis. In 22 (32%) cases, no culprit artery was found. Procedures were classified as successful, failure, or no-treatment in 48 (70%), 9 (13%), and 12 cases (17%). 30 patients (44%) experienced rebleeding (median 2 days (range

0-46)). Rebleeding rates were 29%, 58%, and 100% in success, no-treatment or failure (p<0.001), respectively. Patient management during angiography was the only factor associated with rebleeding (success vs. failure p<0.001; success vs. no-treatment p=0.09, no-treatment vs. failure p=0.04, overall p<0.001). Rebleeding was treated by endovascular treatment, surgery, or both, in 12 (40%), 11 (37%) and 7 (23%) cases, respectively. Overall, 72% of the patients were successfully treated by endovascular procedures alone.
Conclusion: Rebleeding is associated with initial success of the embolization. The majority of patients were successfully treated by endovascular approach alone.

SS 11.10

Cytoreduction after radiofrequency ablation of unresectable pancreatic adenocarcinoma: correlation between CA 19.9 serum levels and necrosis extent at CT

M. D'Onofrio[1], R. De Robertis[1], E. Barbi[2], P. Tinazzi Martini[2], T. Milazzo[1], R. Girelli[2], S. Paiella[1], C. Bassi[1], P. Pederzoli[2]; [1]Verona/IT, [2]Peschiera del Garda/IT

Purpose: To test the correlation between necrosis extent at CT and CA 19.9 serum levels as a possible outcome predictor after radiofrquency ablation (RFA) of unresectable pancreatic adenocarcinomas.
Material and Methods: 51 patients with unresectable pancreatic adenocarcinoma were prospectively treated with RFA. CT exam was performed one week after RFA, while CA 19.9 assessment was performed after one month. Percentage necrosis extent at CT between patients with reduced/stable or increased CA 19.9 was compared with t-test.
Results: CA 19.9 levels were reduced 1 month after RFA in 26/51 (51%) patients, while were stable in 12/51 (24%). 13 patients (25%) presented increased CA 19.9 levels. Mean percentage necrosis difference between patients with stable or <30% reduced CA 19.9 levels and those with >30% reduced CA 19.9 levels was statistically significant (p<0.05). The mean necrosis extent was 43% in patients with >30% CA 19.9 reduction.
Conclusion: RFA of unresectable pancreatic adenocarcinoma induces cytoreduction, as showed by CA 19.9 reduction. It seems that the larger is the ablated area, the more consistent is CA 19.9 reduction. To achieve a reduction greater than 30% in CA 19.9 levels, more than 40% of the lesion must be treated.

11:00 - 12:30 **Leonard de Vinci**

Scientific Session SS 12
Liver malignant tumours

SS 12.01

Image quality and diagnostic performance of dual-source CT with spectral imaging in hepatocellular carcinoma: rad-path correlation

G. Lorenzoni, I. Bargellini, D.L. Lauretti, O. Perrone, F. Turini, D. Campani, E. Neri, C. Bartolozzi; Pisa/IT

Purpose: To evaluate image quality and diagnostic accuracy of dual-source CT (DSCT) in the diagnosis of hepatocellular carcinoma (HCC) in a series of transplanted cirrhotic patients.
Material and Methods: We searched our database for all cirrhotic patients who underwent DSCT with spectral imaging in late arterial phase, <120 days before liver transplantation (LTx). Three sets of images (A: 140kVp polychromatic; B: 70keV monochromatic; C: "iodine-based" material decomposition) were reviewed, assessing image quality (scale 1-5), lesion conspicuity (scale 1-3), number of lesions and lesion-to-liver contrast-to-noise ratio (CNR). Using the pathological findings on the explanted livers as standard of reference, sensitivity, specificity, positive and negative predictive values and accuracy were assessed and compared by DeLong method.
Results: 35 patients were included, with 23 HCC nodules pathologically diagnosed in 18 (51.4%) patients (mean diameter 20.4±8.9 mm). Group B showed non-significantly higher image quality (1.11±0.40) compared to groups A (1.2±0.58) and C (1.17±0.38). Lesion conspicuity scores were 1.59±0.79, 1.23±0.56 and 1.23±0.44 for groups A, B and C, respectively (P>.05). CNR was significantly (P<.05) higher in group C (4.5±3.5) compared to groups A (2±0.9) and B (2.8±1.5). On the nodule-by-nodule and patient-by-patient analyses, group C had the highest diagnostic accuracy (area-under-the-curve, AUC 0,90-0,95), compared to groups A (AUC 0.81-0.84; P=.04/.036) and B (AUC 0.85-0.89; P=.16/.16).
Conclusion: Spectral DSCT provides high-quality images; iodine-based datasets allow the confident diagnosis of HCC with >85% sensitivity and >95% specificity.

SS 12.02

Interobserver variability of gadoxetic acid-enhanced MRI for the non-invasive diagnosis of hepatocellular carcinoma using KLCSG-NCC guidelines: comparison with multiphasic MDCT

I. Joo[1], J.M. Lee[1], D.H. Lee[1], J.Y. Son[1], S.J. Ahn[1], Y.J. Lee[2], H.-C. Kim[1], J.K. Han[1]; [1]Seoul/KR, [2]Seongnam/KR

Purpose: To evaluate interobserver variability of gadoxetic acid-enhanced MRI with comparison of that of multiphasic MDCT for the non-invasive diagnosis of hepatocellular carcinoma (HCC) using the 2014 Korean Liver Cancer Study Group (KLCSG) and the National Cancer Center (NCC) guidelines which include gadoxetic acid-enhanced MRI.
Material and Methods: In this retrospective study, we included 146 patients with chronic liver disease presenting with 153 pathologically proven HCCs (≥1 cm) who had undergone both gadoxetic acid-enhanced MRI and multiphasic MDCT. Three radiologists independently determined the presence of typical imaging features of HCCs including arterial hyperenhancement, washout on portal venous and/or delayed phases, and pseudocapsule on MRI and MDCT, respectively. Interobserver agreement for each imaging feature and KLCSG-NCC diagnosis of HCC on MRI and MDCT were assessed by Fleiss kappa test.
Results: Interobserver agreement of arterial hyperenhancement, washout, and pseudocapsule was moderate to substantial with gadoxetic acid-enhanced MRI and poor to moderate with MDCT. According to KLCSG-NCC, typical enhancement pattern was found in 92.8%, 92.2%, and 83.0% of HCCs on MRI; and 86.9%, 83.7%, and 69.9% on MDCT by reviewers 1, 2, and 3, respectively. Interobserver agreement for KLCSG-NCC either by MRI or MDCT was moderate (0.50, 95% confidence interval [CI] of 0.41–0.59; and 0.49, 95% CI of 0.40–0.58, respectively).
Conclusion: KLCSG-NCC guidelines for the non-invasive diagnosis of HCC showed moderate inter-observer variability both by gadoxetic acid-enhanced MRI and MDCT.

SS 12.03

Intermediate-stage HCC treated with TACE: proposal for a new scoring system

A. Scionti, B. Ginanni, P. Scalise, F. Calcagni, I. Bargellini, E. Neri, C. Bartolozzi; Pisa/IT

Purpose: To identify predictors of overall survival (OS) in intermediate-stage HCC patients undergoing TACE and to establish an objective point score for patients' stratification.

Material and Methods: We retrospectively reviewed clinical and demographic data of 149 patients (125 males; mean age: 65 years) with naïve intermediate-stage HCC treated with TACE between 2006 and 2011. One-month tumour response was defined according to mRECIST criteria. Stepwise Cox regression model was used to identify predictors of OS and develop an objective point score.

Results: Median OS was 22.7 months. At multivariate analysis, negative independent prognostic factors for OS were age >66 years (HR 1.79; P=.005), ascites (HR 2.35; P=.005) and progressive disease after TACE (HR 4.66; P<.0001), while positive independent prognostic parameters were maximum total HCC diameter according to mRECIST ≤60 mm (HR: 0.49; P=.001) and complete response after TACE (HR 0.64; P=.04). A 9-point scale score (range -3 to +6) was created, and three groups of patients were identified. Patients with scores <0 had a significantly longer OS (40.2 months, group A), compared to patients with scores =0 (23.3 months, group B) and scores >0 (13.3 months, group C) (A versus B, P=.0009; B versus C, P=.0026).

Conclusion: Combining pre- and post-TACE parameters, our scoring system enables a simple stratification of intermediate-stage HCC patients that could be helpful for treatment planning.

SS 12.04

HCC differentiation: quantitative MRI study of tumor enhancement on Gd-BOPTA-enhanced hepatobiliary phase

F. Legou, F. Pigneur, L. Baranes, M. Chiaradia, M. Djabbari, J. Calderaro, C. Costentin, A. Laurent, A. Rahmouni, A. Luciani; Creteil/FR

Purpose: To asses the added value of Gd-BOPTA-enhanced hepatobiliary phase imaging to distinguish hepatocellular carcinomas according to their pathological differentiation.

Material and Methods: This study had IRB approval and the requirement for informed consent was waived. Twenty-one patients with 24 resectable HCC BCLC A (5 well differentiated, 10 moderately differentiated and 6 poorly differentiated) naïve of any treatment, and treated by orthotopic liver transplantation or hepatectomy were included in this prospective, monocentric study. All patients underwent a preoperative liver MRI after Gd-BOPTA injection included delayed hepatobiliary phase acquisitions. Two readers reviewed all images in terms of signal intensity (SI) features on unenhanced, and hepatobiliary phase images to establish the lesion-to-liver contrast enhancement ratio (LLCER). The LLCER was compared according to pathological differentiation (Mann–Whitney, ROC).

Results: The LLCER of well-differentiated HCC (mean 46.01% ± 45.78) was significantly higher than that of moderately to poorly differentiated HCC (mean -22.62% ± 16.17) (p<0.0008). 100% of well-differentiated HCC had a positive LLCER and 100% of moderately to poorly differentiated HCC had a negative LLCER. Using a cutoff value of +3% yielded a 100% specificity and sensitivity for discriminating well-differentiated from moderate to poorly differentiated HCC.

Conclusion: LLCER at the hepatocyte phase after Gd-BOPTA injection allows the differentiation of well-differentiated from moderately to poorly differentiated HCC.

SS 12.05

withdrawn by the authors

SS 12.06

Arterio-portal shunts in the cirrhotic liver: CT perfusion for distinction of arterialized pseudolesions from hepatocellular carcinoma

M.A. Fischer[1], S. Gordic[1], B. Leidner[1], P. Aspelin[1], H. Alkadhi[1], T. Brismar[2]; [1]Zurich/CH, [2]Stockholm/SE

Purpose: To determine differences between arterial pseudo-lesions (APL) and hepatocellular carcinoma (HCC) of the cirrhotic liver at perfusion computed tomography (P-CT).

Material and Methods: 41 APL and 28 HCC in 20 cirrhotic patients with arterio-portal shunting (15 men; mean age 65±10), who underwent 4D-spiral P-CT for evaluation of HCC pre- (n=9) and post- (n=11) transarterial-chemoembolisation (TACE), were retrospectively included in this dual-center study using CT-imaging follow-up as the standard of reference. All lesions were qualitatively analyzed for shape (wedge, irregular, nodular) and location (adjunct or not-adjunct to a fistula) as well as quantitatively analyzed for arterial-liver-perfusion (ALP), portal-venous perfusion (PVP), and hepatic perfusion index (HPI).

Results: APL were mainly wedge-shaped (25/41, 61%) or irregular (15/41, 37%), while HCC were mainly nodular (17/28, 61%) or irregular (11/28, 39%). Before TACE, shape of APL and HCC was significantly different (P<0.001), whereas no difference was seen after TACE (P>0.05). PVP and HPI were significantly different between APL and HCC for both pre- and post-treated lesions (all, P<0.001). APL adjunct to a fistula (n=17) showed a similar HPI as HCC (P=0.142), but PVP of HCC was significantly lower than APL regardless of the distance to a fistula (P>0.05).

Conclusion: Arterio-portal shunting should be considered one of the causes of arterialized lesions in the cirrhotic liver, which can mimic HCC. Lesion configuration and PVP allow best for distinction between APS and HCC at P-CT.

SS 12.07

Compartment model analysis of intravenous contrast-enhanced dynamic CT in hepatic hemodynamics: a comparison with intra-arterial contrast-enhanced CT

D. Komatsu, A. Yamada, T. Suzuki, M. Kurozumi, Y. Fujinaga, K. Ueda, M. Kadoya; Matsumoto/JP

Purpose: To evaluate arterial and portal venous vascularity of the liver independently using compartment model analysis of intravenous contrast-enhanced dynamic CT (IVCED-CT).

Material and Methods: Thirty-five consecutive patients with radiologically diagnosed hepatocellular carcinoma (HCC) who underwent both IVCED-CT and intra-arterial contrast-enhanced CT (IACE-CT) were included in this study. Upper abdomen was scanned at pre-contrast and 22, 28, 34, 40, 46, 52, 58, 90, 210 seconds after intravenous administration of contrast media in IVCED-CT. Absolute inflow blood velocity constant of hepatic artery [K_{1a}] and portal vein [K_{1p}] of the background liver and HCC were quantitatively evaluated by compartment model analysis of IVCED-CT. Arterial and portal venous vascularity levels of HCC against background liver were compared between these hemodynamic parameters, IVCED-CT or IACE-CT findings.

Results: According to IACE-CT, all HCCs were hypervascular in arterial blood flow and hypovascular in portal venous blood flow against background liver. The accuracy of evaluating arterial vascularity level was 100% by K_{1a} and IVCED-CT early phase (22–58 s), respectively. The accuracy of evaluating portal venous vascularity level was 100% by K_{1p}, 63% (95%CI: 47–79%) by IVCED-CT delayed phase (90–210 s), respectively.

Conclusion: The arterial and portal venous vascularity of the liver can be evaluated independently and quantitatively using compartment model analysis of IVCED-CT which can be equivalent to IACE-CT.

SS 12.08

Routine staging CT thorax in treatment-naïve hepatocellular carcinoma prior to loco-regional therapy: is there a need?

P.W. Leong, K.S. Lim, U. Pua; Singapore/SG

Purpose: Pulmonary metastases (PM), whilst the commonest site of distant metastasis in hepatocellular carcinoma (HCC), remain a rare occurrence. Their presence, nevertheless, contraindicates curative loco-regional therapy. The role of pre-treatment staging CT thorax is currently unclear. This study aims to assess the utility of pre-treatment CT thorax and predictive value of imaging features of HCC for PM.

Material and Methods: Retrospective review of continuous cases of treatment-naïve HCC referred for locoregional therapy between 2004 and 2013 was done. Patients with pre-treatment CT thorax were evaluated for presence of PM. HCC features (size, numbers, vascular invasion, nodal status, bone metastases) were recorded. Univarate analysis (Chi-square/Fisher's exact test) and multivariate logistic regression were performed with a statistician for significant association.

Results: 780 patients were reviewed, of which 135 patients had staging CT thorax done. PM (n=17, 12.6%), benign (n=41, 30.4%) and indeterminate lung lesions (n=6, 4.4%) were detected. All the patients with PM were eventually declined loco-regional therapy. Univariate analysis showed significant association between PM with number of intra-hepatic lesions (p<0.01), primary tumour size (p=0.018) and presence of vascular invasion (p<0.01). On multivariate analysis, number of intra-hepatic lesions (OR: 9.7; 95% CI: 1.6–57.2, p=0.012) and presence of both hepatic and portal venous invasion (OR: 11.8; 95% CI: 1.1–128.8, p=0.043) are two independent positive predictors of PM.

Conclusion: The yield of staging CT thorax in treatment-naïve HCC is low and its routine use is not recommended. It can, however, be considered in selected HCC cases with multiple lesions or vascular invasion.

SS 12.09

withdrawn by the authors

SS 12.10

Mass-forming intrahepatic cholangiocarcinoma: diffusion-weighted imaging as preoperative prognostic marker

J. Lee, S.H. Kim, T.W. Kang, K.D. Song, K.M. Jang, D. Choi; Seoul/KR

Purpose: To assess value of diffusion-weighted imaging (DWI) as prognostic marker in preoperative evaluation of mass-forming intrahepatic cholangiocarcinoma (ICC).

Material and Methods: Ninety-one patients who had undergone hepatic resection and DWI between October 2008 and February 2014 for mass-forming ICC were included. Two radiologists evaluated degree of diffusion restriction on DWI with apparent diffusion coefficient (ADC) maps in consensus. Patients were classified into two groups: group 1 included those in whom less than one-third of tumor showed diffusion restriction. Group 2 included those in whom more than one-third of tumor showed diffusion restriction. Two groups were compared with respect to disease-free survival and overall survival.

Results: There were 49 patients in group 1 and 42 patients in group 2. The 1-, 2-, and 3-year disease-free survival rates were 28.2%, 13.3%, and 8.9% for group 1, whereas 82.2%, 78.9%, and 78.9% for group 2, respectively. The 1-, 2-, and 3-year overall survival rates were 78.8%, 39.6% and 18.3% for group 1, whereas 92.2%, 83.8%, and 83.8% for group 2, respectively. Disease-free survival rate and overall survival rate for group 1 were significantly lower than those for group 2 (P<.0001). Multivariate analysis revealed that diffusion restriction (P=.002) and intrahepatic metastasis (P=.008) were independent prognostic factors for overall survival.

Conclusion: Degree of diffusion restriction on DWI with ADC maps could play a role as prognostic marker in preoperative evaluation of mass-forming ICC.

11:00 - 12:30 **Goethe**

Scientific Session SS 13

CT colonography and colonic cancer assessment

SS 13.01

CT colonography for selection of colonic polyps for laparo-endoscopic excision

N. Katsoulas, A. Currie, E. Mainta, R. Ilangovan, O. Faiz, D. Burling, R. Kennedy; London/UK

Purpose: To determine the utility of CT colonography for accurate assessment of polyp location in relation to its mesenteric vascular supply (mesenteric versus antimesenteric border of colonic wall), proportion of wall circumference involved and polyp diameter; regarded as key anatomical considerations for safe laparo-endoscopic excision, a new surgical technique for local full thickness polyp excision.

Material and Methods: National Ethics Committee approval was obtained. 20 patients with malignant polyps (cancer confined to the colonic wall and without overt nodal involvement or extramural venous invasion) who had pre-operative CT colonography were selected from a colorectal cancer database for retrospective review. CT colonography examinations were interpreted by two experienced gastrointestinal radiologists in consensus, blinded to post-operative histopathological findings (reference). The percentage of cases accurately located was recorded. Kappa statistic (κ) and Spearman's correlation coefficient (r) were used to compare circumferential involvement and polyp diameter.

Results: Of 20 polyps (median diameter 32.5mm, range 15 to 80), 15 (75%) were located on the mesenteric border and 5 (25%) on anti-mesenteric border. All 20 (100%) polyps were correctly categorized (mesenteric vs. antimesenteric). Agreement between consensus interpretation and reference for proportion of wall circumference involved was good (17/20 cases, κ 0.76). There was almost perfect correlation for polyp diameter between radiology and reference (r 0.926).

Conclusion: CT colonography is an excellent technique for selecting polyps suitable for laparo-endoscopic excision.

SS 13.02

What if my grandpa had gone virtual first? Diagnostic yield of CT colonography in elderly patients with incomplete colonoscopy

D.A. Tiferes, G. Warmbrand, C.A. Matsumoto, R.P. Caldana, G. D'Ippolito, A.H.M. Caiado; Sao Paulo/BR

Purpose: To assess the performance of CT colonography (CTC) in elderly patients who were referred because colonoscopy was incomplete, and to estimate how many colonoscopies could have been avoided if patients had started colonic evaluation with CTC.

Material and Methods: Observational retrospective study of data obtained from radiology and endoscopy reports from 168 consecutive patients ≥66 years (mean age, 74.6 years) referred to CTC because colonoscopy was incomplete.

Results: 120 (71.4%) patients were symptomatic. Major indications for colonoscopy included abdominal pain/diverticular disease (31%), change in bowel habits (22.6%) and hematochezia (10.7%). Introduction of the colonoscope was limited to the sigmoid in 118 (70.2%) of cases. Incomplete colonoscopy detected colorectal cancer in 3 (1.8%) and polyps ≥10 mm in 4 (2.4%) patients. At CTC adequate bowel preparation and distention of the entire colon were achieved in 157 (93.5%) patients. CTC additionally revealed cancer in 6 (3.6%), polyps ≥ 10 mm in 8 (4.8%), inflammatory strictures in 3 (1.8%), radiation colitis in 3 (1.8%) and submucosal lesions (lipomas and GIST) in 5 (3.0%) patients. Diverticular disease was observed in 118 (70%) patients. Significant extracolonic findings were observed in 8 (4.8%) patients.

Conclusion: CTC revealed additional significant colonic lesions (cancer and polyps ≥10 mm) in 8.3% of elderly patients with incomplete colonoscopies. Almost 80% of colonoscopies could have been avoided if patients had started colonic evaluation with CTC.

SS 13.03

Navigation speed along the colonic centreline at CT colonography: effect on eye movement and polyp identification

A. Plumb[1], P. Phillips[2], T. Fanshawe[3], S. Mallett[3], G. Spence[3], A. Gale[4], S.A. Taylor[1], S. Halligan[1]; [1]London/UK, [2]Lancaster/UK, [3]Oxford/UK, [4]Loughborough/UK

Purpose: To determine the effect of variable navigation speed along the colonic centerline during endoluminal CT colonography (CTC) on eye movement behaviour and polyp detection.
Material and Methods: Ethical permission was granted for this prospective study. 23 radiologists (18M:5F; age range 30–63) were asked to indicate their normal preferred CTC navigation speed using an adjustable CTC video. They then viewed a selection of CTC videos presented at different, non-adjustable speeds. Videos were repeated at 4 different speeds (min: 1cm/sec; max: 4.5cm/sec; total=40 videos/participant). Simultaneously, eye positions were logged by a Tobii X60 infra-red eye tracker. Radiologists were also asked to click their mouse when they detected a polyp on the screen ("polyp identifications"). Preferred playback speed was tested again at the end of the viewing period.
Results: Average preferred playback speed was 1.18cm/sec and showed no significant difference by gender (p=0.37) or for experienced (>300 cases) colonographers (p=0.73). There was a consistent decrease in the number of polyp identifications/viewing as speed increased, from 1.2 identifications/viewing at the slowest speed to 0.8 identifications/viewing at the fastest. This was true whether or not the video depicted a true-positive polyp.
Conclusion: Average preferred navigation speed at CTC is approximately 1.2cm/sec; increasing from this speed leads to lower polyp identification rates.

SS 13.04

Patient factors predictive of decreased endoscopic performance from quantitative CTC: does age and body habitus impact colonic morphology and endoscopic performance?

C.N. Weber[1], A.S. Lev-Toaff[1], M.S. Levine[1], B. Geiger[2], H.M. Zafar[1]; [1]Philadelphia, PA/US, [2]Princeton, NJ/US

Purpose: To assess impact of age and body habitus on colonic morphology using CTC quantification software and correlate with endoscopic performance.
Material and Methods: CTC datasets from 32 patients with history of failed optical colonoscopy (OC) were evaluated. Quantitative metrics included colonic/segmental length, tortuosity (number of high curvature points (HCP)), and compactness (boxed volume containing centerline divided by centerline length). Patient factors included age (over/under 65, n=16/16), height (over/under 5'6", n=14/18) and body mass index (BMI) (over/under 25, n=23/9). Each dataset was quantified twice. The groups were compared with two-tailed Student's t test. Distance navigated at colonoscopy was compared.
Results: Older patients had more tortuous colons (p=0.05). Shorter patients had shorter and more compact colons (p≤0.04), with greater tortuosity although not significant (p=0.26). Thinner patients had more compact and tortuous colons (p≤0.02). Although not significant, patient height mostly correlated with distance navigated at colonoscopy, with 67% vs. 47%, 50% vs. 35%, and 33% vs. 17% successfully reaching the transverse segment, hepatic flexure, and ascending segment in taller vs. shorter patients, respectively, despite longer colons in taller patients.
Conclusion: Older, shorter, and thinner patients had more tortuous and compact colons, which trended towards poorer endoscopic performance, most notably in shorter patients. This quantitative evidence supports clinical observations regarding more challenging optical colonoscopies in these patient groups. Patient factors such as age and body habitus should be considered when weighing options of CTC versus OC.

SS 13.05

Prognostic value of the diverticular disease severity score based on CTC: follow-up in patients recovering from acute diverticulitis

N. Flor[1], G. Maconi[1], F. Sardanelli[1], M.A. Lombardi[1], B. Colombo[1], G. Di Leo[1], G.P. Cornalba[1], P.J. Pickhardt[2]; [1]Milan/IT, [2]Madison, WI/US

Purpose: To assess the prognostic value of a diverticular disease severity score (DDSS) based on CT colonography (CTC) after acute diverticulitis.
Material and Methods: Of 252 patients who had an acute diverticulitis episode, 47 underwent conventional CT for the acute episode and were treated with medical therapy, and had CTC after 9±7 weeks; 17/47 finally underwent surgery. Disease severity was assessed with a 0-to-4 modified Hinchey CT-based score and a 1-to-4 CTC-based DDSS. A phone survey was performed 27 months later (range 4–52) for patients not surgically treated.
Results: Significant correlation was found between CTC-based DDSS and clinical follow-up (p=0.022) or risk of surgery (p=0.007), not between clinical follow-up and CT-based score, extraluminal gas, C-reactive protein serum level, age, gender, or first versus recurrent acute diverticulitis episode. CTC demonstrated relevant additional findings in 5/47 (11%) patients: 2 acute diverticulitis complications (enterocolic and enterotubal fistulae), 2 colon cancers, and 1 an extracolonic (lung) cancer.
Conclusion: The CTC-based DDSS showed a prognostic value and correlated with the risk of undergoing surgery and clinically relevant additional findings were found in over 10% of patients. CTC could be the preferred test in patients recovering after acute diverticulitis.

SS 13.06

wihtdrawn by the authors

SS 13.07

Role of CT colonography in early follow-up of acute complicated diverticulitis

M. Bassi, B. Malta, Z. Ferrante, C. Montalto, R. Rizzati, M. Tilli, M. Giganti, G. Benea; Ferrara/IT

Purpose: To investigate value of CT colonography (CTC) in the follow-up after acute complicated diverticulitis to evaluate best therapeutic approach.
Material and Methods: From April 2009 to August 2014, 66 patients underwent unenhanced low-dose CTC follow-up (28 males, 38 females, aged 38–91 years) 6–8 weeks after acute diverticulitis, conservatively treated. All patients previously performed enhanced-CT (CECT) and were classified using modified Hinchey classification. CTC exam evaluated colonic/extracolonic findings, assessing short-term course and staging of diverticular disease. No CTC complications occured.
Results: CTC quality was good in 59/66 patients (89%); in 7 cases we obtain suboptimal distension due to diverticular disease or colonic stenosis. At baseline CECT we found: Hinchey I (n=30, 46%); II (n=22, 33%); III (n=14, 21%); IV (n=0, 0%) stages. CTC findings follow-up allowed to keep conservative treatment in all cases of Hinchey I (100%), in 8/22 cases of Hinchey II (36%) and in 8/14 cases of Hinchey III (57%). Twenty patients not understaged (14/22 Hinchey II, 64%, and 6/14 Hinchey III, 43%) underwent laparoscopic/open surgery. CTC also revealed 4 unknown polyps >6 mm and 28 extracolonic findings, 4 with major clinical relevance that changed treatment strategy.
Conclusion: CTC is a safe and accurate method to evaluate severity and staging in short-term follow-up of acute complicated diverticulitis allowing an overview of colonic/extracolonic findings and guiding correct therapeutic planning.

SS 13.08

CT in the assessment of early response to neoadjuvant therapy of colon cancer

S. Rafaelsen, C. Dam, V. Lund-Rasmussen, J. Pløen, A. Jakobsen; Vejle/DK

Purpose: Neoadjuvant drug therapy is presumed to improve outcome in colon cancer. Using multi-detector computed tomography (MDCT) we aimed to assess the early response of neoadjuvant drug therapy for locally advanced colon cancer.
Material and Methods: MDCT with i.v. contrast were acquired from consecutive 67 patients before and after preoperative drug therapy. All patients had at baseline histologically confirmed colon cancer with ctT4 or ctT3 tumour with extramural invasion ≥5mm and without distant metastases or peritoneal nodules. The tumour diameter in 2 different planes, extension of extramural tumour invasion and number and size of enlarged lymph nodes were measured before and after the therapy.
Results: Mean tumour length was 7.8 cm (95% CI: 5.3–10.4) at baseline and 4.34 cm (95%, CI: 4.0–4.9) after therapy. Mean extramural tumour invasion was 10.6 mm (95% CI: 9.5–11.8) at baseline and 5.7 mm (95% CI: 4.7–6.7) after therapy. Mean number of enlarged lymph nodes was 4.1 (95% CI: 3.4–4.9) at baseline and 2.1 (95% CI: 1.4–2.7) after therapy. According to the RECIST criteria 45% (95% CI: 34–57) of the patients had response and 55% (95% CI: 43–67) had stable disease. No one showed progressive disease.
Conclusion: Using MDCT we demonstrate a significant reduction in tumour size, extramural tumour invasion, number and size of enlarged lymph nodes following neoadjuvant therapy for colon cancer. Using the RESIST criteria 45% had a response.

SS 13.09

Diagnostic accuracy of computed tomography for staging colon cancer: a meta-analysis

E. Nerad[1], M.J. Lahaye[2], M. Maas[2], G.L. Beets[2], P.J. Nelemans[2], F.C.H. Bakers[2], R.G.H. Beets-Tan[2]; [1]Eindhoven/NL, [2]Maastricht/NL

Purpose: To determine the diagnostic value of pre-operative computed tomography (CT) in detecting colon carcinomas with invasion beyond the bowel wall and the presence of malignant lymph nodes.

Material and Methods: A literature search of Ovid, Embase and Pubmed was performed to identify studies reporting on the accuracy of CT for local staging of colon carcinomas. Data extraction was performed by two observers in consensus. The sensitivity, specificity, and diagnostic odds ratio (DOR) were calculated using a bivariate random effects model and summary receiver operating curves (sROC) were generated.

Results: Twenty studies fulfilled all the required inclusion criteria. The pooled sensitivity, specificity, DOR for detection of tumour invasion beyond the bowel wall were 90% (95% CI: 83–95%); 69% (95% CI: 62–75%); 20,6 (CI: 20–41%), respectively. For detection of invasion depth of 5mm beyond the bowel wall these values were 77% (CI: 66–85%); 70% (CI: 53–83%); 7.8 (CI: 4.2–14.2) and nodal involvement; 71% (CI: 58–81%); 66% (CI: 46–83%); 4.8 (CI: 2.5–9.4%).

Conclusion: CT is reliable in detecting colon carcinomas with tumour invasion through the bowel wall (T1/T2 versus T3/T4). However, detecting tumour invasion of >5mm from the bowel wall (T1/T3ab and T3cd/T4) tumours and especially nodal involvement remains a challenge for CT.

SS 13.10

Quality control in the multicentre PROSPeCT trial: perfusion CT of primary colorectal cancer

D. Prezzi, M. Lewis, V. Goh; London/UK

Purpose: To assess the image quality of perfusion CT (PCT) studies across all participating sites in the multicentre PROSPeCT trial.

Material and Methods: IRB approval and informed consent were obtained. PCT studies from 9 sites and 5 different scanner models were reviewed centrally for image quality. Image noise was assessed by placing a region of interest (ROI) over the bladder, recording the mean CT number (HU) and standard deviation (SD). Calculation of an equivalent patient diameter enabled correlation between image noise and patient size. The quality of the arterial input function was assessed by analysing the peak iodine enhancement value (HU) and its full width at half maximum (FWHM). Patient positioning, with respect to centering in the scanner's field of view (FOV) was also assessed.

Results: The bladder was included in 86 of 172 PCT. Mean (SD) noise was 17.8 (3.3) on Siemens scanners and 22.3 (2.0) on GE; it increased when applying a sharper reconstruction kernel. An exponential relationship between noise and equivalent patient diameter was found. Peak arterial enhancement was fairly consistent across scanners (>300HU). Patient centering was accurate in the transverse (x) direction (<30mm from centre) but less so in the anterior–posterior (y) direction.

Conclusion: Image noise was similar across all scanner models, except when the scan protocol varied from standard. The arterial input function quality was generally good. More attention should be paid to accurate patient centering.

11:00 - 12:30 **Darwin 3**

Scientific Session SS 14

Vessels: contrast media and enhancement

SS 14.01

Correlation of 64-channel CT angiography with digital subtraction angiography in the evaluation of non-variceal acute gastrointestinal bleeding

A. Gupta, S. Kumar, I. Garg, A. Gupta; Lucknow/IN

Purpose: To analyse the role of 64-channel CT angiography in the localization of acute gastrointestinal bleeding & correlation of its findings with digital subtraction angiography (DSA) with the radiation dose assessment between the two modalities.

Material and Methods: The prospective study was conducted in the Department of Radiodiagnosis SGPGIMS, Lucknow, India from July 2012 to December 2014. Age was between 19 and 72 years. 67.5% patients were male and 32.5% were female.

Results: 40 patients with GI bleeding were included in our study. 87.5% presented with a upper GI bleed and 12.5% a lower GI bleed. On NCCT 20% showed hyperdensity within bowel lumen and 27.5% within confined space. On CECT localization was possible in 92.5%, out of which 55% presented with pseudoaneurysm, extravasation in confined space in 22.5%, hyperemia in 7.5%, A-V fistula in 5% and extravasation in bowel lumen in 2.5%. On DSA pseudoaneurysm was seen in 52.5%, extravasation in confined space in 17.5%, hyperemia in 7.5% and A-V fistula in 5%. Sensitivity of CTA was 96.9% and specificity was 28.5%. Both were positive in 32/40 (80%), DSA was positive alone in 2.5% and CT alone in 12–5%. Overall agreement between DSA and CT was observed in 85%. Statistically it was found to be fair (k=0.33) and significant (p<0.020). The mean CT and DSA effective dose was 19.7 & 1.55 mSv, respectively.

Conclusion: CT angiography is reproducible, repeatable and localizes the bleeding site which determines suitable intervention and reduced interventional time. DSA offers both the diagnostic and theraputic option.

SS 14.02

Role of ultrasound imaging in detection of dysfunctional transjugular intrahepatic portosystemic shunts (TIPS)

C.N. Weber, G.J. Nadolski, M.C. Soulen; Philadelphia, PA/US

Purpose: To investigate impact of ultrasound (US) imaging on detection of polytetrafluoroethylene (PTFE)-covered TIPS dysfunction.

Material and Methods: Patients who received PTFE-covered TIPS (2002–2012) were retrospectively reviewed. Those with suspected shunt dysfunction (recurrent symptoms and/or abnormal US) were identified; only patients with subsequent TIPS venograms were included. Venographic and sonographic findings were recorded and compared. TIPS dysfunction was defined as stenosis/occlusion or portosystemic gradient >12mmHg. Sensitivity, specificity and positive and negative predictive values (PPV, NPV) of US were compared between patients with and without pre-venographic US abnormalities, as well as between ascites and bleeding patient groups.

Results: 50 patients underwent 72 TIPS venograms (53 in 31 ascites patients, 19 in 19 bleeding patients) for suspected shunt dysfunction. Sensitivity (83% vs. 69%), specificity (67% vs. 38%), PPV (91% vs. 85%) and NPV (50% vs. 19%) of US predicting shunt dysfunction were higher in the bleeding group. PPV markedly increased for the bleeding group with addition of pre-venographic US (38%→91%), whereas the ascites group already demonstrated high PPV based on physical exam findings (84%→85%). Imaging alone detected 50% (7/14) of dysfunctional TIPS in the bleeding group, which was higher than the ascites group (9%, 4/45).

Conclusion: Although equivocal/unremarkable TIPS US may not exclude shunt dysfunction, abnormal sonographic findings correlated highly with proven dysfunction. Ultrasound may be of more value in patients receiving TIPS for hemorrhagic varices, as physical exam is limited in indirectly monitoring patency compared with ascites patients during extended follow-up.

SS 14.03

Congenital portosystemic shunts: feasibility of closure and effect on complications in 50 cases

S. Franchi-Abella, F. Guerin, E. Gonzales, G. Morcrette, S. Branchereau, D. Pariente; Le Kremlin Bicêtre/FR

Purpose: Congenital portosystemic shunts (CPSS) are rare vascular malformations. They can lead to severe cardiopulmonary complications, hepatic tumors and portosystemic encephalopathy. Feasibility of closure is debated and its efficiency to prevent or treat complications is not well known. We report on a paediatric series of CPSS closed surgically (S) or by interventional radiology (IR).

Material and Methods: Between 1999 and 2014, 50 patients had a closure of CPSS (median age: 8.6 years, 0 to 15.6 y.). CPSS consisted of 7 patent ductus venosus, 14 porto-hepatic shunts, 26 side-to-side and 3 end-to-side extrahepatic communications. Technique of closure, complications related to CPSS and their outcomes after closure are described.
Results: Thirty-five patients had closure of CPSS because of complications that were benign hepatic tumors (23), pulmonary arterio-venous shunts (3), pulmonary hypertension (4) and portosystemic encephalopathy (9). Fifteen patients had a preventive closure of CPSS. Closure of CPSS was performed surgically in 28 and with IR in 20 and combined technic in 2. None had significant portal hypertension or other complication after closure. Hepatic tumors disappeared in 14 and decreased in size in 9. Pulmonary shunts resolved in 2 and improved in 1. Pulmonary hypertension stabilized in all. Portosystemic encephalopathy resolved in all.
Conclusion: CPSS can be closed safely whatever their location. Complications secondary to CPSS may resolve or improve after closure except for pulmonary hypertension. Preventive closure is safe and should be discussed.

SS 14.04

Study of prognostic factors of evolution in non-malignant acute portal vein thrombosis

M. Kulik, J. Boursier, F. Oberti, J. Lebigot, P. Cales, A. Aubé; Angers/FR

Purpose: The main objective of this study is to look for prognostic parameters of evolution in non-malignant acute portal vein thrombosis (PVT).
Material and Methods: From the databases of imaging and hepatology department, we retrospectively included 76 patients with acute PVT diagnosed between April 2007 and December 2011. For each patient, we collected biological, clinical and radiological data, before diagnosis, at the diagnosis, and 6 and 18 months after diagnosis.
Results: 52/76 patients were cirrhotics. 55.8% of cirrhotic patients were treated versus 87.5% of non-cirrhotic patients. 48% had complete portal vein occlusion. The rate of thrombosis response (partial and complete regression) was 44.8% in treated patients, and 43.5% in untreated patients. As regards the response, we did not highlight difference according to the treatment or the initial degree of occlusion. At 6 and 18 months, the worsening of liver function (Child Pugh) was significantly lower in treated cirrhotic patients' group. The presence at the time of diagnosis of an ascites associated to an extension of the PVT to the superior mesenteric vein and/or splenic vein was a factor of non-response.
Conclusion: Treatment and initial degree of obstruction were not prognostic factors of response. However, in cirrhotic patients treatment was a factor of non-aggravation of hepatic function.

SS 14.05

ESGAR consensus statement on the use of liver-specific contrast agents in MR imaging

E. Neri[1], M.A. Bali[2], A. Ba-Ssalamah[3], P. Boraschi[1], G. Brancatelli[4], F. Caseiro Alves[5], L. Grazioli[6], T. Helmberger[7], J.M. Lee[8], R. Manfredi[9], L. Martí-Bonmatí[10], C. Matos[2], E. Merkle[11], W. Schima[3], S.J. Skehan[12], V. Vilgrain[13], B. Op De Beeck[14], C.J. Zech[11], C. Bartolozzi[1]; [1]Pisa/IT, [2]Brussels/BE, [3]Vienna/AT, [4]Palermo/IT, [5]Coimbra/PT, [6]Brescia/IT, [7]Munich/DE, [8]Seoul/KR, [9]Verona/IT, [10]Valencia/ES, [11]Basel/CH, [12]Dublin/IE, [13]Clichy/FR, [14]Edegem/BE

Purpose: To develop a consensus and provide updated guidelines on the clinical use of liver specific CA, the European society of Gastrointestinal and Abdominal Radiology (ESGAR) composed a multinational European panel of experts in the field of liver MR imaging.
Material and Methods: The panel used a modified Delphi process to draft a list of statements. Descriptive and Cronbach's statistics were used to rate levels of agreement and internal reliability of the consensus.
Results: Three Delphi rounds were conducted and 76 statements composed, on MR technique (n=17), clinical application of liver-specific CA in benign focal liver lesions (n=7), malignant liver lesions in non-cirrhotic (n=9) and in cirrhotic patients (n=18), diffuse and vascular liver diseases (n=12), and bile ducts (n=13). The overall mean score of agreement was 4.84 (SD ±0.17). Full consensus was reached by the experts panel in 22% of the statements regarding the state-of-the-art MR protocol and the application of liver-specific CA in cirrhotic patients.
Conclusion: Covering most important aspects of the clinical use of liver-specific CA in MR imaging, the consensus also provided updated guidelines on the methodology and clinical indication of MRI in the study of liver diseases.

SS 14.06

Usefulness of Sonazoid-enhanced ultrasound in the assessment of acute rejection or recurrent hepatitis in liver transplant recipient: a preliminary study

I. Joo, J.Y. Lee, D.H. Lee, J.H. Jeon, J.K. Han; Seoul/KR

Purpose: To investigate the feasibility of Sonazoid-enhanced ultrasound in the non-invasive assessment of acute rejection or recurrent hepatitis in post-liver transplantation follow-up.
Material and Methods: In this prospective study, 41 patients who had undergone liver transplantation within 5 years were enrolled (group 1, ≤4 weeks after transplantation, n=17; group 2, >4 weeks after transplantation, n=24). Patients received Sonazoid-enhanced ultrasound during the vascular phase and Kupffer phase followed by liver biopsy. Hepatic filling rate [(HFR) time interval between contrast agent arrival in the right hepatic artery and maximum hepatic parenchymal intensity during the vascular phase] and parenchymal intensity difference (PID) before and after instantaneous high power emission on the Kupffer phase were compared between patients with normal biopsy, acute rejection, and recurrent hepatitis.
Results: By histopathologic analysis, 23 patients were classified as normal, 3 as acute rejection, and 15 as recurrent hepatitis. HFR and PID showed significant differences between patients with normal biopsy, acute rejection, and recurrent hepatitis ($P<0.05$). Subgroup analyses according to the interval of transplantation and Sonazoid-enhanced ultrasound revealed that HFR was significantly greater in patients with acute rejection or recurrent hepatitis than those with normal biopsy in group 1, whereas PID was significantly greater in patients with recurrent hepatitis than those with normal biopsy in group 2 ($P<0.05$).
Conclusion: Sonazoid-enhanced ultrasound may be a promising tool for the assessment of acute rejection or recurrent hepatitis in liver transplant recipient.

SS 14.07

Evaluation of a low iodine concentration contrast media in abdominal multiphasic computed tomography using spectral imaging: a prospective study on 210 patients

C. Roy, F. Severac, M. Ohana, A. Labani; Strasbourg/FR

Purpose: To demonstrate the non-inferiority of a low iodine concentration CM for abdominal multiphasic CT acquired with spectral imaging in comparison with usual CT obtained with high-concentration CM.
Material and Methods: 210 patients (BMI<35, GFR>45) with clinically indicated multiphasic abdominal CT were prospectively randomized into three groups of 70 patients. Examinations were performed on a single-source dual-energy CT (GE Discovery 750HD). Two groups underwent conventional CT with iomeprol 400mgI/ml and iomeprol 350mgI/ml. One group was acquired with Iobitridol 250 mgI/ml using spectral with monochromatic images at 75, 65 and 60 keV. Quantitative analysis consisted of HU+SD in aorta, hepatic parenchyma and portal vein, obtained for arterial and portal phases. Image quality of all phases was independently assessed. Quantitative statistical analysis was performed using the Bayesian method with a 95% credibility interval to assess for non-inferiority. HU thresholds were set at 20% for the arterial and 10% for the portal phase. Radiation doses were recorded.
Results: For qualitative evaluation, spectral images revealed an excellent image quality. At 60 KeV, 250 was superior for the venous phase. At 65 KeV, 250 revealed no significant differences between the 350 or 400 concentrations for all sites. At 75 KeV, 250 was inferior for all sites. Increase in radiation doses was less than 10%.
Conclusion: Low iodine contrast offers equivalent image quality and enhancement for both phases, when using spectral imaging, allowing up to 37.5% iodine reduction.

SS 14.08

Optimal visualization of focal nodular hyperplasia: quantitative and qualitative comparison of single and multiphasic arterial phase acquisition at 1.5 T

C. Rousseau[1], M. Ronot[1], I. Boulay Coletta[2], V. Vilgrain[1], M. Zins[2]; [1]Clichy/FR, [2]Paris/FR

Purpose: To compare the arterial enhancement and lesion contrast of FNH explored with triple or single arterial phase MR sequences.
Material and Methods: Between 2007 and 2014, patients undergoing MR imaging for the exploration of FNH were included. Protocol included single (2007-2010) or triple arterial phase (2011-2014). Arterial phases were divided into 1/angiographic (contrast in hepatic artery, not in portal veins), 2/early (mild opacification of portal veins), 3/late (contrast in portal veins, not in hepatic veins), 4/portal (contrast in hepatic veins). For each lesion, signal intensity on arterial phase (SI_{art}) was visually recorded as intense, moderate or low. Lesion-to-liver contrast (LC) and relative-lesion-enhancement (RE) were calculated and compared between the two groups using Mann-Whitney test.

Material and Methods: Between 2007-2014, patients undergoing MR imaging for the exploration of FNH were included. Protocol included single (2007-2010) or triple arterial phase (2011-2014). Arterial phases were divided into 1/ angiographic (contrast in hepatic artery, not in portal veins), 2/early (mild opacification of portal veins), 3/late (contrast in portal veins, not in hepatic veins), 4/portal (contrast in hepatic veins). For each lesion, signal intensity on arterial phase (SI_{art}) was visually recorded as intense, moderate or low. Lesion-to-liver contrast (LC), and relative-lesion-enhancement (RE) were calculated and compared between the two groups using Mann-Whitney test.
Results: 35 women were included (mean 45 years (20-66), 50 FNH mean 30 mm). "Single" group: 20-patients/30-FNH; "Triple" group: 15-patients/20-FNH. SI_{art} was intense in 100% and 73% of the lesions in the "triple" and single" group respectively (p=0.041). Early arterial phase showed more frequently intense signal (p<0.001). RE was not significantly different between "single" and "triple" (1.78±0.84 vs. 1.98±1.81, p=0.430), but LC was significantly higher in the "triple" group (0.32±0.10 vs. 0.22±0.10, p=0.005). LC was significantly higher in the first two arterial phases in the "triple" group (p<0.001).
Conclusion: Acquisition of three arterial phases improves the detection of FNH hypervascularity, with high visual signal intensity and a higher contrast. Optimal phase is the early arterial phase.

SS 14.09

Focal nodular hyperplasia versus inflammatory adenoma: clues for a confident differential diagnosis during MR imaging with a hepatobiliary (Gd-EOB-DTPA) contrast agent

V. Battaglia, L. Turturici, A. Mantarro, D. Cioni, C. Bartolozzi; Pisa/IT

Purpose: To identify reliable clues to formulate a confident differential diagnosis between focal nodular hyperplasia (FNH) and inflammatory adenoma (IA) in non-cirrhotic, healthy livers.
Material and Methods: Thirty-one nodules (3 males, 14 females) were evaluated at MR imaging. For each lesion, biopsy diagnosis was obtained (21 inflammatory adenomas; 10 focal nodular hyperplasia). Lesions' characteristics such as the presence of intralesional fat component, scar on baseline T2W images, and post-contrastographic enhancement on dynamic and hepatobiliary phases were evaluated by two readers by consensus.
Results: Hyperintensity on baseline T2W imaging was detected in 20/21 IAs and in 3/10 FNHs. Lesion scar on baseline T2W imaging was specific for FNH diagnosis. No intracellular fat component was appreciable in FNHs, while it was detected in 11/21 IAs. All IA became hypointense on HB phase, while 8/10 FNH showed as iso- or hyperintense; perilesional halo of enhancement on HB phase was present in 17/21 IA and no FNH. Lesions' uptake on both early arterial and parenchymal arterial phases was not a significant clue for differential diagnosis.
Conclusion: Lesions' hyperintensity on baseline T2W imaging associated with lesion central hypointensity and perilesional enhancement halo on HB phase is strongly related to a diagnosis of IA. The presence of intralesional fat does further support the diagnosis of IA.

SS 14.10

Diagnostic management of atypical benign hepatocellular lesions imaged at MR-CEUS vs. hepato-biliary phase imaging

L. Tselikas[1], F. Pigneur[1], M. Roux[1], L. Baranes[1], C. Costentin[1], V. Roche[1], J. Calderaro[1], A. Laurent[1], D. Azoulay[2], A. Mallat[1], D. Cherqui[1], A. Rahmouni[1], A. Luciani[1]; [1]Creteil/FR, [2]Paris/FR

Purpose: To compare the added value of delayed hepatobiliary phase (HBP) imaging using gadolinium (Gd)-BOPTA-enhanced MRI and contrast-enhanced ultrasound (CEUS) in patients with atypical benign hepatocellular lesions (BLT).
Material and Methods: Eighty-three BLT—46 focal nodular hyperplasia (FNH) and 37 hepatocellular adenomas (HCA)—with atypical presentation on liver contrast-enhanced MR using extracellular Gd chelates (CE-MRI), in 54 patients were retrospectively included in this IRB-approved study. All patients underwent HBP-MRI and CEUS. Two radiologists independently reviewed 2 sets of images; set-1: CE-MRI and HBP-MRI; set-2: CE-MRI and CEUS. All HCA and 30.4% of all FNH were documented on pathology, the remaining FNH being diagnosed in board decisions and a minimum follow-up of 12 months. Sensitivity (Se) and specificity (Spe) were compared between the two sets, and subgroup analyses according to lesion's size were performed.
Results: Regardless of lesion size, the respective Se and Spe of both data sets were not statistically different (95.7 and 100% vs. 78.3 and 94.6% for set 1 and 2, respectively; p=0.18). For lesions larger than 35mm, although both sets had similar excellent specificity (100%), sensitivity was higher for CE-MRI + HBP-MRI set (100% vs. 40%); p=0.04.
Conclusion: Although the overall performances of CE-MRI + HBP-MRI and CE-MRI + CEUS are similar, the use of HBP imaging should be advocated over CEUS in larger than 35mm benign hepatocellular lesions.

11:00 - 12:30 Darwin 4

Scientific Session SS 15

Rectum and colon cancer: evaluation of tumour response

SS 15.01

Dynamic contrast-enhanced MR imaging in rectal cancer: study of inter-software accuracy and reproducibility using simulated and clinical data

L. Beuzit, P.-A. Eliat, E. Bannier, J.-C. Ferré, S. Manfredi, Y. Gandon, V. Brun, H. Saint-Jalmes; Rennes/FR

Purpose: To test the reproducibility and accuracy of pharmacokinetic parameter measurements on five analysis software packages (SPs) for dynamic contrast-enhanced magnetic resonance (DCE-MR) imaging, using simulated and clinical data.
Material and Methods: This retrospective study was institutional review board approved. Simulated tissues consisted of pixel clusters of calculated signal changes for combinations of pharmacokinetic parameters (volume transfer constant [K_{trans}], extracellular volume fraction [v_e]), T1 and noise. The clinical group comprised 27 patients treated for locally advanced rectal cancer, with 36 DCE-MR scans. The imaging protocol included dual-flip angle T1 mapping and a dynamic post-contrast T1-weighted sequence. The clinical and simulated images were postprocessed with five SPs to measure K^{trans}, v_e and the initial area under the gadolinium curve (iAUGC). Modified Bland–Altman analysis was conducted; intraclass correlation coefficients and within-subject coefficients of variation were calculated.
Results: Measurement errors were observed on the simulated data for all the pharmacokinetic parameters and SPs, with a bias ranging from -0.19 min^{-1} to 0.09 min^{-1} for K^{trans}, -0.15 to 0.01 for v_e, and -0.65 to 1.66 $mmol.L^{-1}.min$ for iAUGC. The intraclass correlation coefficient between SPs revealed moderate agreement for the simulated data (K^{trans}: 0.50; v_e: 0.67; iAUGC: 0.77) and very poor agreement for the clinical data (K^{trans}: 0.10; v_e: 0.16; iAUGC: 0.21).
Conclusion: Significant errors were found in the calculated DCE-MR imaging pharmacokinetic parameters (K^{trans}, v_e, iAUGC) for the perfusion analysis SPs, resulting in poor inter-software reproducibility.

SS 15.02

Reproducibility of evaluation of invasion depth of rectal cancer into the mesorectal fat: can we reliably discern T3ab from T3cd tumours?

M. Maas[1], G.L. Beets[1], M. Ageitos Casais[2], X. Li[3], S.-X. Rao[4], M.M. Van Heeswijk[1], R. Beckers[1], R.G.H. Beets-Tan[1]; [1]Maastricht/NL, [2]Santiago de Compostela/ES, [3]Beijing/CN, [4]Shanghai/CN

Purpose: One of the important aspects of rectal cancer staging is the measurement of the invasion depth of a tumour into the mesorectal fat in millimetres. This determines whether there is a T3ab (<5mm) or T3cd (>5mm) tumour, which can change treatment. Measurement of this factor can be arbitrary. Aim was to evaluate reproducibility of the measurement of invasion depth into the mesorectal fat by different readers.
Material and Methods: Sixty-one patients with a pathologically proven T3 tumour were selected. Two readers with different experience in reading rectal cancer MRI (2 years and 5 years) measured the maximal depth of invasion of tumour into mesorectal fat in the axial plane perpendicular to the tumour axis. Clock position of the measurement was registered. ICC and Bland–Altman plots were used for analyses.
Results: Intraclass correlation coefficient was 0.61. The Bland–Altman plot showed a mean difference between measurements of 2.45 (SD 3.53) mm with limits of agreement of -4.45 to 9.39. Differences between measurements ranged from -9 to 15 mm. In 36% of patients, the clock position of the measurements of both readers was not in the same quadrant.
Conclusion: Reproducibility of measurement of tumour invasion depth into mesorectal fat is low, both with regard to the depth and to the location of the deepest invasion. Therefore, the distinction between T3ab and T3cd tumours is unreliable and should not be used for treatment decisions.

SS 15.03

Assessment of MRI heterogeneity in primary rectal cancer: day-to-day reproducibility of MRI locoregional and global texture parameters

S. Gourtsoyianni, G. Doumou, M. Siddique, B. Taylor, J. Stirling, G.J. Cook, V. Goh; London/UK

Purpose: To assess the day-to-day reproducibility of loco-regional and global MRI textures features derived from primary rectal cancer.

Material and Methods: Following IRB approval and informed consent, 28 MRIs performed on consecutive days as part of a prospective study in 14 patients with rectal cancer were analysed. 30 locoregional (second-order and higher order statistical) and global (first-order statistical and model-based) texture features were extracted for the whole tumour from the T2-W axial images by 2 different readers. Reproducibility was assessed using Bland–Altman statistics and coefficient of variation (wCV%) recorded.

Results: Day-to-day reproducibility was best for global first-order statistical (wCV range: 3–25%), global model-based fractal parameters (wCV range: 2–28%) and second-order locoregional parameters (wCV range: 3–27%). Higher order locoregional parameters had poorer reproducibility, e.g. higher order complexity and short-zone emphasis wCV >50%.

Conclusion: Assessment of tumour heterogeneity has shown promise in rectal cancer with a focus to date on global features. Day-to-day reproducibility is good for global texture parameters boding well for clinical practice.

SS 15.04

DWI for assessment of rectal cancer nodes after chemoradiotherapy: does the absence of nodes on DWI predict a ypN0 status?

M.M. Van Heeswijk, D.M.J. Lambregts, W. Palm, B. Hendriks, G.L. Beets, R.G.H. Beets-Tan; Maastricht/NL

Purpose: Diffusion-weighted MRI (DWI) is a very sensitive technique to detect nodes. Assessment of a node-negative status after chemoradiaton (CRT) is important, mainly when considering organ-saving treatments in patients with a good tumour response. Aim was to test the hypothesis that the absence of nodes on DWI after CRT is concordant with a ypN0 status.

Material and Methods: 91 rectal cancer patients treated with CRT followed by a restaging MRI (1.5T) including DWI (highest b value b1000) were included. Two independent readers counted the number of nodes visible on DWI after CRT. The number of nodes observed on DWI (0 vs. ≥1) was compared with the number of positive nodes at histopathology (yN0 vs. yN+).

Results: 72 patients were ypN0 and 19 were ypN+. In 11 patients, no nodes were observed on DWI by both readers, which was concordant with a yN0-status in all 11 (100%) cases. In the other 61 ypN0 patients, a mean number of 4 (range 1–17) nodes were counted. In the 19 ypN+ patients, a mean number of 4 (range 1–7) nodes were observed on DWI.

Conclusion: Although the absence of lymph nodes on DWI is not a frequent finding, it is a reliable predictor of a ypN0 status after neoadjuvant CRT in patients with rectal cancer. As such, DWI can be a helpful tool to select node-negative patients after CRT.

SS 15.05

Multiparameteric PET-MR assessment of response to neoadjuvant chemoradiotherapy in locally advanced rectal cancer: PET, MR, PET-MR and tumor texture analysis

U. Metser, K.S. Jhaveri, G. Murphy, J. Halankar, D. Hussey, P. Dufort, E. Kennedy; Toronto, ON/CA

Purpose: Pre-operative chemoradiation therapy (CRT) has now become the standard of treatment for locally advanced rectal cancer (LARC). Patients achieving complete pathologic response (pCR) have significantly improved long-term survival. Preoperative detection of pCR may enable a conservative therapeutic approach in some patients (e.g. those at high risk for surgery). The purpose of the current prospective pilot study was to assess multiparametric qualitative and quantitative MR, PET, PET-MR and tumor texture features in predicting complete pathologic response to CRT in patients with LARC.

Material and Methods: Eighteen LARC patients underwent staging with FDG-PET and MR-rectum and 15 had post-CRT restaging. Response was assessed qualitatively and quantitatively. SUV (tumor/background), SUV/ADC, and tumor texture parameters derived via machine learning algorithms (MLA) from PET and multiple MR sequences were correlated with histopathology.

Results: A third of patients had pCR. Sensitivity, specificity & accuracy of PET, MR and combined PET-MR were 90, 60, & 80; 90, 20 & 66.7; 90, 80 & 86.7, respectively. Quantitatively, only tumor-muscle (SUV/ADC) ratio improved prediction of pCR. Of all texture features assessed using MLA, only the classifier trained on pretreatment PET was significant (p=0.034; accuracy, 92.8%). Combined PET and MR texture features did not improve performance.

Conclusion: Combined PET-MR has improved specificity compared to PET or MR alone. Tumor to muscle SUV/ADC ratios post-therapy and texture features on baseline PET show promise in predicting pCR post-CRT in LARC.

SS 15.06

MRI detected extramural venous invasion in rectal cancer: diagnostic performance and its prognostic significance

E.S. Lee, M.J. Kim, S.C. Park, H.J. Change, J.Y. Baek, S.Y. Kim, D.Y. Kim, J.H. Oh; Goyang-si, Gyeonggi-Do/KR

Purpose: Extramural venous invasion (EMVI) is one of the poor prognostic factors in rectal cancer. This study is aimed to assess the diagnostic performance of magnetic resonance imaging for EMVI in post-treatment rectal cancer patients (yMR-EMVI) and determine its prognostic significance.

Material and Methods: A total of 60 surgically proven rectal cancer patients who had undergone preoperative MRI following neoadjuvant chemoradiation treatment were included in this study. Two radiologists evaluated the yMR-EMVI and checked inter-observer agreement with weighted kappa analysis. The diagnostic performance based on the histopathologic results using receiver operating characteristic curve was also assessed. In addition, correlation of yMR-EMVI and 5-year disease-free survival (DFS)/overall survival (OS) was identified using Kaplan–Meier survival analysis.

Results: Mean observation time was 64 months (range, 3 to 84 months). Inter-observer agreement for yMR-EMVI revealed good agreement (weighted kappa, 0.732). Area under the curve of yMR-EMVI by consensus reading of two radiologists was 0.795 (sensitivity 46.2%, specificity 97.3%). The 5-year DFS for yMR-EMVI-positive patients was significantly lower than yMR-EMVI-negative patients—46.4% (95% CI: 27.3%–65.5%) versus 65.8% (95% CI: 59.0%–72.6%) (log rank test, P=0.013). Regarding 5-year OS, yMR-EMVI-positive patients showed lower survival than yMR-EMVI-negative patients—66.7% (95% CI: 52.7%–80.8%) versus 73.8% (95% CI: 68.0%–79.7%), but not significant (log rank test, P=0.094).

Conclusion: After neoadjuvant chemoradiation in rectal cancer, yMR-EMVI was well correlated with histopathologic results and significantly related with 5-year DFS in prognosis.

SS 15.07

Distal location and larger thickness may predict a more intense peritumoral inflammatory response to neoadjuvant therapy and shorter disease-free survival in moderate/high-risk rectal cancer patients

I. Santiago, R. Rocha, R. Theias, A. Gomes, A. Costa, T. Fiuza, V. Nunes; Amadora/PT

Purpose: To evaluate MR T2-weighted imaging markers of peritumoral inflammatory response (PIR) after neoadjuvant (NA) therapy in moderate/high-risk rectal cancer patients and to assess their relation to patient outcome.

Material and Methods: All rectal cancer patients with preoperative staging pelvic MR who underwent long-course chemoradiotherapy followed by total mesorectal excision, diagnosed at our Institution between 01-01-2004 and 02-17-2014 were included, totalizing 47 patients (64.8±13.2 years, 30 males). Staging MR high-resolution T2-weighted images were retrospectively evaluated by a radiologist with 5 years of experience in pelvic MR. Tumor dimensional, morphological and signal intensity-derived parameters were recorded, as well as key localizing distances. Variables assessed included maximum thickness (MT), and distances to anal verge, recto-sigmoid junction and peritoneal reflection (DPR). The latter was considered positive when the upper limit of the tumor was located below, null when involved and negative when the lower limit of the tumor was located above. Histopathologic variables were analyzed, including PIR, which was graded as weak/moderate/intense; as well as patient outcome.

Results: A significant correlation between the degree of PIR and DPR was found (r=0.600; p=0.002). The degree of PIR was positively correlated to MT (r=0.492; p=0.013). An inverse correlation was found between PIR and months to distant disease recurrence (r=-0.683, p=0.043).

Conclusion: Tumors located in the low rectum and with large maximum thickness may respond with higher PIR to NA therapy. The degree of PIR may be inversely related to disease-free survival in moderate/high-risk rectal cancer patients.

SS 15.08

Evaluation of rectal cancer response to therapy: role of MR tumour regression grade to predict pathological complete response

D. De Santis, D. Caruso, M. Ciolina, C.N. De Cecco, M. Rengo, S. Marzi, A. Laghi; Rome/IT

Purpose: To determine if a pathological complete response to therapy in rectal cancer can be predicted by tumour regression grade evaluated by MR (MRTRG).
Material and Methods: Thirty-seven patients, diagnosed with locally advanced rectal cancer were prospectively enrolled in the study. All patients underwent MRI on a 3 Tesla before, during and after chemoradiotherapy (CRT). All patients underwent total mesorectal excision (TME). MRTRG was evaluated on T2-weighted fast spin echo (FSE) multiplanar imaging. The MRTRG was determined by the fibrosis/tumour ratio and was divided into 4 grades based on the percentage of fibrosis (<25%, <50%, <75%, 100%). Measurements were performed on all axial images including the tumour. MRTRG evaluated on the second examination (during therapy) was correlated with the pathological finding after surgery, defined as partial response or complete response.
Results: A complete pathologic response was observed only in patients (17) with MRTRG 4 (100% fibrosis) with a negative predictive value of 100%. In lower MRTRG groups (1, 2 and 3), a partial response was observed (20 patients).
Conclusion: MRTRG 4 is an accurate predictor of complete response after CRT. When a lower MRTRG is observed, the persistence of disease should be suspected. This method, applied during therapy, may reduce the time to surgery.

SS 15.09

The value of diffusion-weighted MR imaging to identify responders after neoadjuvant chemo-radiation therapy in patient with locally advanced rectal cancer

E. Quaia, A.G. Gennari, M. Pontello, M.A. Cova; Trieste/IT

Purpose: To define the value of diffusion-weighted MR imaging sequences to identify responders in patients with locally advanced rectal carcinoma after neoadjuvant chemo- and radiation therapy (CRT).
Material and Methods: Thirty consecutive patients (mean age ± SD: 71 years ± 6,48; range 53–84; M:F=18:12) with locally advanced rectal carcinoma underwent CRT followed by surgery. Each patient underwent MR imaging before and 6 weeks after the completion of CRT. The tumor ADC percent variation was calculated as: (ADC_{post} - ADC_{pre}) x 100 / ADC_{pre}. The amount of viable tumor versus fibrosis after CRT was assessed according to the Mandard criteria applied to the surgical specimen.
Results: Nineteen patients were classified as responders due to partial (n=14) or complete response (n=5), while 11 patients were classified as non-responders due to stable disease (n=9) or disease progression (n=2). Responders can be differentiated from non-responders based on ADC variation (Wilcoxon test; P< 0.05) which represents the best independent predictor of therapeutic outcome. Diffusion-weighted MR imaging sequences showed a sensitivity of 100% (25/25), a specificity of 60% (3/5), a positive predictive value of 92% (23/25) and a negative predictive value of 100% (3/3) in the detection of complete response.
Conclusion: Diffusion-weighted MR images can differentiate responders from non-responders to CRT based on ADC variation which represents the best independent predictor of therapeutic outcome.

SS 15.10

3T MR quantitative imaging in rectal cancer staging: variability in reporting among radiologists

E. Guidi[1], L. Faggioni[1], G. D'Ippolito[2], E. Neri[1], C. Bartolozzi[1]; [1]Pisa/IT, [2]Sao Paulo/BR

Purpose: To evaluate the interobserver agreement between two radiologists in local staging of rectal cancer with 3T MRI.
Material and Methods: Fifty patients with rectal cancer underwent 3T MRI for preoperative staging and all examinations were assessed by two experienced radiologists. The following tumor markers were measured: site, longitudinal extent, maximum thickness, distance between lesion and puborectalis muscle, depth of extramural spread, distance between lesion and mesorectal fascia. Qualitative parameters were also evaluated: overcoming of anterior peritoneal reflection, mesorectal, iliac and obturator lymph node involvement, pelvic organs and levator ani muscles infiltration. Findings were compared and interobserver agreement was calculated for each parameter using the Cohen's kappa statistics.
Results: The interobserver agreement was 0.91 for the lesion site, 0.914 for the distance between lesion and puborectalis muscle, 0.791 for the tumour longitudinal extent, 0.758 for the depth of extramural spread, 0.734 for the maximum thickness of the lesion and 0.48 for the distance between lesion and mesorectal fascia. There was also an agreement between the two observers of 100% for the pelvic organs involvement, of 96% for the overcoming of the anterior peritoneal reflection, of 88% for the mesorectal lymph nodes involvement and of 82% for the levator ani muscles infiltration.
Conclusion: The overall interobserver agreement was good, but the few differences in tumor marker measurement testify the need to improve the reproducibility of reporting by a standardized approach.

11:00 - 12:30 Darwin 5

Scientific Session SS 16

Liver intervention and response assessment

SS 16.01

Usefulness of a second biopsy when the first one is inconclusive in patients with a liver nodule developing in chronic liver disease

V. Cartier[1], V. Vilgrain[2], B. Gallix[3], S. Michalak[1], M. Esvan[4], O. Seror[5], F. Oberti[1], C. Aubé[1]; [1]Angers/FR, [2]Clichy/FR, [3]Montpellier/FR, [4]Paris/FR, [5]Bondy/FR

Purpose: To evaluate usefulness of a second biopsy when the first one is inconclusive in patients with a liver nodule identified during screening of chronic liver disease.
Material and Methods: This study was a part of a study that evaluated accuracy of imaging for the diagnosis of small hepatocellular carcinoma (HCC) in chronic liver diseases. Among the 439 patients included, in 265 cases inconclusive imaging lead to nodule biopsy of 280 lesions. The following histological results were considered as conclusive: HCC, dysplastic or regenerative nodule, other tumor (benign or malign tumors). When results were inconclusive, a second biopsy was suggested, but not obligatory.
Results: 265 patients with 280 nodules underwent a first biopsy (80.8% of men, mean nodule size: 18.96 +/- 5.66 mm (range: 7–33)). First biopsy was conclusive in 72.5% of cases (203 nodules): 168 HCCs (82.8%), 13 regenerative nodules (6.4%), 12 dysplastic nodules (5.9%), 10 other tumors (4.9%). Among the 77 cases of inconclusive first biopsy, a second biopsy was performed for 20 nodules within the 6 months after the first one that was conclusive in 75% of cases (15/20 nodules): 12 HCCs, 2 dysplastic nodules, 1 other tumor. In 5 (25%) cases no definitive diagnosis could be provided.
Conclusion: Diagnostic accuracy of a second biopsy is not decreased compared to the first in our study. Repeating biopsy could be recommended in patients with a first inconclusive biopsy.

SS 16.02

Intravoxel incoherent motion MR imaging for monitoring treatment response of hepatocellular carcinoma after sorafenib treatment: correlation with histologic findings in animal models

Y. Lee[1], S.S. Lee[2], H.H. Cheong[2]; [1]Busan/KR, [2]Seoul/KR

Purpose: To evaluate the feasibility of intravoxel incoherent motion (IVIM) imaging for monitoring treatment response of hepatocellular carcinoma (HCC) after sorafenib treatment in mouse models of HCC.
Material and Methods: Twenty-four nude mice bearing Huh-7 xenografts were randomly allocated into control or one of two treatment groups (i.e. sorafenib doses of 5mg/kg [5mg-Tx] or 30mg/kg [30mg-Tx]). IVIM imaging was performed using 9 b values (0–900 sec/mm^2) before and 12 days after the treatment. The apparent diffusion coefficient and IVIM parameters were measured in the entire tumor and at the periphery of the tumor, and they were compared with histologic microvessel density (MVD) and tumor necrosis/apoptosis.
Results: The control group showed significantly greater tumor volume and MVD than the treatment groups (P <.001). The final perfusion fraction (f) values (control, 0.41±0.06; 5mg-Tx, 0.29± 0.06; 30mg/kg, 0.22±0.09; P<.001) at the tumor periphery for control group were significantly larger than those for treatment groups. The final true diffusion (D) values (control, 0.37±0.09 $x10^{-3}$ mm^2/sec; 5mg-Tx, 0.46±0.09; 30mg/kg, 0.54±0.06; P<.001) at the tumor periphery were significantly larger in the treatment groups than in the control group. MVD had significant positive correlations with the f (r=.584, P=.003), while no parameter showed significant correlation with tumor necrosis/apoptosis.
Conclusion: The IVIM-derived perfusion fraction reflects MVD in animal models of HCC, and may be useful in monitoring anti-angiogenic effect of sorafenib in patients with HCCs.

SS 16.03

Portal vein embolization using N-butyl-cyanoacrylate compared to N-butyl-cyanoacrylate plus Amplatzer™ vascular plugs in 102 patients

G. Baudin, F. Germain, L. Avril, M. Chassang, A.S. Schneck, A. Ianelli, J. Gugenheim, P. Chevallier; Nice/FR

Purpose: To compare efficacy and tolerance of portal vein embolization (PVE) using N-butyl-cyanoacrylate (NBCA) versus NBCA plus Amplatzer™ vascular plugs (NBCA+AVP).

Material and Methods: 102 patients with malignant hepatobiliary disease underwent PVE using either NBCA (n=52) or NBCA+AVP (n=50) between July 2005 and July 2014. Groups were retrospectively compared for age, sex, comorbidities, type of tumor, technical details of PVE procedure, volume of the future liver remnant (FLR) and FLR ratio before PVE. Primary endpoint was the increase in FLR volume after PVE. Secondary endpoints were the increase in FLR ratio after PVE, resection rate, embolization tolerance and peri-operative complications rate.

Results: Both groups were similar in terms of age, sex ratio, type of tumor, comorbidities, FLR volume and FLR ratio before PVE. PVE procedure was similar in both groups except for the access route (most contralateral approach in NBCA group). The increase in FLR volume after PVE was similar with NBCA and NBCA+AVP (+46.2% and +45.5%, NS). The increase in FLR ratio, resection rate, PVE tolerance and peri-operative complication rates were similar in both groups. PVE procedure time was also similar (64 min for NBCA; 72 min for NBCA+AVP, NS).

Conclusion: PVE with NBCA + AVP is as efficient and safe to induce hypertrophy of FLR as PVE with NBCA alone. However, adjonction of AVP does not shorten the procedure time in teams experienced with the use of NBCA.

SS 16.04

Hepatocellular carcinoma treated by transarterial chemoembolization: prediction of treatment failure using tumoral morpho-phenotypic features on pre-treatment biopsy

M. Ronot[1], M. Wagner[1], A. Sciarra[2], L. Di Tommaso[2], C. Raschioni[2], J. Belghiti[1], L. Castera[1], P. Bedossa[1], V. Vilgrain[1], M. Roncalli[2], V. Paradis[1]; [1]Clichy/FR, [2]Milan/IT

Purpose: To identify tissue predictors of tumor resistance to TACE for use in clinical practice on pre-treatment biopsies.

Material and Methods: We investigated the association of residual tumor (RT) in post-TACE-resected HCC with pathological and immunophenotypical features, mainly related to hypoxia and angiogenesis. Comparison of tumor phenotype between post-TACE HCC and both paired pre-TACE biopsies and control TACE-untreated HCC was performed by Chi-squared test. Cases showing >50% RT were defined as TACE-resistant. TACE resistance score was calculated using binary logistic regression model.

Results: A consecutive series of 108 HCC from 41 patients (39 males, mean age 58.5±8 years) was studied. Overall, 45/108 (44%) HCC were classified as TACE-resistant. Among these, 28 (62%) and 40 (89%) showed diffuse CD34 vascular staining and negative VEGF staining, respectively ($p<0.05$). The association of these 2 parameters in a weighted score was able to predict TACE resistance with 81% accuracy, 85% sensitivity and 67% specificity. The effectiveness of the score was validated in an independent series of 28 HCC biopsies from patients subsequently treated with TACE and for whom radiologic follow-up was available (23 men (82%), mean age 65±10 years (range, 46-80 years)), and showed 68% accuracy, 78% sensitivity, 63% specificity, 50% PPV and 86% NPV for the detection of TACE resistance.

Conclusion: This study demonstrates the potential value of pre-treatment tumor biopsy as predictors of TACE resistance in HCC.

SS 16.05

^{90}Y-loaded glass microspheres versus sorafenib for hepatocellular carcinoma with portal vein thrombosis: a retrospective study

Y. Rolland, J. Edeline, E. Boucher, E. Garin; Rennes/FR

Purpose: The goal of this study is to analyse retrospectively HCC patients with PVT treated with therasphere (T) or sorafenib (S) or both therasphere plus sorafenib (T+S).

Material and Methods: 61 consecutive PVT patients were included. Patients treated with therasphere were treated using a personalized dosimetric approach. Median progression-free survival (PFS) and overall survivals (OS) were estimated with the Kaplan–Meier method and compared with a log-rank test.

Results: 18 patients received T only, 29 S only and 14 received both T+S. Main PVT was present in 38% of the patients treated by T and 52% for those treated by S only (ns). For patients treated with T the mean lobe dose was 146Gy and 13 patients received an intensification (mean lobe dose = 197Gy). PFS was 7.7 m in the group T vs. 3.5 in the group S only ($p=0.026$). OS was 23.4 months in the group T vs. 5.1 in the group S alone ($p<0.001$). In the group T, OS was not significantly different if the patients received T alone or both T+S, respectively, 24.0 months vs. 21.5 months ($p = 0.96$). For patients with unilateral PVT results were still significantly better for T; OS was 24.0 vs. 6.5 months for patients treated, respectively, with T or S alone ($p<0.001$).

Conclusion: In this study therasphere, using a personalized dosimetric approach, significantly increases OS of PVT patients versus sorafenib.

SS 16.06

Predictive factors for complete response of chemoembolization with drug-eluting beads (DEB-TACE) for hepatocellular carcinoma

G. Vesselle, C. Quirier-Leleu, S. Velasco, S. Boucebci, P. Ingrand, J.P. Tasu; Poitiers/FR

Purpose: To identify clinical and imaging features associated with a complete response (CR) to transarterial chemoembolisation (TACE) with drug eluting beads (DEB) in patients with hepatocellular carcinoma.

Material and Methods: In this prospective historical cohort, 172 patients who received at least one DEB-TACE from 2007 to 2013 were studied. Imaging response was evaluated according to the modified response evaluation criteria in solid tumors (mRECIST). Age, gender, etiology of cirrhosis, child and BCLC scores, particles size, location in the liver, size of the tumor, presence of a capsule, hypervascularisation on DSA and CT or MRI scans and blush extinction were analysed.

Results: After one cure, CR was observed in 36% of the 315 tumors treated. Nodule size, location in the liver and complete blush extinction on DSA were statistically correlated to response whereas capsule aspect on imaging and demographic criteria did not. In multivariate analysis, only location in the liver and nodule size were significant features (with location in the 4th liver segment and tumor size >5 cm as pejorative factors).

Conclusion: Tumor location in the segment 4 is a pejorative factor for CR whereas tumor size <5 cm is a positive predictive factor. These criteria could, therefore, be taken into consideration to improve the selection of patients for DEB-TACE compared to curative treatment and combination therapies.

SS 16.07

Long-term outcome of sequential transarterial chemoembolization and portal vein embolization for hepatocellular carcinoma

M. Ronot, M. Wagner, F. Cauchy, B. Gregoli, M. Abdel Rehim, A. Sibert, O. Soubrane, V. Vilgrain; Clichy/FR

Purpose: To investigate long-term outcome of patients with hepatocellular carcinoma (HCC) undergoing sequential transarterial chemoembolization (TACE) and portal vein embolization (PVE).

Material and Methods: From 2004-2012, all patients with HCC undergoing TACE-PVE before major liver resection were retrospectively analyzed and the following elements were noted 1/surgical resection, 2/recurrence after resection, 3/further treatments in non-resected patients and in patients with recurrence. Overall and recurrence-free survivals were calculated.

Results: 54 patients (50 male, mean 68±10.5 years, 69% F3-4, mean HCC size 7.8±4cm) were analyzed. After 66 TACE/54 PVE, 39 patients (72%) were resected. Twenty-two (56%) experienced tumoral recurrence (mean delay 15.5±5 months). 50% of non-resected patients underwent other TACE without adverse event or marked toxicity. Resection was associated with a better survival (median OS 44 vs. 18 months, 1-, 3-, and 5-year survival rates 86%, 70%, and 32% vs. 53%, 17%, and 0%, $p<0.0001$). Recurrence was associated with a poorer prognosis (median OS not reached vs. 43 months, 1-, 3-, and 5-year survival rates 82%, 71%, and 71% vs. 85%, 58%, and 17%, $p = 0.0004$).

Conclusion: In HCC patients with sequential TACE-PVE, surgical resection is performed in most cases, with good oncological outcome taking into account the large tumor burden. Patients not resected presented with a poorer outcome but could be managed with usual antitumoral treatments, including TACE despite portal vein occlusion.

SS 16.08
Sloughing of biliary tumor thrombi of hepatocellular carcinoma after chemoembolization
H.-C. Kim; Seoul/KR

Purpose: To describe the image findings, clinical course, and implications of sloughing of biliary tumor thrombi of HCC after chemoembolization.
Material and Methods: We reviewed 13 patients who experienced sloughing after chemoembolization. We evaluated the patients' characteristics, clinical manifestations, and treatment modalities. We also reviewed CT scans to determine the characteristics of tumors and the sloughed thrombi including length, attenuation, and fate.
Results: The biliary invasion was segmental or extended to the lobar duct in eight patients and to the common bile duct in five. The length of the sloughed thrombi ranged from 0.6 to 9.0 cm. Their Hounsfield units ranged from 35 to 729. Five thrombi were misreported as biliary stones and one was not reported at all in the initial report of the CT scan. At the time of sloughing, eight patients complained of cholestatic symptoms, while the other five had no symptoms. Four patients underwent sphincterotomy and thrombus removal under ERCP, two underwent PTBD, and one underwent PTBD followed by ERCP. The remaining six were managed conservatively. Five thrombi were removed by ERCP, six disappeared spontaneously within 3 months, and one remained but without any symptoms. One patient had no follow-up image.
Conclusion: Sloughing of tumor thrombi is not a rare event after chemoembolization of HCC with biliary invasion. It can cause biliary obstruction and can be misdiagnosed as biliary stone.

SS 16.09
withdrawn by the authors

SS 16.10
Long-term outcomes of percutaneous transhepatic balloon angioplasty with stent deployment for portal vein stenosis after liver transplantation
H. Jung; Seoul/KR

Purpose: To evaluate retrospectively the long-term outcomes of percutaneous transhepatic balloon angioplasty with stent deployment for portal vein stenosis (PVS) after liver transplantation (LT).
Material and Methods: Between October 1997 and December 2014, of 794 patients (LDLT: 524, DDLT: 270) who underwent LT in a single institution, 33 patients (male 25, female 8, mean age 49.5 years) were confirmed to have portal veins stenosis at follow-up CT or ultrasonography. All patents performed percutaneous transhepatic or transsplenic interventions, including direct portography with manometry and balloon angioplasty with stent placement. Technical success, clinical success, laboratory findings, manometry findings, patency rates, and major complications were evaluated. Follow-up periods after initial balloon angioplasty ranged from 2 to 47 months (mean 18.3 months).
Results: Technical success was achieved in all patients, and clinical success was achieved in 29 of 33 patients (87.8%). Of 33 patients undergoing manometry, 12 patients showed significant improvement of pressure gradient across the stenosis after percutaneous transhepatic balloon angioplasty with stent deployment. At 1, 3, 6, and 12 months and last follow-up after balloon angioplasty with stent deployment, the rates of primary patency were 100%, 96.7%, 96.7%, 96.7%, and 96.7%. One major complication subsequent to balloon angioplasty with stent deployment was noted: portal vein thrombosis with hepatic infarction.
Conclusion: Percutaneous transhepatic balloon angioplasty with stent deployment is a safe and effective treatment with long-term patency for PVS. after LT.

11:00 - 12:30 **Dickens 1+2**

Scientific Session SS 17
Stomach and oesophagus

SS 17.01
Multiparametric fully integrated PET/MRI of advanced gastric cancer for prediction of chemotherapy response: a preliminary study
D.H. Lee, S.H. Kim, H.-C. Kim; Seoul/KR

Purpose: To investigate feasibility and usefulness of multiparametric fully integrated PET/MRI for prediction of treatment response in patients with unresectable advanced gastric cancer (AGC).
Material and Methods: This prospective study was approved by our Institutional Review Board. Ten patients with unresectable AGC underwent multiparametric PET/MRI examination including dynamic, contrast-enhanced MRI (DCE-MRI), diffusion-weighted image (DWI), and positron emission tomography (PET) on a 3T fully integrated PET/MRI system before chemotherapy. Perfusion parameters obtained by DCE-MRI, afferent diffusion coefficient (ADC) values from DWI, and standardized uptake values (SUV) from PET were measured for primary gastric cancer by two independent reviewers. For parameters obtained from PET/MRI data, inter-observer agreement was obtained with intraclass correlation coefficient (ICC) and relationship with response to chemotherapy was evaluated using the Mann–Whitney test and receiver operating characteristic (ROC) analysis.
Results: After chemotherapy, partial response (PR) was achieved in six patients, stable disease (SD) in two, and progressive disease (PD) in two. For all PET/MRI parameters, moderate to almost perfect agreement was achieved (ICC=0.405–0.826). K^{trans} value of gastric cancer in the responder group was significantly higher than that in the non-responder group for both reviewers (P=0.038). The area under the curve of K^{trans} value was 0.917.
Conclusion: Multiparametric approach using fully integrated PET/MRI system was feasible for patients with unresectable gastric cancer. K^{trans} value of primary gastric cancer can be used as a predictive marker for response evaluation to chemotherapy.

SS 17.02
The diagnostic accuracy of MDCT in evaluating T and N parameters in preoperative non-cardial gastric cancer
G. Donatelli, R. Scandiffio, S. Santi, P. Vagli, C. Bartolozzi; Pisa/IT

Purpose: To evaluate diagnostic accuracy of currently used MDCT criteria in T- and N-staging of non-cardial gastric cancer and to identify more accurate staging criteria.
Material and Methods: Nineteen patients with non-cardial gastric cancer underwent CT and then surgery. Only patients who did not take neoadjuvant therapy were considered. The gold standard was the pathological evaluation. MDCT was performed using a 64-detector row CT scanner; images were obtained before and after intravenous administration of non-ionic contrast material in arterial and venous phases, if necessary, a later phase and/or an acquisition in lateral or prone position was made. T- and N-staging were blinded evaluated according to currently used CT criteria; subsequently another not-blinded N-staging evaluation was made.
Results: Tumor volume significantly correlates with pT and maximum tumor thickness with pT2 and pT3; none of these variables have shown a relation with pN. T-staging overall diagnostic accuracy ranges from 0.62 to 0.89 and was comparable between a series of imaging of 2.5mm slice thickness/2.5mm reconstruction interval and a series of 2.5mm/1.25mm. N-staging accuracy ranges between 0.68 and 0.84, sensitivity between 0.69 and 0.93, specificity between 0.50 and 0.67, PPV between 0.79 and 0.82, NPV between 0.50 and 1.
Conclusion: MDCT has a good diagnostic accuracy in T- and N-staging of non-cardial gastric cancer that can be improved using volumetric MDCT acquisition with isotropic or near-isotropic voxel and subsequent MPR.

SS 17.03

Prognostic value of volumetric metabolic tumor parameters in patients with advanced and metastatic gastroesophageal cancer

J. Ta, D. Tamandl, M. Paireder, A. Haug, S.F. Schoppmann, A. Ba-Ssalamah; Vienna/AT

Purpose: 18F-fluorodeoxyglucose (FDG) positron emission tomography (PET)/CT is considered the gold standard in the staging of patients with esophageal cancer (EC). Metabolic volumetric parameters such as metabolic tumor volume (MTV) and total lesion glycolysis (TLG) have been shown to be of superior prognostic value compared to maximum standardized uptake values (SUV_{max}) in surgical patients, but their impact on managing patients in the palliative situation remains unclear.
Material and Methods: A total of 83 consecutive patients with advanced or metastatic EC who had ^{18}F-FDG PET/CT within 2008 to 2012 were included in this study. Besides clinical and tumor-related variables, PET/CT TNM staging, and metabolic volumetric parameters (SUV_{max}, MTV, TLG, tumor length [TL]) were analyzed. Survival analysis of overall survival (OS) was performed using Cox proportional hazards and Kaplan–Meier analysis.
Results: The optimal cutoff values for MTV, TLG and TL were 25.85mL, 67.34mL and 10.5cm. Of these values, all three variables were associated with impaired OS (MTV: hazard ratio, HR 1.98, 95% confidence interval, CI: 1.07–3.67, p=0.026; TLG: HR 2.13, 95% CI: 1.08–4.20, p=0.025; TL: HR 3.08, 95% CI 1.54–6.20, p<0.001). SUV_{max} was not prognostic for OS in this analysis.
Conclusion: MTV, TLG and TL predict impaired OS in patients with advanced and metastatic EC. SUV_{max} should not be used as a prognostic parameter in this setting.

SS 17.04

Accurate prediction of overall survival using volumetric parameters measured with PET/CT in patients with esophageal cancer

D. Tamandl, B. Fueger, M. Hejna, M. Paireder, A. Haug, S.F. Schoppmann, A. Ba-Ssalamah; Vienna/AT

Purpose: The prognostic value of volumetric parameters measured with CT and PET/CT in patients with neoadjuvant chemotherapy (NACT) and resection for esophageal cancer (EC) is yet to be determined.
Material and Methods: We retrospectively analyzed patients with locally advanced EC, who had NACT and subsequent resection. Data from CT volumetry and ^{18}F-FDG PET/CT (maximum standardized uptake [SUV_{max}], metabolic tumor volume [MTV], and total lesion glycolysis [TLG]) were recorded before and after NACT. The association of volumetric parameter (DMTV, DTLG, etc.) to overall survival (OS) was assessed using a uni- and multivariable Cox proportional hazards model.
Results: Eighty-six patients were assessed using CT volumetry and 52 also had PET/CT before and after NACT. On univariate analysis, CT volume and thickness, MTV, TLG, and SUV_{max} were all associated with OS (p<0.05), as were ΔCT thickness, ΔMTV, ΔTLG, and ΔSUV_{max} (p<0.05). In the multivariate analysis, only ΔMTV (hazard ratio, HR 2.52 [95% confidence interval, CI 1.33–4.78], p=0.005) and ΔTLG (HR 3.89 [95%CI 1.46–10.34], p=0.006), as well as surgical margin status (p<0.05), were independent predictors of OS.
Conclusion: ΔMTV and ΔTLG independently correlate with survival in patients after NACT and resection for EC.

SS 17.05

Is the pre-treatment FDG-PET/CT examination able to predict the response to the neo-adjuvant chemotherapy in patients with esophageal adenocarcinoma?

P. Fencl, T. Harustiak, O. Belohlavek, M. Zemanova; Prague/CZ

Purpose: The aim of the study was to prove whether FDG-PET/CT pre-treatment examination was able to predict the response to the neo-adjuvant chemotherapy.
Material and Methods: According to the PERCIST protocol, 113 patients were prospectively examined prior (BL) and after the end of neo-adjuvant chemotherapy (ChT3) by FDG-PET/CT. Metabolic signs were tested for their predictive ability: maximal tumor uptake (SUV_{peak}, and SUV_{max}), total lesion glycolysis (TLG); and also tumor length was exploited. Using univariate analysis, the data at BL were compared to the ones at ChT3 in all four signs.
Results: Distinct heterogeneity of FDG-PET/CT signs was registered at BL. The value of metabolic signs expressed as median (min–max) was 7.51 (38.54–3.03) for SUV_{peak}, 8.34 (39.27–3.21) for SUV_{max}, and 173.81 (2332.49–2.85) for TLG; the median length of the tumor was 6.4cm (18.5cm–1.7cm). The comparison between BL and ChT3 examinations did not reveal dependence of any of four tested pre-treatment FDG-PET/CT characteristics on the level of therapeutic response, expressed as a decrease of SUV_{peak} beyond -30%. The pre- and post-treatment data correlated with the significance level (p) for SUV_{peak} p=0.234, for SUV_{max} p=0.193, for TLG p=0.764, and for tumor length p=0.479.
Conclusion: Neither metabolic characteristic of esophageal adenocarcinoma (SUV_{peak}, SUV_{max}, TLG) nor the tumor length on pre-treatment examinations was able to predict metabolic response to the neo-adjuvant chemotherapy.

SS 17.06

The value of sarcopenia and body composition parameters as prognostic factors after esophagectomy for cancer

D. Tamandl, M. Paireder, R. Asari, S.F. Schoppmann, A. Ba-Ssalamah; Vienna/AT

Purpose: Assessment of the predictive value of sarcopenia and other body composition parameters (BCP) on survival in patients undergoing potentially curative resection of esophageal or esophagogastric cancer (EC).
Material and Methods: Two hundred patients were selected from our institutional database, which had resection for EC between 2006 and 2013. Besides demographic and tumor-specific parameters, preoperative CT scans were used to assess established markers of sarcopenia and BCP. Cox regression and Kaplan–Meier analysis were used to assess the association with overall survival (OS) after surgery.
Results: Two hundred patients (49F/151M) underwent surgery in the observed time period. Median age was 63.9 years (IQR 56.7–70.0). Sarcopenic patients showed impaired survival compared to individuals who were within physiologic range (hazard ratio [HR] 1.87, 95% confidence interval [CI] 1.15–3.03, p=0.011). Furthermore, low skeletal muscle attenuation <40 HU (HR 1.91, 95% CI 1.12–3.28, p=0.019) and increased fat mass index (HR 3.47, 95% CI 1.27–9.50, p=0.016) were associated with impaired outcome. A composite score (CSS) was generated using those 3 variables. In the multivariable analysis including the CSS and the most relevant clinical variables with survival, only CSS, T-stage and surgical resection margin remained as significant predictors of OS.
Conclusion: Patients with sarcopenia have impaired long-term outcome after surgery for EC. This information can be easily extracted from any preoperative CT scan and might help to better manage those patients.

SS 17.07

Role of two-phase dynamic MDCT in differential diagnosis of post-inflammatory esophageal strictures (corrosive, peptic) from esophageal cancer

S.A. Buryakina, G.G. Karmazanovsky, Q. Yang, D.V. Ruchkin, O.A. Rymar, E.V. Kondratiev, A.V. Vishnevskaia; Moscow/RU

Purpose: To investigate quantitative features which allow to differentiate benign esophageal strictures from esophageal cancer.
Material and Methods: CT scans of patients with histopathologically confirmed 26 corrosive esophageal strictures, 12 peptic strictures, 31 esophageal cancer in whom a two-phase dynamic MDCT was performed (arterial and venous phases at 10, 35 seconds, the delayed phase at 6–8 minutes after the injection of contrast media) were reviewed for quantitative features: regions-of-interest measurement of the zone of stenosis and normal esophageal wall and the difference between them. The phase which showed the highest attenuation in the stenosis and stenosis-to-normal esophageal wall attenuation differences (mean ΔCT) was determined. A paired t-test was used to determine which phase showed the highest tumor attenuation and tumor-to-normal esophageal wall attenuation differences.
Results: The greatest attenuation of esophageal tumor was in the arterial phase (105 HU), and the mean ΔCT in arterial phase was 23,86±19,31 HU. The greatest attenuation of post-inflammatory strictures was in the delayed phase (104 HU), and the mean ΔCT in delayed phase was 34,03±15,94 HU (P<.01).
Conclusion: Although barium studies and endoscopy are more sensitive modalities for detecting benign esophageal stenosis, an additional assessment of the dynamics of contrast material accumulation by benign esophageal strictures using a two-phase dynamic contrast material-enhanced MDCT revealed that arterial and delayed phases are optimal for differentiation of benign esophageal strictures from cancer.

SS 17.08

9.4T-MRI assessment during cisplatin and trastuzumab therapy in oesophageal adenocarcinoma xenografts

C. Yip, A. Weeks, K. Shaw, D.B. Landau, G.J. Cook, M. Siddique, V. Goh; London/UK

Purpose: To evaluate MRI changes during trastuzumab and cisplatin therapy in HER2-positive OE19 gastro-oesophageal adenocarcinoma xenografts.
Material and Methods: Following IRB approval, 3 groups of SCID mice (n=15) bearing OE19 xenografts were treated with intraperitoneal (IP) saline twice a week (controls), Cisplatin 4mg/kg once a week (group C) or trastuzumab

20mg/kg twice a week (group T) for 2 weeks. Animals underwent 9.4T MRI before (T0), after one IP treatment (T1) and on therapy completion (T2). Contrast-enhanced T1-weighted (T1w), T2-weighted (T2w), diffusion-weighted (DW) and T2*-weighted (T2*) sequences were acquired. Early (T1–T0) and late (T2–T0) parameter changes, and tumour volumes were compared between the groups using Kruskal–Wallis test.
Results: Group T had reduced growth rates (ΔT2–T0 volume=106%) compared to controls (680%) and group C (305%) (p = 0.041). DW skewness increased in group T (107%) but decreased in group C (-28%) and controls (-89%) (p=0.048). Group T had a greater reduction in T2* entropy (group T -7.1% vs. group C -0.2% vs. controls -2.2%, p=0.032) and a greater increase in T2* uniformity was found in group T (48%) compared to group C (3%) and controls (18%) (p=0.032).
Conclusion: Trastuzumab-treated tumours demonstrated reduced growth rates and significant changes in DWI and T2* versus controls. Neoadjuvant trastuzumab should be considered in HER2-positive tumours to improve tumour control and resectability.

SS 17.09

Can radiographer 'hot' review in the radiology department reduce the occurrence of 'never events' from feeding through misplaced nasogastric tubes (NGT)?

G. Roe, K. Harris, H. Lambie, D.J.M. Tolan; Leeds/UK

Purpose: To determine whether radiographer 'hot' review in the radiology department reduces the occurrence of 'never events' from feeding through misplaced nasogastric tubes (NGT), in a large teaching hospital.
Material and Methods: Despite UK National Patient Safety Agency (NPSA) guidance on safe practice to confirm safe positioning of NGTs, a number of 'never events' (death or serious harm) still occur due to misinterpretation of the check X-ray by ward staff. A practice change was introduced, which included specific training to allow immediate radiographer provisional comments for each check X-ray. The success of the new system was determined comparing the accuracy of radiographer comments against a reference standard of the radiologist final report to see whether the system is likely to reduce the number of 'never events'.
Results: 2890 check NGT X-rays were undertaken during the first six months of the new system (80 excluded for absent or incomplete provisional comments). Overall radiographer provisional comment accuracy was 98.1% (CI 97.7–99.5%) with sensitivity and specificity of 96.7% (CI 95.1–97.9%) and 98.7% (CI 98.1–99.1%), respectively, and positive predictive value of 96% and negative predictive value of 98.9%.
Conclusion: Radiographer comments are accurate and a safe, workable and cost-effective solution for addressing image interpretation issues relating to NGT 'never events'.

SS 17.10

Radiologically inserted gastrostomy (RIG): a comparison of the pull versus the push techniques.

S. Buraundi, T. Le, D. Ranatunga, A.R. Owen; Melbourne, VIC/AU

Purpose: To establish if there is a difference in either the technical success or the rate or severity of complications between the 'pull' and 'push' techniques of radiologically-inserted gastrostomy (RIG).
Material and Methods: A retrospective review of RIGs was performed over the preceding 4-year period using the electronic patient record. Technical success was recorded and complications were categorised as either major or minor using the Clavien Dindo classification of surgical complications.
Results: 123 RIGs were reviewed. 77/80 (96.2%) of the push and 42/43 (97.7%) of the pull RIGs were technically successful. >75% of RIGs were inserted for patients with either oropharyngeal carcinoma (OPC) or motor neuron disease (MND). 76% of the pull procedures were performed in patients with MND. 75% of the push procedures were nearly equally divided between patients with OPC or MND. Complications occurred in 16 (20.8%) patients using the push technique (13% minor, 7.8% major) and in 7 (16.7%) patients using the pull technique (14.3% minor, 2.4% major). There was no clear relationship between the clinical indication and the rate or severity of complications. Hospital re-presentations within 30 days occurred in 4 (5.2%) versus 0 patients using the push versus the pull technique.
Conclusion: RIG has a high technical success. The pull RIG is associated with a lower complication rate (a difference that is largely explained by fewer major complications) and should be the preferred technique.


European Society
ESGAR
Gastrointestinal and Abdominal Radiology

European Society
ESGAR
Gastrointestinal and Abdominal Radiology

JUNE 14 - 17

ESGAR 2016

PRAGUE

CZECH REPUBLIC

European Society of Gastrointestinal and Abdominal Radiology

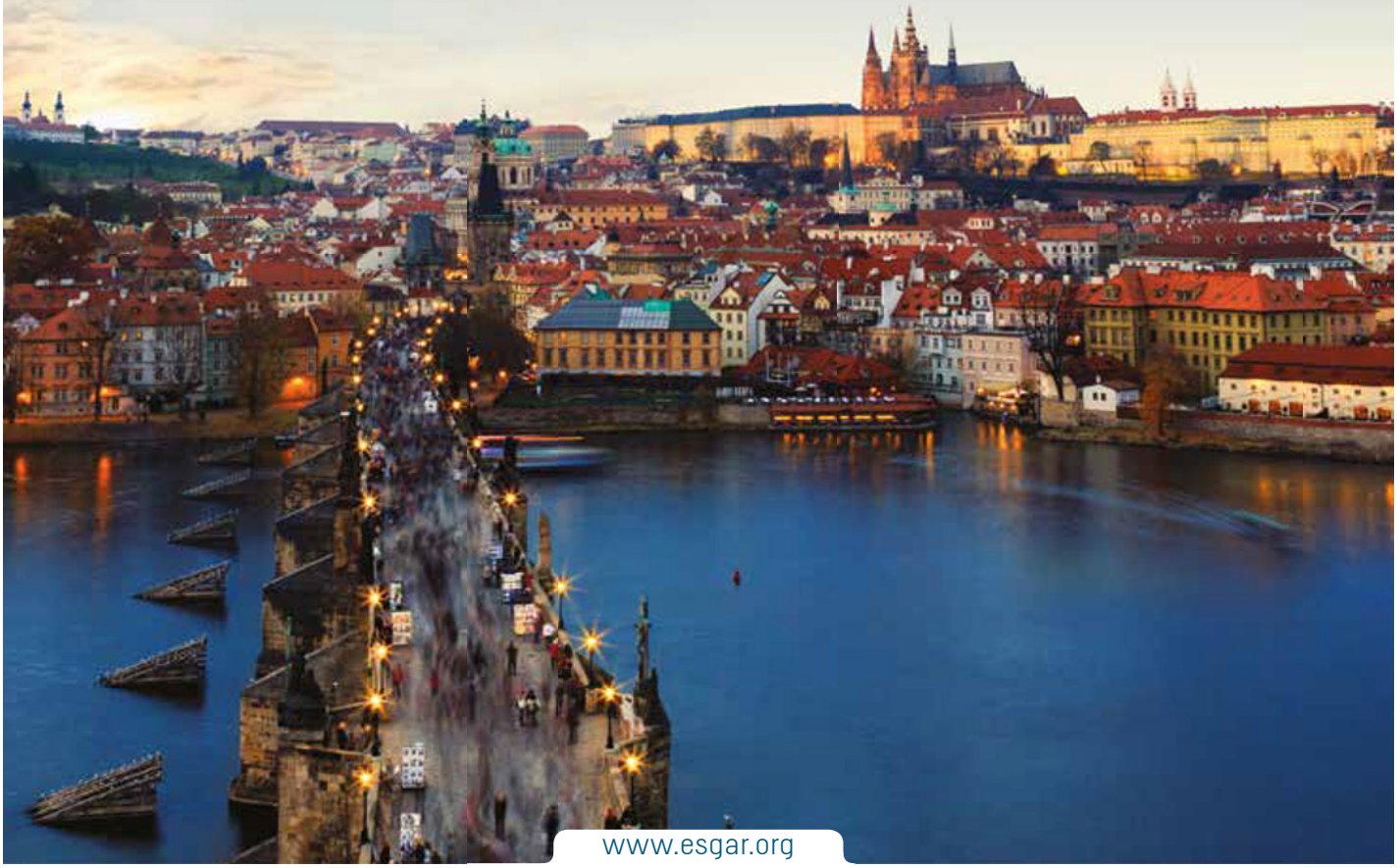

www.esgar.org